# Study on Microwave-Driven Electric Vehicle for Agriculture( Dissertation_全文 )

AUTHOR(S):

Miyasaka, Juro

CITATION:

Miyasaka, Juro. Study on Microwave-Driven Electric Vehicle for Agriculture. 京都大学, 2014, 博士(農学)

ISSUE DATE:

2014-03-24

URL:

https://doi.org/10.14989/doctor.r12823

# Study on Microwave-Driven Electric Vehicle for Agriculture

Juro Miyasaka

2014

# Study on Microwave-Driven Electric Vehicle

# for

# Agriculture

Juro Miyasaka

Division of Environmental Science and Technology
Graduate School of Agriculture
Kyoto University
Japan

2014

## Contents

# 1. Introduction

## 1.1 Background

Global warming is one of the most important environmental issues now we are facing. Though there are still pros and cons for that matter, the Kyoto Protocol on environmental protection came into effect on 2005. Developed countries are now tackling on reducing greenhouse gases, such as carbon dioxide ($CO_2$), methane ($CH_4$), nitrous oxide ($N_2O$), hydrofluorocarbons (HFCs), perfluorocarbons (PFCs), and sulphur hexafluoride ($SF_6$).

Another important issue is limited energy problem. According to Scheer, an energy and materials dependent economy (i.e. a fossil fuel economy) was established by the Industrial Revolution, transforming energy technology (Scheer, 2000). Our industrialized society is depending on this economy. However, the fossil resource is finite and ,despite of the efforts of developing technologies that enhance the utilization of the resources, these resources are basically limited and we cannot depend on them forever.

The following three characteristics of global economy that depend on fossil fuel are described by Scheer (Scheer, 2000) Followings are translation by A. Oida (Oida, 2006):

(1) Fossil resources are limited. For example, petroleum, an estimated 1020 billion barrels of which still lie underground, and which comprises about 40% of the world's total energy consumption, will be completely exhausted after 40 years. Therefore, it is feared that an exponential rise in oil prices would result in economic and political crises. Furthermore, there is the danger of an energy war.

(2) The emissions, which are produced during the energy conversion of fossil resources, cause worldwide destruction of the environment.

(3) Fossil fuel resources are found in some specific areas, but are also required by people living elsewhere. Therefore, the fossil resource is extensively exploited, mostly by huge enterprises. However, it is consumed by a large number of users. Infrastructures and companies can effectively arrange the mining, transportation, conversion and delivery of resources to the fossil fuel dependent economy. Thus, humans are bound to the fossil fuel

resource, and the fossil energy dependent economy has to continuously move toward the concentration, monopolization, and globalization of resources.

To reduce the emission of greenhouse gases, diminution of consumption of fossil fuels and enhancement of utilization efficiency of them will be necessary. These two issues are closely connected. In the agricultural machinery field, dependency on fossil fuels should be reexamined. According to IPCC 1990 report, agriculture amounts to 9 % of total contribution of human activities on global warming (Fig. 1.1).

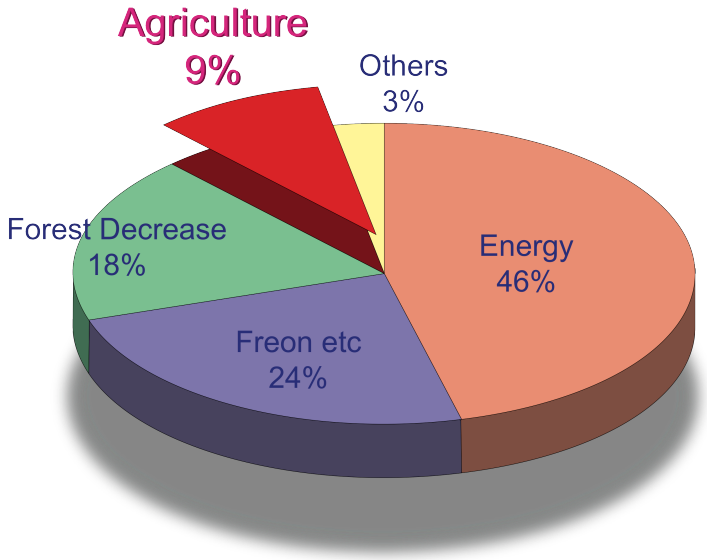


Fig. 1.1 Contribution of Human Activities on Global Warming

Electrification of Agricultural Machinery is one of the prospective solutions. However, there are problems on it. One is that the original source of electricity must not depend on fossil fuels. Another problem is utilization of batteries. Density of power (power output per battery mass) and density of energy (charged electric energy per battery mass) are relatively low than fossil fuels.

As the original source of electricity for electrification of agricultural machinery, solar power energy is one of the prospective candidates. Utilization of solar batteries for electric power plants is now increasing. If the handling of the electricity from solar

energy for agricultural machinery is established, utilization of it will spread.

Due to the low power density and energy density, batteries are considered as inappropriate for heavy duties of farm work by agricultural machinery (Fig. 1.2). Its low power density limits the load of the farm work, and its low energy density makes impossible to operate long hours of farm work.

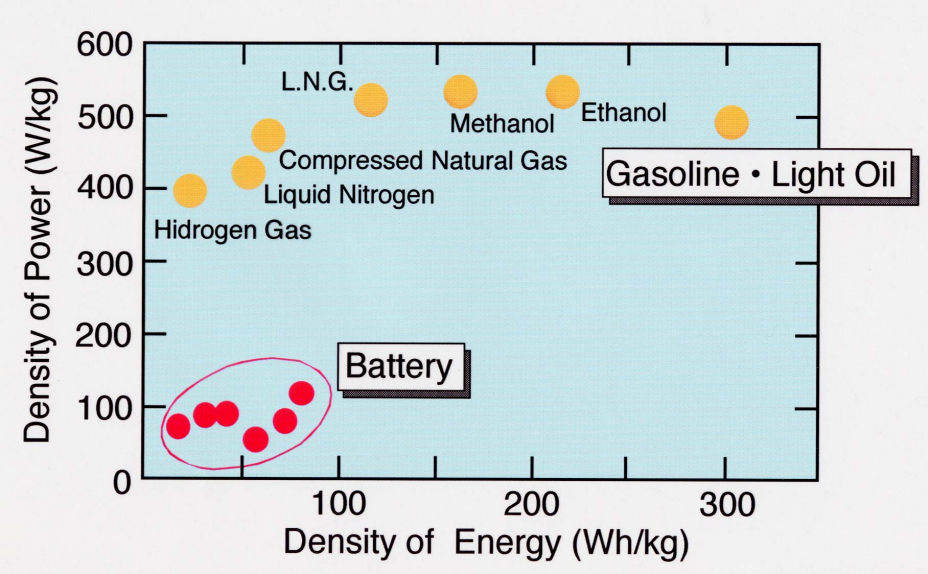


Fig. 1.2 Density of Power and Density of Energy

Considering these problems on application of electric agricultural machinery, microwave power transmission technology of solar power satellite (SPS) suggests strong solution for them. SPS (as described in Chapter 2) is power plant using huge solar batteries launched in a geosynchronous orbit (Fig. 1.3). Electricity is generated by solar batteries, and is transformed into microwave and is transmitted wirelessly to the ground rectifying facilities.

This technology has a potential of solving the two problems on electrification of agricultural machinery mentioned above. The electricity is generated by solar batteries without fossil fuels. Microwave power transmission enables to convey the power to a running agricultural machine continuously and the machine does not have to mount batteries on it.

However, the utilization of the microwave power transmission technology still has potential challenges. One is the establishment of technology to transmit stable

electricity to a moving agricultural machine. Another one is effect of microwave power on human and plants in fields. These points should be carefully examined.

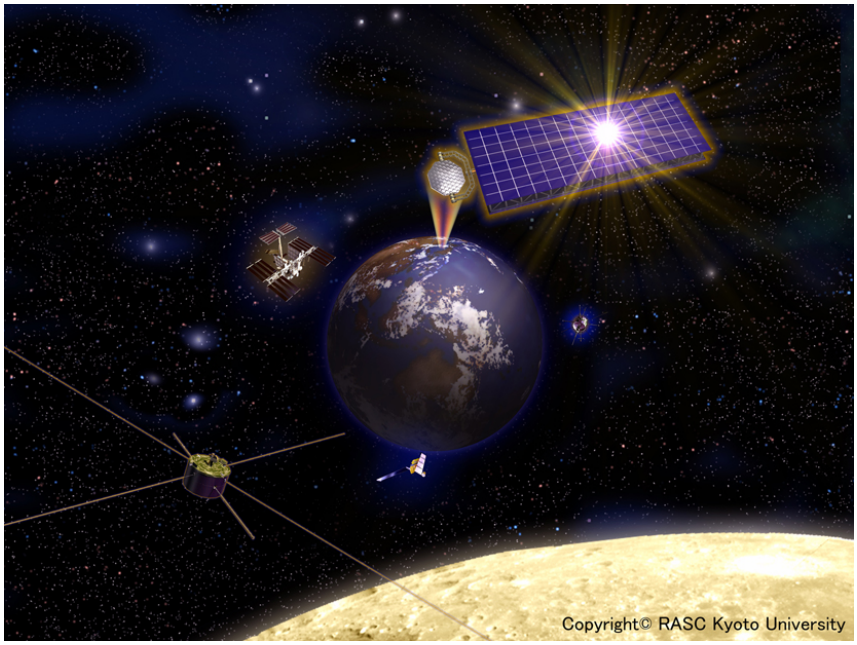


Fig. 1.3 Solar Power Satellite
(Research Institute for Sustainable Humanosphere, Kyoto University)

## 1.2 Objectives

The final objectives of the study are the development of a microwave-driven agricultural vehicle for electrification of agricultural machinery, coping with the environmental and energy issues. To achieve this goal, the investigation of the possibility of application of microwave-driven vehicles to agriculture should be conducted. In this study, followings were conducted to establish the technology of a microwave-driven agricultural vehicle.

(1) Fundamental experiments of transmitting microwave power to a running model vehicle mounting fixed receiving device (rectenna).
(2) Enhancement of efficiency of power transmission by utilizing a transmitting parabolic antenna and rotating rectenna panel on the vehicle.
(3) Improvement of the model vehicle by down-sizing the vehicle and revision of the

both transmitting and receiving system.

(4) Examination of effects of microwave on plants. To determine the effects on outer figure on plants, experiments of long-term exposure of microwave at certain intensity levels in strictly controlled environment was conducted. In this study, effects of long-term exposure of 2.45 GHz microwave on growth of *Spinacia oleracea* in soil under controlled environments of growth chamber were examined, which were not conducted in our previous study. Growth measurement of leaf area and weight was conducted to determine the existence of the effects.

The objectives of this study are examination of applicability of microwave-driven agricultural machinery and the reviewing of effects of microwave on crops in fields where this microwave-driven agricultural machinery is utilized.

[Reference]

Oida, A. 2006. Electric Drive of Agricultural Machinery by Microwave Power Transmission in the Air, Final Report on Research Project (No. 14360149) under Grant-in-Aid for Scientific Research (B) for 2002 to 2005 from the Ministry of Education, Culture, Sports, Science and Technology, Japan.

Scheer H. 2000. Solar energy era. Zeitshrift Deutschland, Germany; 2000;5:46–9 [in Japanese].

# 2. Microwave Power transmission and Its History

Before explaining the details of this study, in this chapter, a brief history of microwave power transmission (MPT) is described to give a better idea of the background of this study. The history of MPT goes back to the 19th century, when the existence of electromagnetic waves and its propagation in free space were proved.

## 2.1 The Early Experiments of Radio Wave Power Transmission

Heinrich Hertz (1857-1894) demonstrated electromagnetic wave propagation in free space and, in his experiments, he used parabolic reflectors at both ends of transmitting and receiving system (Brown 1984). Brown mentioned that Hertz's experiments resembled present practice more than Tesla's work (Brown, 1984).

Maybe the most famous experiments of radio wave power transmission were gigantic ones conducted by Nicola Tesla (1856-1943). In Colorado in 1899, Tesla built a gigantic coil connected to 200-ft height mast with a 3-ft-diameter copper ball at the top. This coil resonated at 150 kHz, which is relatively low frequency compared to microwaves. 300 KW of electricity was fed to the coil and the RF potential produced on the sphere reached 100 MV. However, in Tesla's experiments, no clear records of the amount of transmitted and received power was existed (Brown, 1984, Matsumoto, 2002).

In the early 1930's, H. V. Noble of the Westinghouse Laboratory conducted wireless power transmission experiments using 100 MHz dipoles for transmitting and receiving located about 25 ft from each other. Several hundred watts of power were transferred between the both dipoles (Brown, 1984).

During the World War II, related technologies such as antennas and microwave generators was developed and progressed. However, no greater interest in MPT was appeared until after a decade from the end of the World War II.

## 2.2 Microwave Power Transmission and Solar-Power Satellite (SPS)

W. C. Brown et al. conducted experiments of microwave-driven helicopter in 1964 at Raytheon's Spencer Laboratory. String type rectenna were installed on the helicopter. The flight height was constrained to a few inches. However, this was the first flight of a heavier-than-air object powered by microwave beam.

In 1968, Dr. Peter Glaser of the Arthur D. Little Company proposed the concept of the solar-power satellite (SPS). In his SPS concept, the solar energy was converted into electricity in satellites on geosynchronous orbit. This electricity was transformed into microwave power and beamed to receiving facilities on Earth. The received microwave power is converted into electric power and utilized (Glaser, 1968).

After the Glaser's SPS concept, the Jet Propulsion Laboratory (JPL) conducted experiments of microwave transmission in 1975. They obtained 30 kW from the distance of one mile with a ratio of DC output to incident microwave power of 0.84 (Brown, 1984).

In 1977, Project that was identified as DOE/NASA Satellite Power System Concept Development and Evaluation Program was initiated. This program contained a lot of related detailed studies and completed in 1980. Its concept described large-scale power infrastructures in space including about 60 solar-power satellites. One SPS delivers 5 GW of electricity and total delivered power is designed as 300 GW according to the concept.

## 2.3 SPS in Japan

Also in Japan, feasibility studies of SPS were conducted. The New Energy and Industrial Technology Development Organization (NEDO). According to the NEDO's estimation, costs for generating one million kW using SPS would be 23 Yen per 1 kWh. This was estimated under conditions of 30 years of SPS's economic life, construction cost of 2.4 trillion Yen, annual interest of 6%, annual maintenance and repair cost of 1% of the construction cost, utilization rate of 98.4%.

On the other hands, the Japan Aerospace Exploration Agency (JAXA) estimated 8.9 Yen per 1 kWh with the same size of SPS as NEDO.

Institutes and universities in Japan now conducting researches for SPS and some plans were presented. Institute of Humanosphere, Kyoto University is one of the research centers of SPS in Japan and the study of this thesis was conducted in corporation with researchers in that institute.

## 2.4 MPT to Moving Objects

Experiments of microwave-driven airplanes were conducted in Canada and Japan. In 1987, Schlesak et al. conducted experiments of prototype of microwave-driven airplane

named SHARP (Stationary High Altitude Relay Platform). The prototype was 1/8-scale SHARP airplane with 4.5m wingspan. 10 kW of 2.45 MHz microwave power was transmitted to the airplane at the altitude of 150 m as 3.5 m diameter beam. The airplane flew for about 20 minutes and the power flux density was about 400 W/m$^2$. Dual-polarized rectennas were used to receive microwave without problems of depolarization (Schlesak, 1988).

In Japan, the Microwave Lifted Airplane Experiment (MILAX) was conducted in 1992. To install rectennas on the plane, a new lightweight rectenna was developed. Phased-array antenna was used as a transmitting antenna, which chased the flying airplane utilizing pattern recognition of the airplane and two CCD cameras (Matsumoto 2002).

Under the assumption of utilization of robot platform, Nagano *et al.* conducted experiments microwave-drive rover using 5.8 GHz 100 W microwave. A small model vehicle was placed on an arc shaped track and transmitting antenna was installed at the center position of the arc. As a transmitting antenna, active phased array system was used. This study will be mentioned again in later chapters as a comparison with our study.

Hiraoka et al. developed a small model airplane MAV (Micro Aerial Vehicle) driven by microwave power transmission for the Mars flight exploration (Hiraoka et al., 2012). They conducted tests of the airplane in an anechoic radio wave chamber and they confirmed the capability of flight of the MAV. Their study of utilizing this technology for planet exploration showed another possibility of application of the microwave power transmission to moving objects.

## 2.5 Study on Effects of Microwave on Plants

When utilizing the microwave power transmission technology in agricultural fields, effects of microwave on crops must be carefully examined. However, though study and reports of the effects of microwave on plants were easily found, study of the effects in MPT are not enough.

As a related study of SPS, Skiles conducted experiment of long-term 2.45 GHz microwave exposure (7 weeks) on alfalfa (*Medicago sativa*, L.). In his study, the intensities of microwave were 0.5-1.2 mW/cm$^2$. No significant differences of

chlorophyll content by SPAD measurement, fresh weight, and dry weight were observed (Skiles, 2006).

Jonas exposed relatively high amplitude (2.45 GHz, 600 W) of pulsed microwave with 16 and 60Hz pulses for short time to *Momosa pudica* L. The change of circadian response by measuring of petiolar folding and recovery was observed (Jonas, 1979). Jonas also exposed short-period pulsed microwave (600 W) to *Zea mays* L. and obtained the result that the maize seedlings were the most resistant when irradiated at sunrise and the least resistant at sunset (Jonas, 1983).

Shmutz *et al*. conducted experiments of exposure of 2.45 GHz with power flux density ranged from 0.007 to 300 W/m$^2$ microwave to young spruce and beech trees in field plots. The continuous exposure period was 3.5 years. No visual symptoms of damage were observed during the whole period. During the first 2 years, negative relationship between power flux density and foliar concentrations of calcium and sulfur in beech trees was found. However, in the third year these effects were not found (Shmutz *et al*., 1996).

[References]

Brown, W. C., 1984. The History of power Transmission by Radio Waves, IEEE Transaction on Microwave Theory and Techniques, Vol. MIT-32, No. 9 ,1230-1242.

Hiraoka, K., et al. 2012. Flight Capability Verification of a Micro Aerial Vehicle that is Propelled by Microwave Power Transmission, IEICE Technical Report WPT2011-33 (2012-03).

Glaser, P. E., 1968. Power from the Sun: Its Future, Science, Vol. 162, No. 3856, 857-861.

Jonas, H. 1979. Circadian Response to Microwaves by *Mimosa pudica* L. Z. Pflanzenphysiol., 91: 95-101.

Jonas, H., 1983. Responses of Maize Seedlings to Microwave Irradiations.

Environmental Pollution (Series B) 6: 207-219.

Matsumoto, H., 2002. Research on Solar power Satellites and Microwave Power Transmission in Japan, IEEE Microwave Magazine, Dec. 2002, 36-45.

McSpadden, J. O., 2002. Space Solar power Programs and Microwave Wireless Power Transmission Technology, IEEE Microwave Magazine, Dec. 2002, 46-57.

Nagano, K., et al. 2007. Microwave Power Transmission Experiment Report to the Robot for the Work, Technical Report of IEICE SPA2006-22.

Schlesak, J. J., A. Alden, T. Ohno, 1988. A microwave powered high altitude platform, IEEE MIT-S Digest Vol.1, 283-286.

Schmutz, P., et al. 1996. Long-term exposure of young spruce and beech trees to 2450-MHz microwave radiation. The Science of the Total Environment, 180: 43-48.

Skiles, J. W. 2006. Plant response to microwaves at 2.45 GHz. Acta Astronautica 58: 258–263.

# 3. Fundamental Experiments

## 3.1 Basic Concepts of the System

A small model of microwave-driven off-road vehicle with fixed receiving antennas (rectennas) was developed to confirm the transmission and reception of microwave power.

Fixed rectennas were mounted on the vehicle as quadratic panels, which faced to four directions to receive microwave power from all direction even when the vehicle moved to any directions.

In this system, the direction of transmitter antenna was controlled to direct the moving vehicle. The vehicle's path was controlled from out side PC with cables. Measured data were also sent to the loggers through the cables.

With this system, we examined the quantity of transmitted microwave power to the moving vehicle, along with the tracking performance of directional control of the transmitting system.

As an experimental field, running field of about 4 m x 4 m in an anechoic chamber was used. This field is relatively small compared with actual agricultural field size, however the size of the anechoic chamber was limited and the application of the system in greenhouses was assumed in this experiment.

## 3.2 Materials and Methods

### 3.2.1 Vehicle with Fixed Rectennas

1) Vehicle Platform

The dimension of the model vehicle was as follows:

Length 450 mm
Width 290 mm
Height without rectenna 230 mm
Mass 3.7 kg
Wheel base 330mm
Tread 280mm

This vehicle was developed with the base of Tamiya Mammoth Damp Truck model.

A 7.2W 24V DC driving motor (Japan Servo, DME37BB) and a steering servo motor (Futaba FP-S3003) were mounted on the vehicle. On this vehicle, quadratic Rectenna panels, microcomputer controller, and measuring devices were installed.

2) Quadratic Rectenna Panel

A rectifying antenna, also called a ‘‘rectenna,’’ was used as a microwave energy receiving device (Fig. 3.1). The rectenna receives microwave energy and converts it into DC power. The rectenna is generally composed of an antenna, input filter, rectifier, and an output filter. The antenna is a circular microstrip antenna with a diameter of 46 mm.

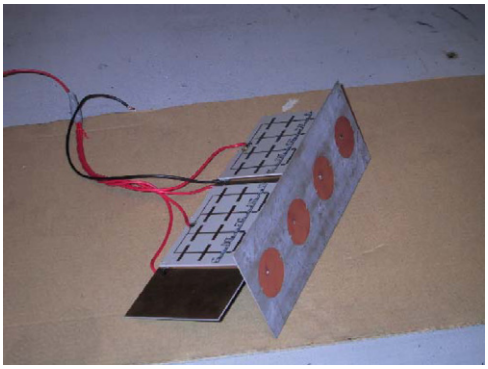

Fig. 3.1 Rectifying Antenna (Rectenna)

The distance between the centers of the two circular antennas is set at 0.6 times the microwave wavelength, i.e. 73.5 mm, to avoid interaction between the antennas. The rectifying circuit is constructed using microstrip lines, as shown in Fig. 3.2. The substrate of the circuit is made of glass-cross-Teflon with a specific permittivity of 2.21 and thickness of 1.6 mm. The microwave energy enters the circuit at point A, and the DC power is obtained between points B and the ground. Point C refers to a chip condenser, which prevents the backward flow of DC power to the antenna. Points D are silicon Schottky barrier diodes (1SS281). To achieve high-power output, a rectifying circuit with parallel units of three diodes in series was used in a 4-way power divider in the experiment. The output filter is composed of quarter-wavelength transmission lines (E1 and E2) and one-eighth-wavelength open stubs (F1 and F2). Microwave to DC energy conversion efficiency (RF–DC conversion efficiency) of the rectifying circuit varies depending on input power and load. For of this experiment, the rectenna was

designed to have an RF–DC conversion efficiency of 60%, an input power of 4–8 W, and a load of 50–60 W. The flow of microwave power conversion with rectenna is shown in Fig. 3.3.

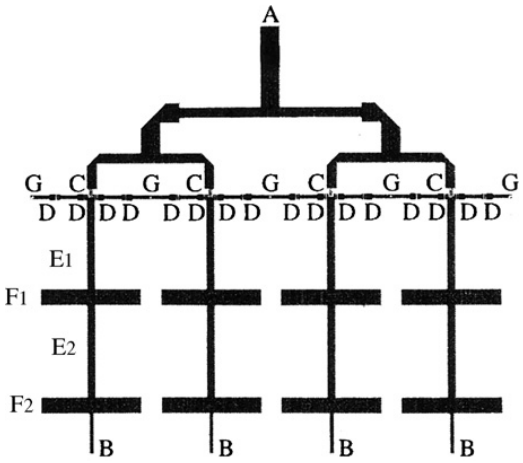


Fig. 3.2 Rectifing Circuit

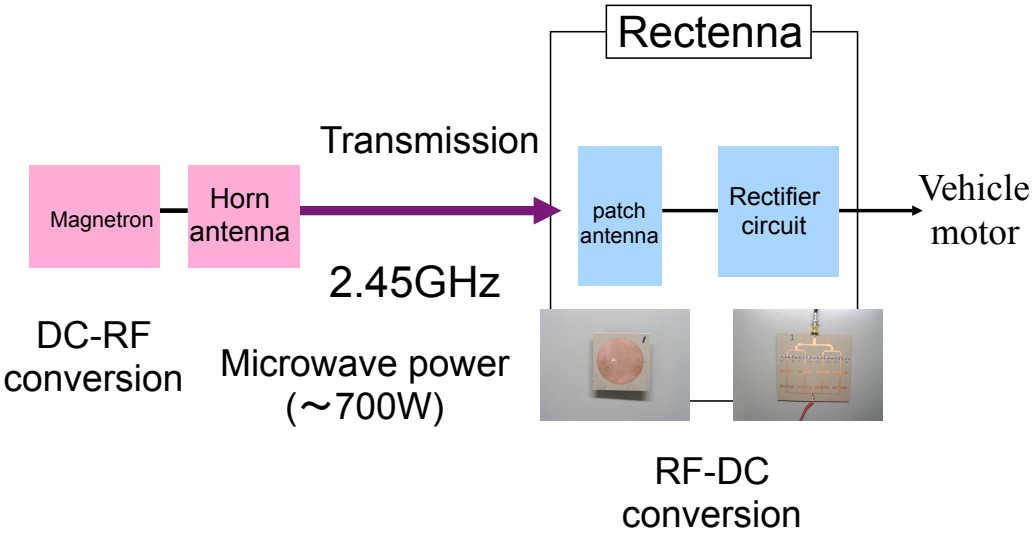


Fig. 3.3 Microwave Power Conversion

The vehicle had a four-sided quadratic rectenna, as shown in Fig. 3.4. Six circular microstrip antennas were attached to each side. The rectenna itself was fixed to the vehicle such that some circular microstrip antennas always face the microwave

transmitter. A small cylinder with stripes on the top of the rectenna is used as a marker for controlling the directions of two cameras and locating the position of the vehicle.

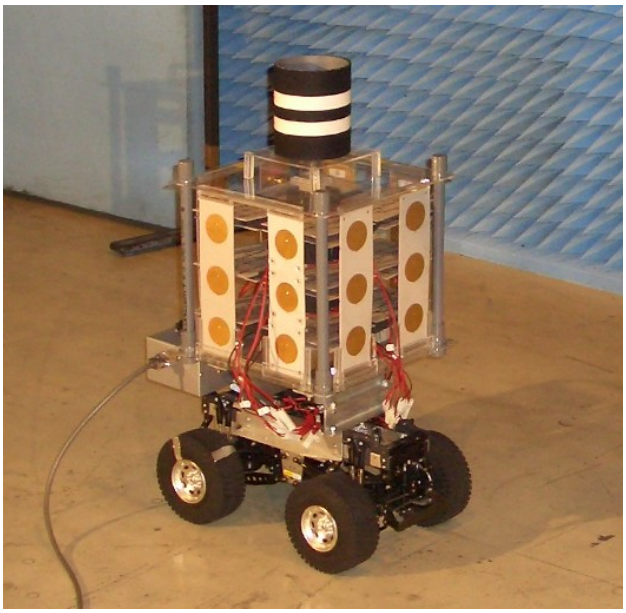

Fig.3.4 Model vehicle with 4-side quadratic rectenna

3) Microcomputer Controller

Fig. 3.5 shows the flows of electric power, control signals, and data signals. A PIC16F873A (Microchip) was used to control and measurement. The PIC computer controls the flows as given below.

(1) The PIC computer generates a 50 Hz control pulse, for the servo motor, to change the steering angle. Varying the pulse width from 1.3 to 1.7 ms according to a programmed running pattern causes either a straight run, a circular turn, or a U-turn.

(2) The computer monitors the voltages of the steering servo motor and driving motor and stops these motors when the voltages drop below their set values.

(3) When the driving motor stops, the computer switches power flow to a dummy load. The on–off switching of the driving motor and dummy load is done using a field effect transistor (FET) controlled through the PIC computer output port.

(4) The PIC computer receives vehicle steering commands from a personal computer (PC), i.e. an image processor, through a serial communication cable.

(5) First, the PIC computer measures the voltages of the two motors and the rotary encoder pulses of the driving motor. Next, the computer sends data to the PC by serial communication through a RS–232C interface.

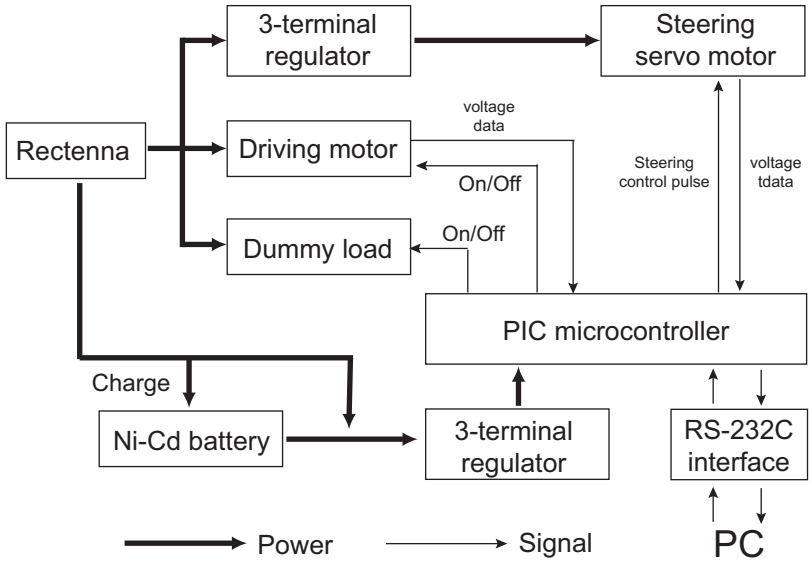


Fig. 3.5 Vehicle Control Unit

The driving motor and the steering motor were powered by the received microwave. A Ni–Cd battery was used as a stable power source for the PIC computer. Surplus power from the rectenna can be used to charge the battery.

The microcomputer controller unit was attached to the vehicle as shown in Fig. 3.6.

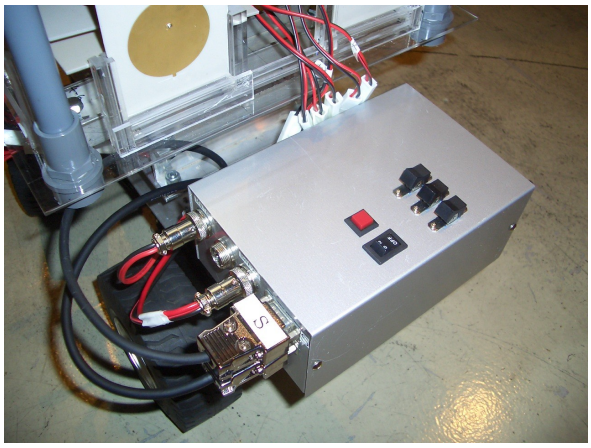

Fig. 3.6 Microcomputer Control Unit

### 3.2.2 Transmitting System

1) Turntable

To track the moving vehicle, the transmitting system was mounted on a turntable, which can direct to the vehicle. To locate the position of the vehicle, two cameras were used. One camera (camera 1) was mounted on the transmitting device and the other camera (camera 2) was installed on the rotating motor on a tripod. Fig. 3.7 shows the transmitting system to track the vehicle. Details of this marker detection were reported by Miyasaka et al. (2004).

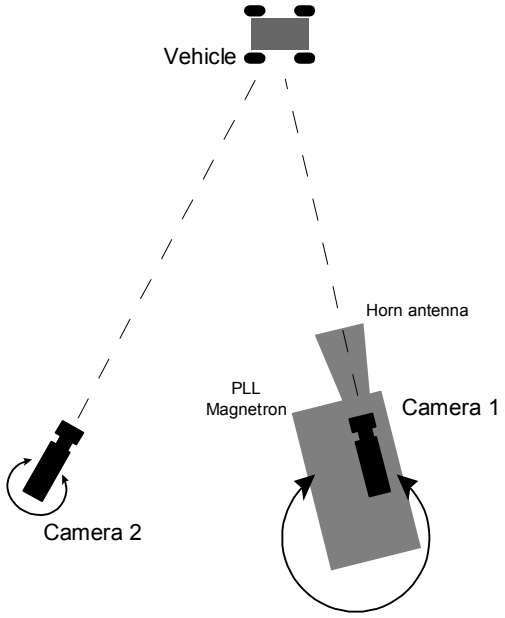


Fig. 3.7 Turntable and Camera System

The turntable was controlled by a PC through GPIB board and GPIB turntable controller. The PC calculates the vehicle position from acquired marker images from cameras and sends control commands to the turntable controller. The camera 1 rotates with the transmitter on the turntable. The camera 2 was rotated by a stepping motor on the tripod, which motor was controlled by the same PC through a motor controller and driver (Fig. 3.8).

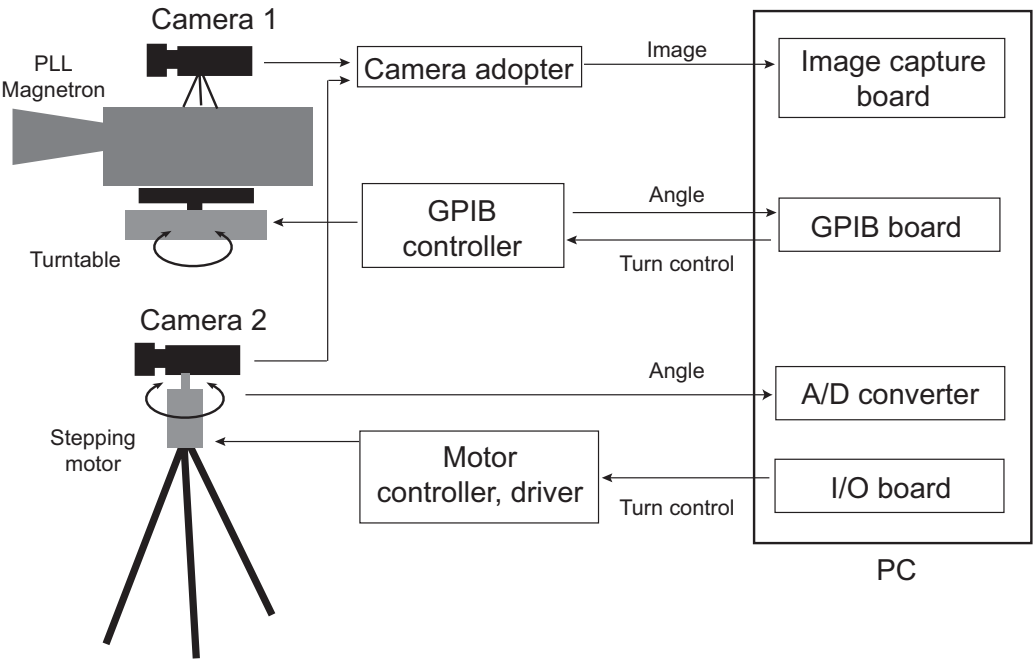


Fig. 3.8 Turntable and Camera Control by PC

2) Magnetron and Horn Antenna

A phase locked loop (PLL) magnetron (Tamaoki Electronics Co. Ltd.) was used to generate a microwave of a certain frequency, for instance at 2.45 GHz, with negligible side robe. A horn or a parabolic antenna was used to discharge the microwaves generated in the magnetron. Fig. 3.9 shows a horn antenna attached to a PLL magnetron.

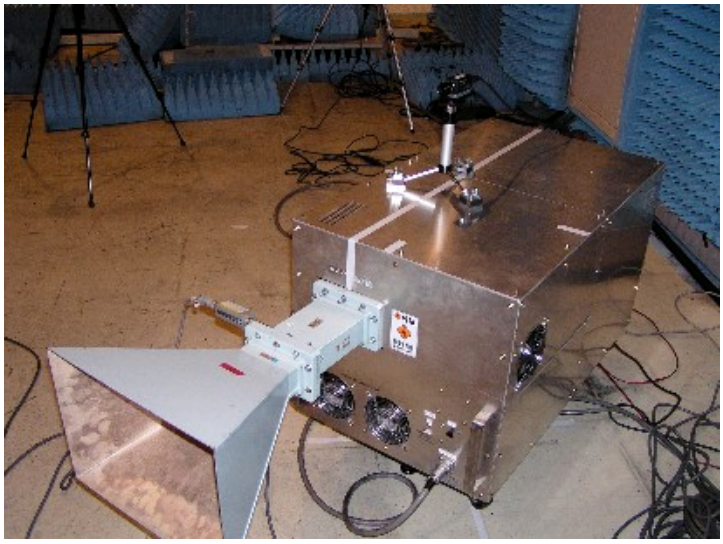

Fig. 3.9 PLL Magnetron with a Horn Antenna

This microwave transmitter was used to drive the model vehicle, which is explained later. The maximum output power was about 900 W from the PLL magnetron. The Magnetron and the horn antenna mounted on the turntable, along with the two cameras, are shown in Fig. 3.10.

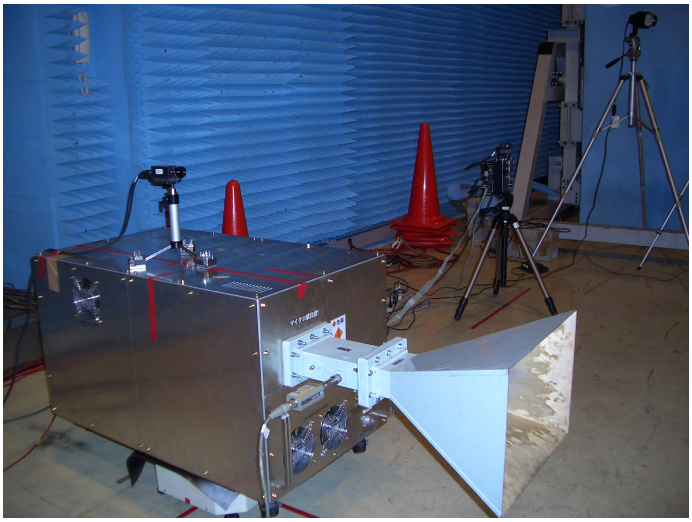

Fig. 3.10 Transmitting System (Magnetron, Horn Antenna, Turntable, and Cameras)

### 3.2.3 Measurement System

The following items were measured by a data logger through the cable from the vehicle.

(1) Driving motor voltage
(2) Driving motor current
(3) Steering servo motor voltage
(4) Steering servo motor current
(5) Steering servo motor control pulse
(6) Rotary encoder pulse of driving motor
(7) Magnetron power output from power sensor and power meter
(8) Rotation angle of camera 1 and camera 2
(9) Control commands sent to turntable and steering servo motor

Currents were measured as voltages of shunt resistor inserted in the motor driving line. In addition to the items above, the followings were also measured by A/D converter of the microcomputer in the control unit and the measured data were sent to the PC through the RS-232C wire as digital data.

(10) Driving motor voltage
(11) Steering servo motor voltage
(12) Pulse per second of rotary encoder of driving motor

Fig. 3.11 shows the measurement system of this experiment.

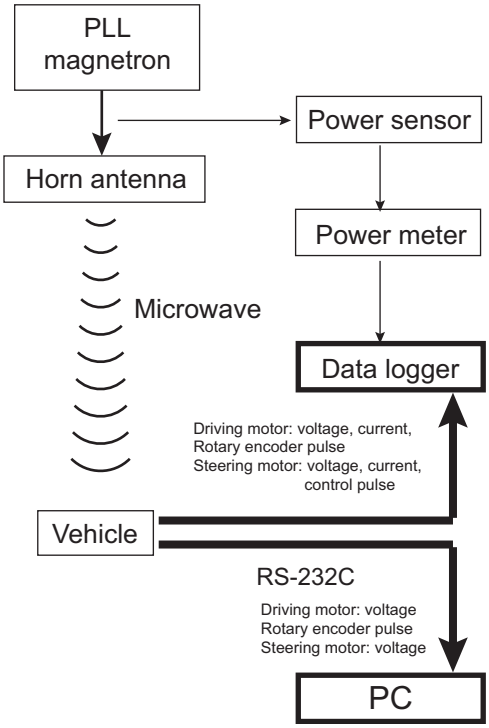


Fig. 3.11 Measurement System

## 3.3 Experiment

### 3.3.1 Experiment Field in Anechoic Chamber

The Experiments were conducted in a radio wave anechoic chamber of the Microwave Energy Transmission Laboratory (METLAB) at the Research Institute for Sustainable Humanosphere, Kyoto University. The system was installed in an anechoic chamber except measurement equipment and data were monitored in the measurement room next to the chamber.

### 3.3.2 Output Power of Microwave

The output power of the magnetron was set to about 700 W. This output power can be fluctuated. Thus, the output power was monitored and recorded by the power sensor, the power meter, and the data logger, which were mentioned above.

### 3.3.3 Measured Items

The measured items were described in the section 3.2.3 "Measurement System". In

addition to those items, vehicle stripe marker was detected from images by the two cameras and the vehicle position was estimated by the image processing and the angles of the cameras.

### 3.3.4 Path Settings

The following three paths were programmed in the microcomputer controller installed in the vehicle. These paths were set to examine the vehicle control response, tracking ability, and transmitted power to the vehicle.

#### 1) Straight Line Path

The straight line path experiment was conducted to observe the most simple vehicle running, along with the tracking performance and power transmission. The path was set as shown in Fig. 3.12. This straight line was programmed in the microcomputer on the vehicle. The vehicle controller tried to keep the straight path by controlling the steering servomotor on the vehicle.

The minimum distance between the vehicle and the center of the rotation of the transmitter was set at 4 m. The length of the running path was set to 3.6 m.

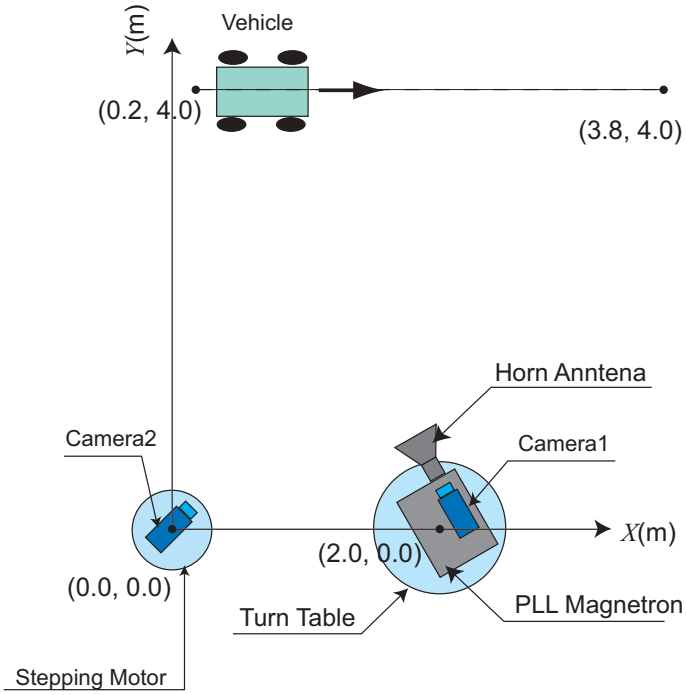


Fig. 3.12 Straight Line Path

2) Circular Path

The circular path was programmed as shown in Fig. 3.13. This rotation of the vehicle as obtained by keeping the constant steering angle by the servomotor controlled by the microcontroller on the vehicle. This path was programmed to examine the tracking ability of the transmitter when the vehicle steers, along with the control of the turning of the vehicle.

The radius of the circle was set to 1.2 m and the distance between the center of the circle and the center of the rotation of the transmitter was set to 3.2 m.

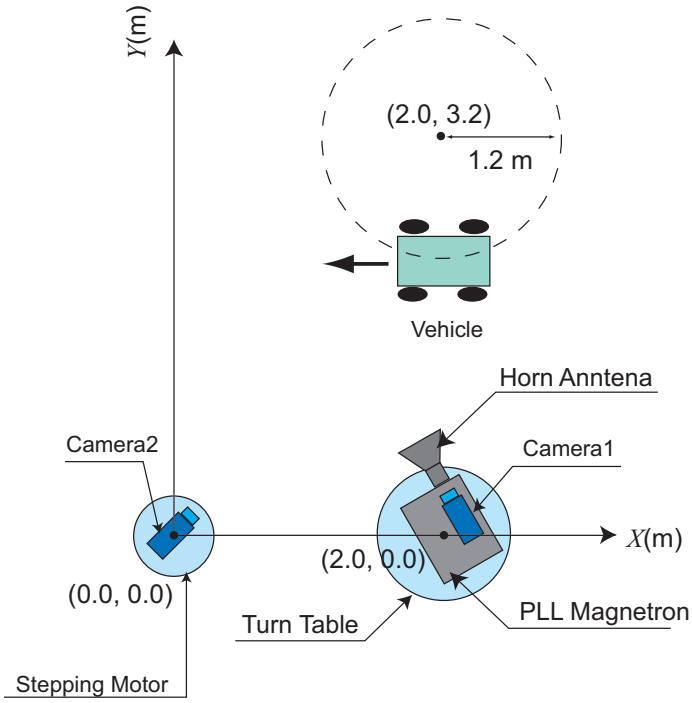


Fig. 3.13 Circular Path

3) U-Turn Path

The U-turn path was programmed as shown in Fig. 3.14. In this experiment vehicle used the position information of itself provided from the outside PC which calculates the position of the vehicle from the camera images and image processing.

First the vehicle ran in the straight path. When the vehicle approached the right end of the experimental field, the vehicle steered left at $x$ = 2.5 m. After turning, when the vehicle reaches at $x$ = 2.5 m again, vehicle stopped the steering and took the straight line

again. This experiment was conducted to examine the basic vehicle control by the position information from the outside PC.

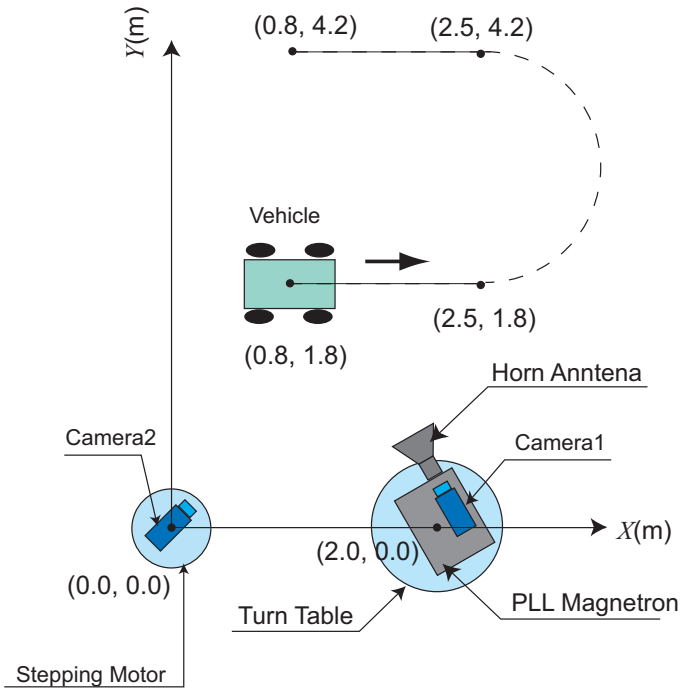


Fig. 3.14 U-Turn Path

## 3.4 Results

### 3.4.1 Path Setting and Actual Path

1) Straight Line Path

The detected path by image processing PC in the straight line experiment is shown in Fig. 3.15. The actual path was observed as slightly inclined straight line. The detected path showed the zigzag pattern and this pattern was not the actual movement of the vehicle.

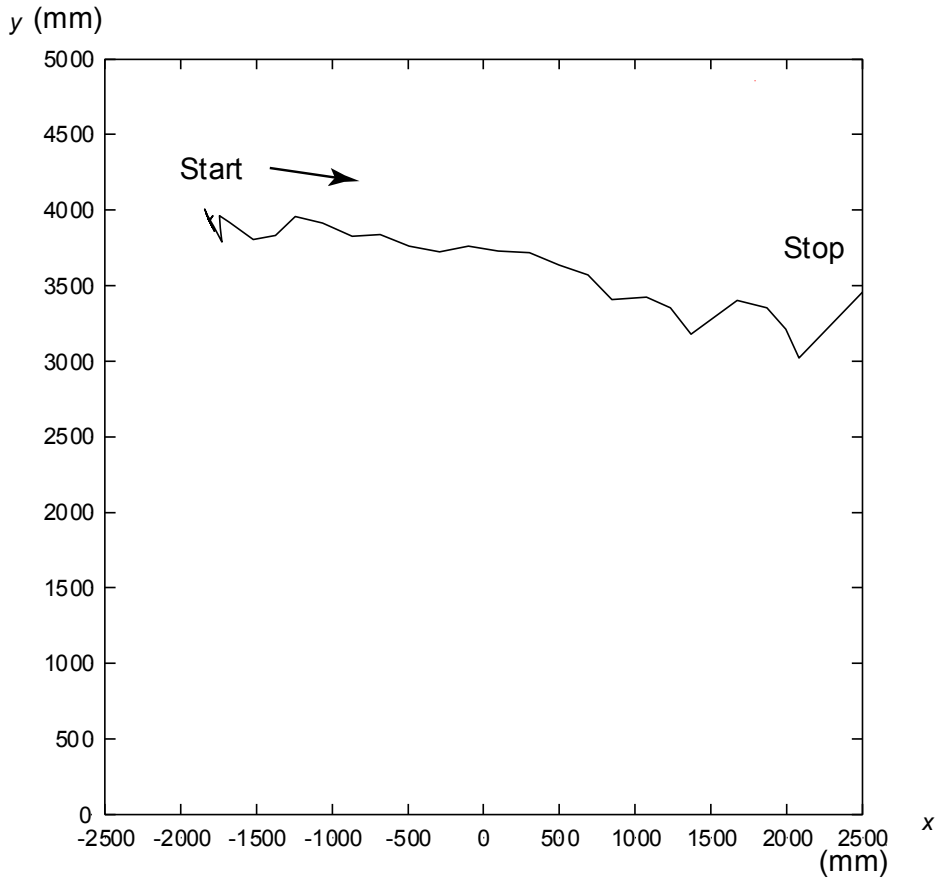


Fig. 3.15 Detected Path by Image Processing (Straight Line Path)

2) Circular Path

The detected circular path of the vehicle by image processing is shown in Fig. 3.16. This detected pattern showed almost circular shape. However, the zigzag pattern, which was not the actual movement, was also observed, as in the detected straight line path. These zigzag pattern was derived from the slow speed of the tracking ability and the image processing of the cameras and the PC as discussed in the Chapter 7.

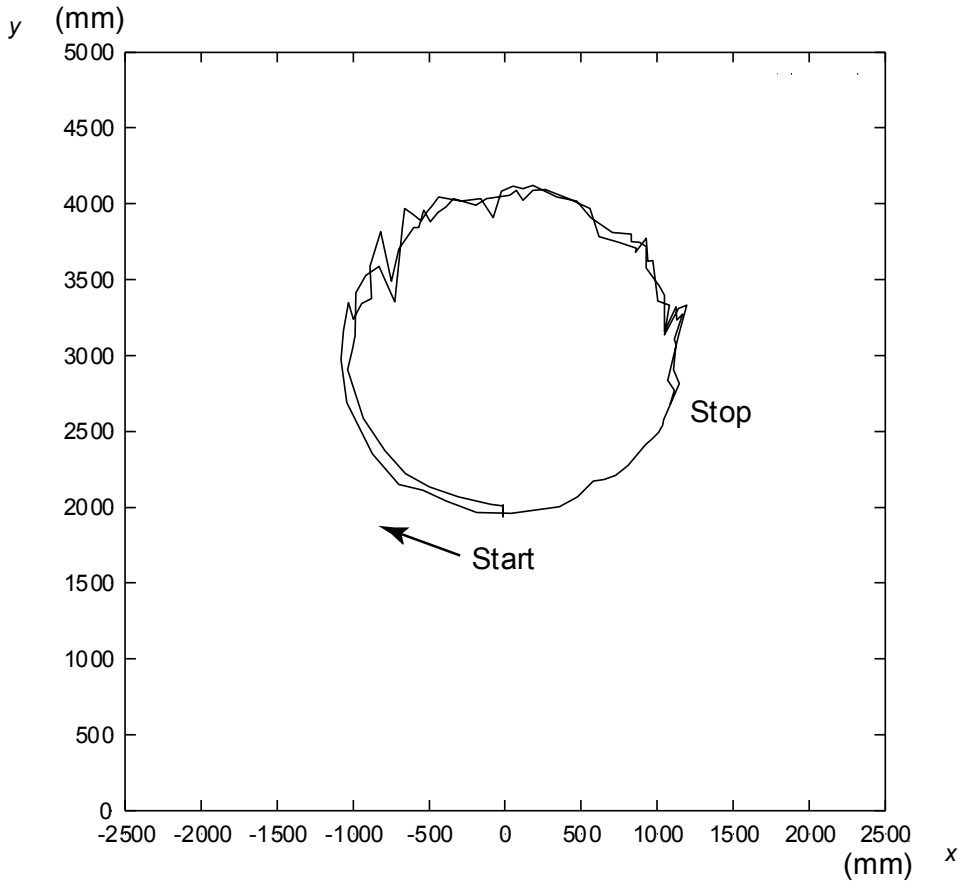


Fig. 3.16 Detected Path by Image Processing (Circular Path)

3) U-Turn Path

The detected U-turn path of the vehicle by image processing is shown in Fig. 3.17. In this experiment, the zigzag pattern was also shown. From this graph, the radius of turning was exceeded from programmed 1.2 m and the vehicle tried to recover the line at $y$ = 4.0 m after turning.

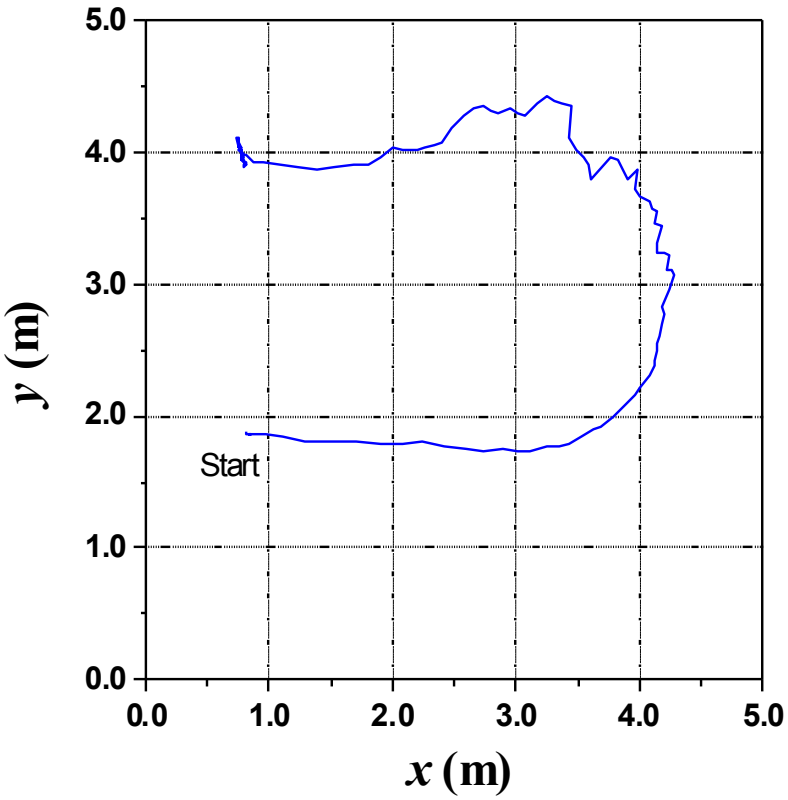


Fig. 3.17 Detected Path by Image Processing (U-Turn Path)

### 3.4.2 Power Consumption

1) Straight Line Path

The power consumption of the vehicle driving motor is shown in Fig. 3.18. The output power from the magnetron and the horn antenna is also shown in the same graph. The output power was about 700 W and the power consumption of the driving motor was about 5 W. The efficiency of the power transmission was less than 1%. However, from this graph, the tracking itself was successfully controlled.

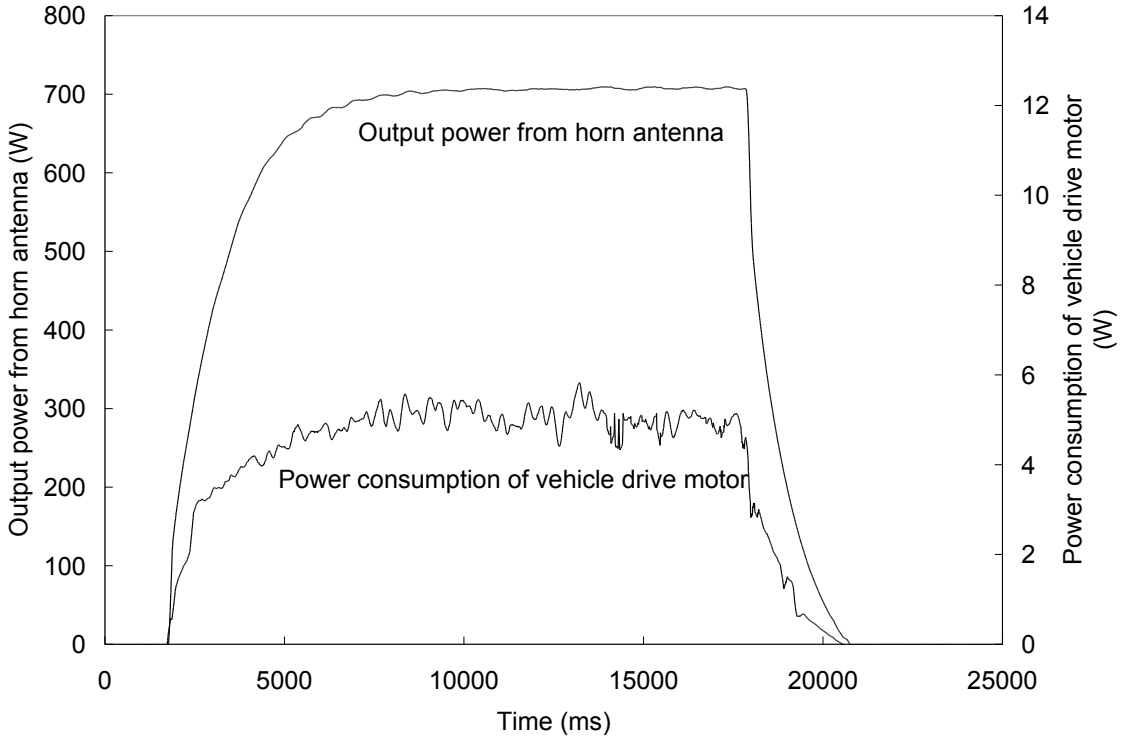


Fig. 3.18 Power Consumption of the Vehicle Driving Motor (Straight Line Path)

2) Circular Path

The power consumption of the vehicle driving motor and steering servomotor is shown in Fig. 3.19. The output power from the magnetron and the horn antenna is also shown in the same graph. The output power was about 700 W and the power consumption of the driving motor was changed according to the position of the vehicle. The quadratic rectenna panel was fixed on the vehicle, and when a corner of the quadratic panel faces to the horn antenna, the received power decreased. On the other hand, when a panel faced to the horn antenna, the received power increased. The

efficiency of the power transmission was less than 2%. However, from this graph, the tracking itself was successfully controlled.

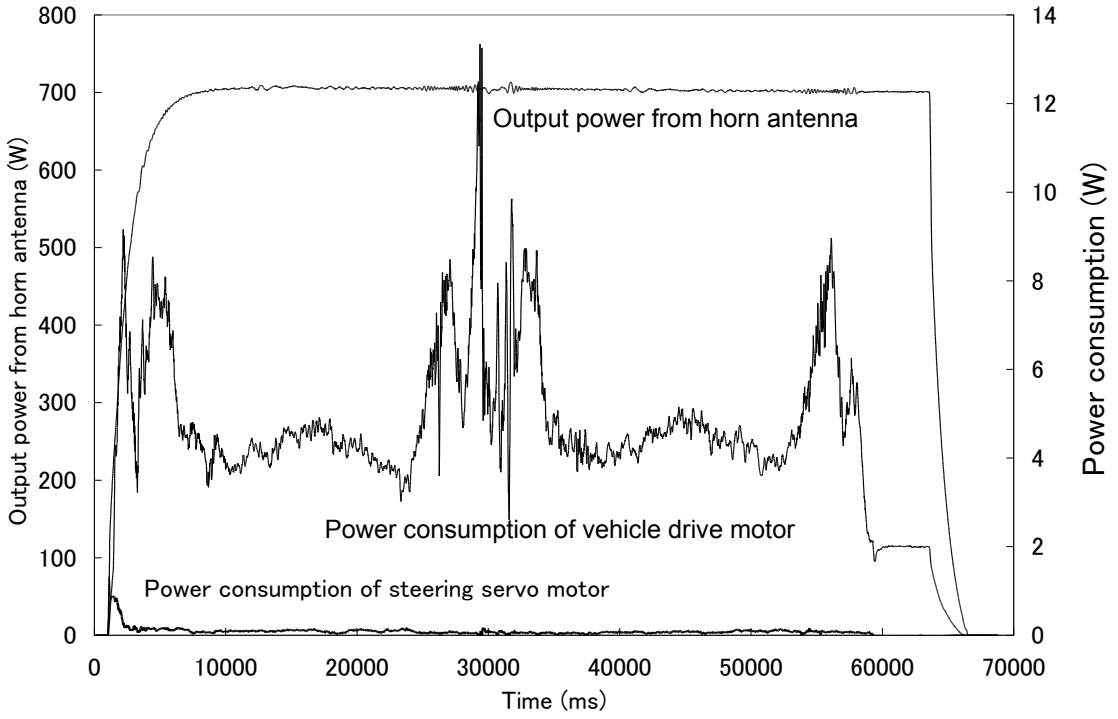


Fig. 3.19 Power Consumption of the Vehicle Driving Motor and Steering Motor (Circular Path)

3) U-Turn Path

The power consumption of the vehicle driving motor and steering servomotor is shown in Fig. 3.20. The output power was the same with the experiment of straight line path and circular path (about 700 W) and the power consumption of the driving motor was changed according to the position of the vehicle. The quadratic rectenna panel was fixed on the vehicle, and when a corner of the quadratic panel faces to the horn antenna, the received power decreased. Other than that occasion, the power consumption fluctuated largely compared to the cases of the straight line path and the circular path.

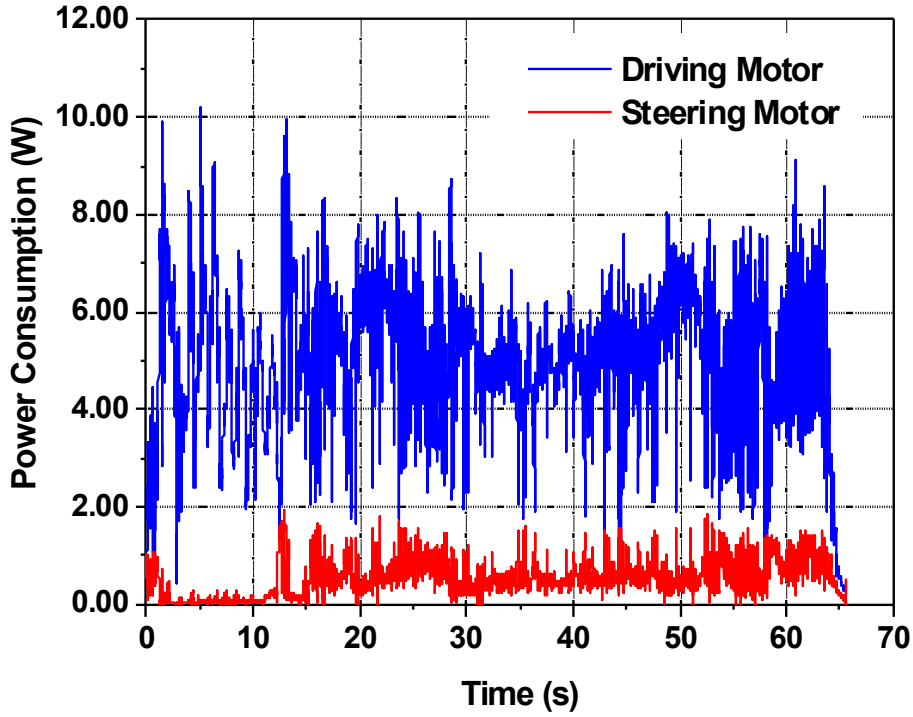


Fig. 3.20 Power Consumption of the Vehicle Driving Motor and Steering Motor (U-Turn Path)

## 3.5 Discussion

### 3.5.1 Tracking

From the results, considering the spread of microwave beam, the tracking of the transmission system to the vehicle was adequate. From the estimated paths of the vehicle, the following possible problems must be considered.

1) Precision of the position detection

From the estimated paths, zigzag patterns were obtained. However, the vehicle actually did not run on these kinds of zigzag path. These zigzag results were derived from the slow speed of image processing of the vehicle marker from the camera images. To enhance the precision of the position detection, faster speed of image processing is required. Considering the higher speed of the vehicle and faster movement of the marker in the acquired images especially when the distance between the cameras and

the vehicle is smaller, quicker response of the image processing is needed.

Nagano *et al.* reported a similar experiment using a small vehicle and different microwave frequency (Nagano *et al*., 2007). In Nagano's report, a smaller vehicle ran only along the arc shaped track and the transmitting antenna was installed at the center position of the arc. In there system, the distance between the transmitter and the receiving antenna was fixed and the size of the target on camera images was considered to be almost constant, because the vehicle runs on the arc track and the rectenna was always directed to the center of the arc, i.e. the position where the transmitting antenna was installed. In these conditions, they obtained quicker response. However, compared to our system, the movement of the vehicle was restricted.

Introducing the faster computer and higher resolution of the cameras are required to improve the performance of the vehicle position detection.

2) Response (Rotation speed)

Rotation speed of the turntable of transmitting antenna is also an important factor to obtain quicker tracking of the vehicle. Also, the rotation speed of the cameras restricted the tracking speed of the system, because the rotation speed limited the image acquisition and reduced the image processing speed.

Compared to Nagano's system mentioned above, our system required two cameras, because the vehicle can run freely in the field, while in Nagano's system, the vehicle path was fixed on the arc. They used commercial system of position detection and turntable. By using these equipment, they obtained higher rotation speed of the transmitting antenna.

### 3.5.2 Transmission Efficiency

From the experiments, obtained efficiency of power transmission was very low. The reasons for the low efficiency were as follows:

1) Spread of microwave from the horn antenna

By using a horn antenna, microwave beam from the horn was spread and power density of microwave at vehicle position became very low.

Introducing other types of transmitting antenna must be considered. In Nagano's

experiments mentioned above, transmitting array antenna panel was used. This panel consisted 32 patch antenna and phase of the microwave was controlled. In addition to that, in their experiment the distance was shorter than our experiments.

Introduction of a parabolic antenna was considered from these result for the next improvement of the system.

2) Fixed rectennas

The rectenna panels were fixed on the vehicle and was not directed to the transmitting antenna. This restriction reduced the efficiency of power transmission. In Nagano's experiment, the rectenna panel was also fixed on the vehicle. However, by running on the fixed arc path, the rectenna paned was always directed to the transmitting antenna automatically. This enhanced their efficiency of power transmittion.

In the next step, rotatable rectenna panel on the vehicle was designed to improve the efficiency.

3) Smaller number of the rectenna patch antennas

Number of the patch antenna was not adequate, considering the possible distance between the transmitting antenna and the vehicle. However, more rectennas on the vehicle increase the heavier weight of the vehicle. The required number of the rectenna must be carefully considered.

[Reference]

Miyasaka, J., et al. 2004. Study on Mobility of Microwave-Driven Agricultural Vehicle – Orientation Control of Power Transmitter Using Image processing –. Technical Report of IEICE: SPS2003-14, 21-28.

Nagano, K., et al. 2007. Microwave Power Transmission Experiment Report to the Robot for the Work, Technical Report of IEICE SPA2006-22.

# 4. Transmitting System with Parabolic Antenna

## 4.1 Improvement of the System

As shown in the previous Chapter 3, microwave power transmission to drive the small model vehicle was confirmed and the running of the vehicle on the straight path, the circular path, and the U-turn path was experimented. However, the following conditions restricted the efficient power transmission and the obtained efficiency was very low value.

(1) Number of the rectenna was little.
(2) Rectenna panel was fixed.
(3) Dispersion of microwave from the horn antenna cannot be ignored.

To solve the problems above, the following improvements were tested.

(1') Larger rectenna panel and a vehicle
(2') Rotating and elevating rectenna panel
(3') Applying a parabolic antenna for transmission

### 4.1.1 Transmitting System with Parabolic Antenna

1) Microwave Power Transmission System

The microwave power to the vehicle is generated by a magnetron (TE01-884-KT800; Tamaoki Electronics Co., Ltd.). In our previous system (Miyasaka et al. 2005, Oida et al. 2004), microwaves were radiated from a horn antenna installed in the front of the magnetron. To reduce microwave radiation diffusion, a parabolic antenna was introduced into our new transmission system. The magnetron and the parabolic antenna were installed on a frame mount on a turntable. A new larger turntable was introduced to accommodate a heavy transmitter on it. The turntable diameter, which is 2 m, is controlled by the GP-IB interface with a PC. To direct the transmitted microwave power to the running vehicle, the turntable rotation angle is controlled by the PC. The height of vehicle rectennas and that of the parabolic antenna differed. The depression angle must be changed according to the vehicle distance. To

increase transmission efficiency, the depression angle of the frame mount can also be controlled. This depression angle is changed using a stepping motor mounted on the frame. Two rotary potentiometers were attached to the turntable and the frame mount to detect each angle. Fig. 4.1 presents a photograph of the transmitting system.

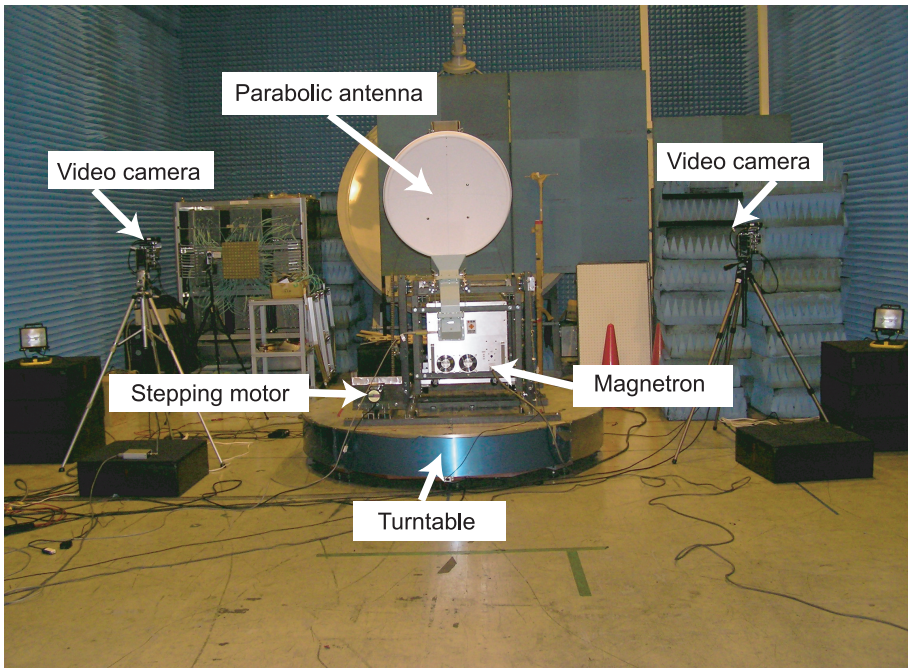


Fig. 4.1 Microwave Transmission System

2) Vehicle Position Detection

Two monochrome CCD cameras (XC-55; Sony Corp.) mounted on stepper motors (ASM46A22; Oriental Motor Co. Ltd.) were used to capture images of the cylindrical stripe marker mounted on the experimental vehicle. An image capture board (FDM-PCI; Photron Ltd.) was used to acquire the marker images to the PC. Rotation of the two cameras is controlled by the PC through a digital I/O board, motor controllers (XG9200T-G; Oriental Motor Co. Ltd.) and motor drivers (ASD13A-A; Oriental Motor Co. Ltd.). The actual rotation angles are measured by rotary potentiometers, the voltage signals of which are acquired by the PC through a 12-bit 16-ch PCI-bus A/D converter card (PCI-3153; Interface Corp.).

### 4.1.2 Development of New Vehicle

1) Platform

The microwave-driven vehicle was built as a model of a small type seeder. A driving motor (24 V rated voltage, 26 W rated output, DME-60B8HPB; Nidec Servo Corp.) is equipped to the vehicle. A rotary encoder is attached to the drive shaft to measure the vehicle speed. For steering, a DC motor (24 V rated voltage, 14.8 W rated output, DME-44B8HPB; Nidec Servo Corp.) was used. The actual steering angle was measured using a rotary potentiometer attached to the steering motor shaft. Fig.4.2 shows the photos of the experimental vehicle.

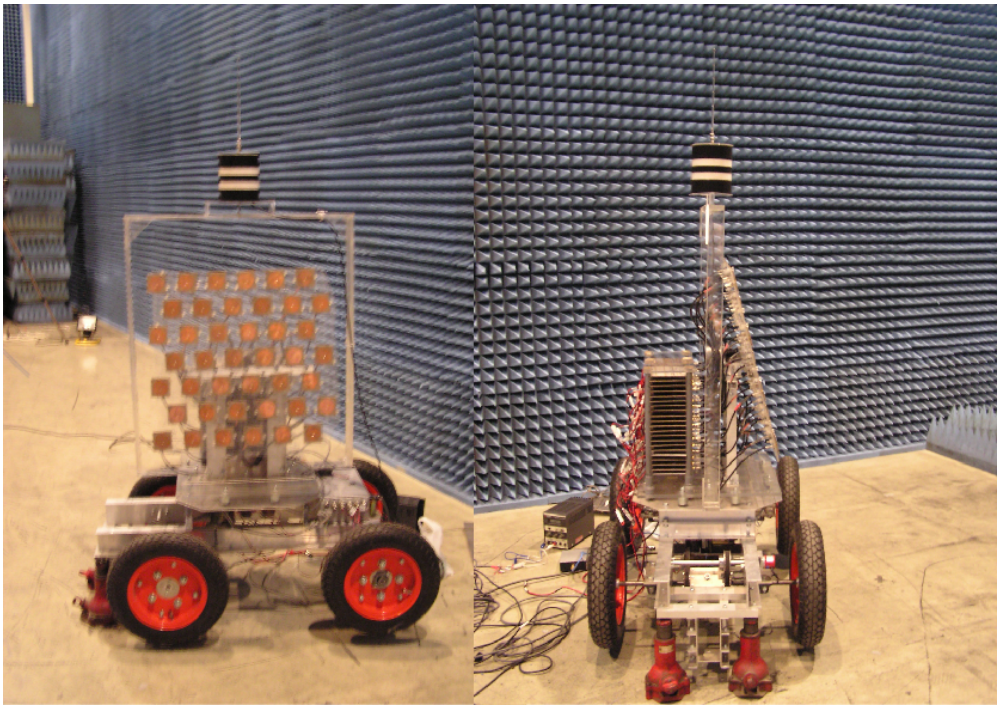

Fig. 4.2 Experimental Vehicle

2) Rectenna Panel with Control of Direction and Angle of Elevation

A rectenna panel was installed on the vehicle. This rectenna panel, placed on a turntable, can be turned to the transmitting parabolic antenna, whereas the second model had four-sided fixed rectenna panels with 24 patch antennas. Compared to our previous model, the mass, size, and power consumption of the new vehicle were greater. To increase the power supply to the vehicle, 42 rectennas were placed (Fig. 4.3). As shown in Fig. 4.3, each rectenna was assigned to drive the driving motor, the steering motor, the rectenna turntable motor, and the rectenna elevation motor. These rectennas receive microwave power and convert it into DC electricity. The turntable is rotated using a DC motor (24 V rated voltage, 14.8 W rated output, DME-44B8HPB; Nidec Servo Corp.). The depression angle of the rectenna panel is also changed using a stepping motor.

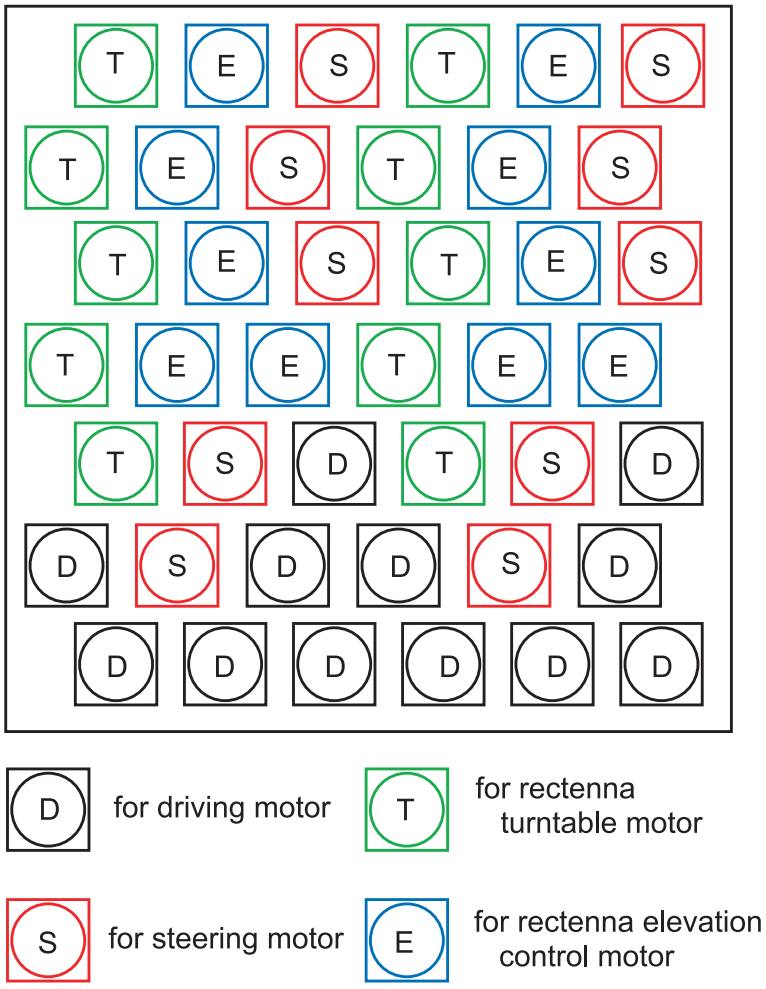


Fig. 4.3 Placement of the Rectennas on the Panel

3) Microcomputer Controller and Wired Communication

The vehicle is controlled by a microcomputer circuit with three PIC microcontrollers (PIC16F876A). Fig. 4.4 shows the diagram of the vehicle controller. The control circuit was powered by Ni-Cd batteries. With two additional motors from the second model, four motors were installed. To control these four motors, three microcontrollers were introduced, whereas the second model had only one microcontroller. The rotary encoder signal and rotary potentiometer signal are sent to this controller. A piezoelectric gyro sensor is connected to a PIC microcontroller. This control circuit is connected to the outside PC through RS-232C cable. Through this wire, the controller receives control commands from the PC and sends data of vehicle state to the PC. A black–white stripe marker was placed on the top of the vehicle. The position-detection system finds this stripe pattern on the CCD camera images.

Fig. 4.5 depicts the total diagram of the transmitting system, the controlling/ measurement PC, and the vehicle controller.

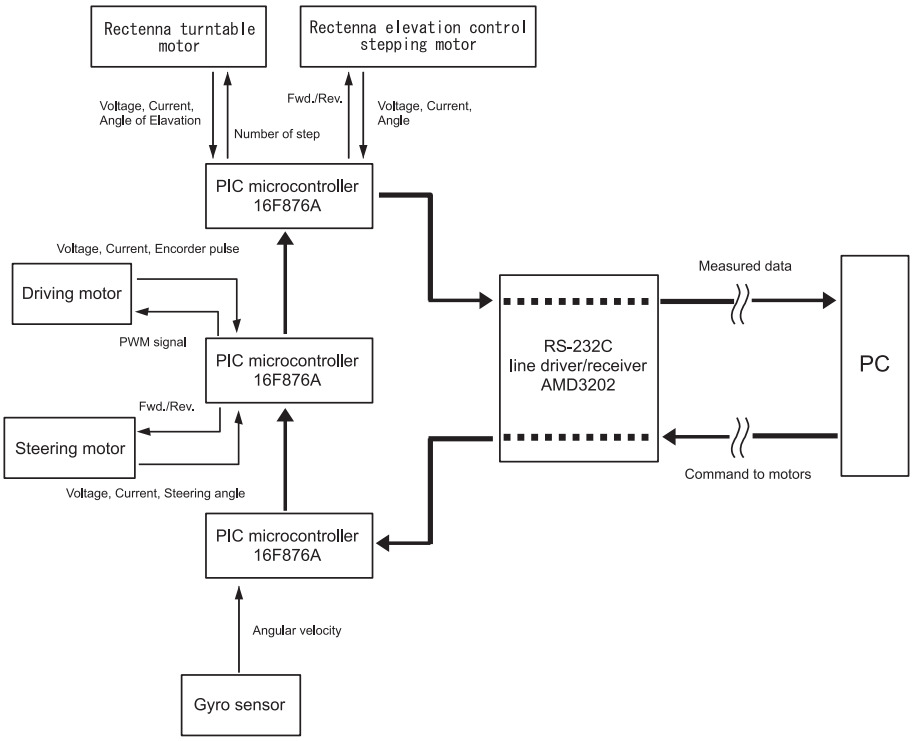


Fig. 4.4 Block Diagram of Vehicle Controller

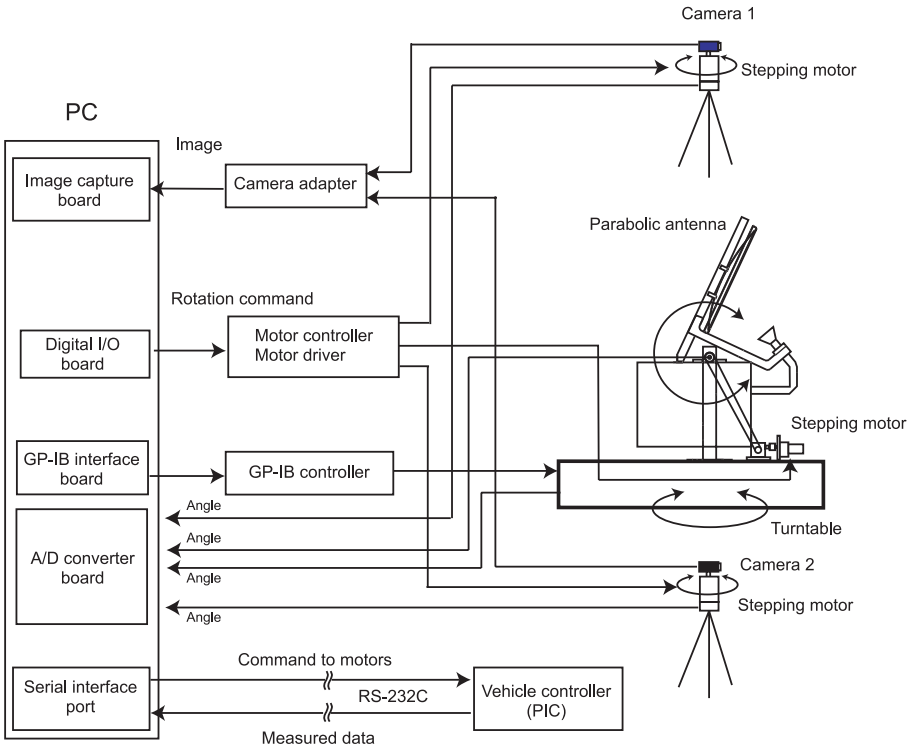


Fig. 4.5 Diagram of the Total System

## 4.2 Experiments

### 4.2.1 Experiment Field in Anechoic Chamber

The experiment was conducted during 1–5 Feb. 2006 at METLAB, the Research Institute for Sustainable Humanosphere, Kyoto University. The system was installed in an anechoic chamber. The magnetron output power was set to 800 W.

### 4.2.2 Characteristics of Microwave Power from Parabolic Antenna

Before the vehicle running experiment, the characteristics of the parabolic antenna was measured. A patch antenna was placed on an x-y positioner which were confronted to the parabolic antenna and the magnetron. Changing the position of the patch antenna, received power was measured at the distance of 1.83 m (near field) and 5.86 m (far field). The measured characteristics in case of 200 W output power is shown in Fig. 4.6.

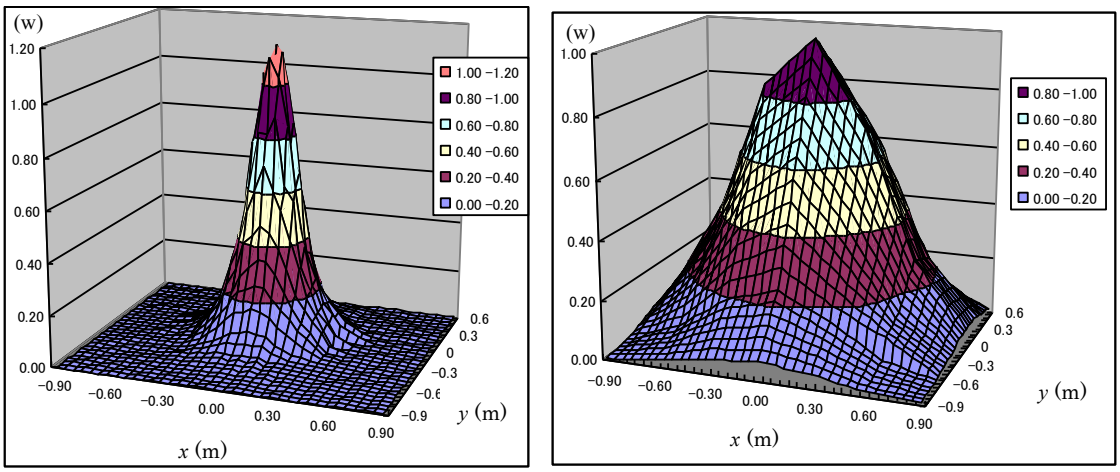


(a) Near Field (1.83 m) (b) Far Field (5.86 m)

Fig. 4.6 Microwave Power Distribution
of Received Power of Parabolic Antenna (Sasaki, 2005)

According to this measurement, expected receiving power of the rectenna panel on the vehicle which is faced directly to the parabolic antenna is approximately 62 W at 200 W output power, that shows the efficiency of 31 % in transmission. This was obtained by overlapping the rectenna placement (Fig. 4.3) on the parabolic antenna characteristics (Fig. 4.6), as shown in Fig. 4.7.

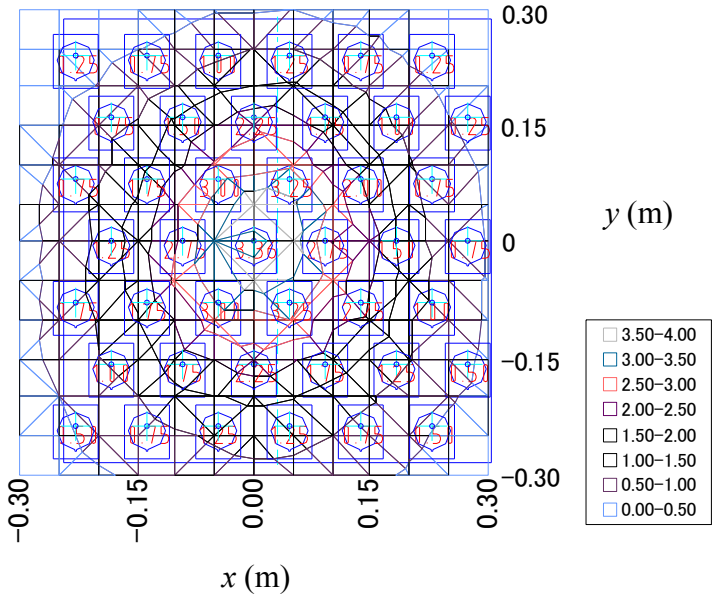


Fig. 4.7 Estimation of Receiving Power (Sasaki, 2005)

4.2.3 Vehicle Detection by Image Processing

The stripe marker on the image was detected using image processing by the PC. Template matching was used to find vertical stripe patterns. Templates of various lengths of stripe with one pixel width were prepared in the detection program. The program tests matching of templates on the acquired camera images, changing the length of stripe template and positions on the image. Details of this marker detection were reported by Miyasaka et al. (Miyasaka et al., 2004).

4.2.4 Orientation Control of Cameras and Transmitting Antenna

The CCD cameras are rotated to capture vehicle marker images. The camera rotation is controlled to capture the stripe pattern of the marker on the horizontal center of the image. However, the marker cannot always be on the center because of the response of this system. To calculate the vehicle position, the horizontal position of the marker on the image is used to compensate the rotation angles ($q_1$, $q_2$) of the cameras. The following equations were used to obtain the rotation angle of the turntable on which the transmitting antenna was installed.

$$x = 2 - 4 \times \sin(\pi - \theta_1) \times \cos\theta_2 / \sin(\theta_1 - \theta_2) \qquad (4.1)$$

$$y = 4 \times \sin(\pi - \theta_1) \times \sin\theta_2 / \sin(\theta_1 - \theta_2) \qquad (4.2)$$

$$\theta_3 = \begin{cases} \pi - \arctan(y/x) & (x \neq 0) \\ \pi/2 & (x = 0) \end{cases} \qquad (4.3)$$

In those equations, $x$ and $y$ are the marker coordinates, $q_1$ and $q_2$ are rotation angles of the cameras, and $q_3$ is the turntable rotation angle. Fig. 4.8 shows the vehicle placement, the cameras and the turntable.

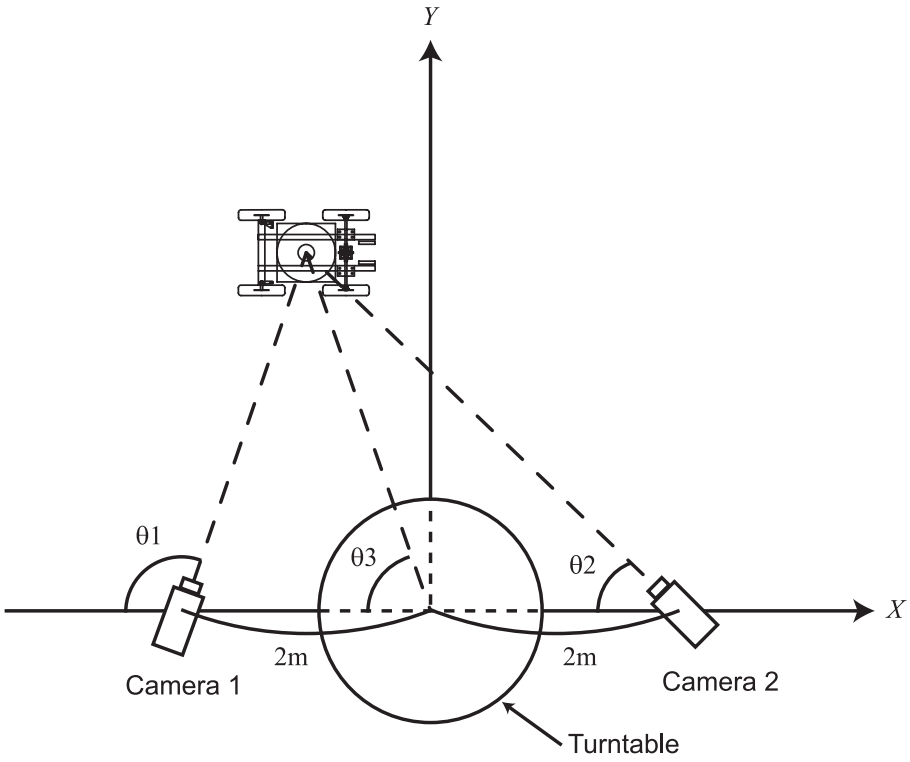


Fig. 4.8 Placement of Vehicle, Cameras, and Turntable

4.2.5 Vehicle Control

The model vehicle is controlled by the controller circuit depicted in Fig. 4.4. The vehicle speed is controlled by monitoring the pulse of the rotary encoder on the driving shaft and by changing the duty ratio of the control pulse to the motor driver device. In the ‘off’ state of the pulses, the dummy load driver is set to ‘on’ state, which enables consumption of unused DC electricity to protect the power source (rectenna circuit). The steering angle is detected by A/D conversion of the potentiometer and is maintained by feedback control to the target angle.

The PICs measure the voltage signal of the gyro sensor, the potentiometer of the turntable and the potentiometer of the angle of depression of the rectenna panel. The measured voltage values are sent to the PC through the wired communication. Using these data from the vehicle, the PC calculates the target angles of the turntable and depression of the rectenna and sends commands to the vehicle controller. The vehicle controller changes the angle according to the commands from the PC.

4.2.6 Path Settings

Programmed paths of the vehicle were set as depicted in Fig. 4.9. The paths were set at distances of 2 m, 3 m, and 4 m from the parabolic antenna. These paths were designed to simulate the movement of agricultural vehicles in crop fields.

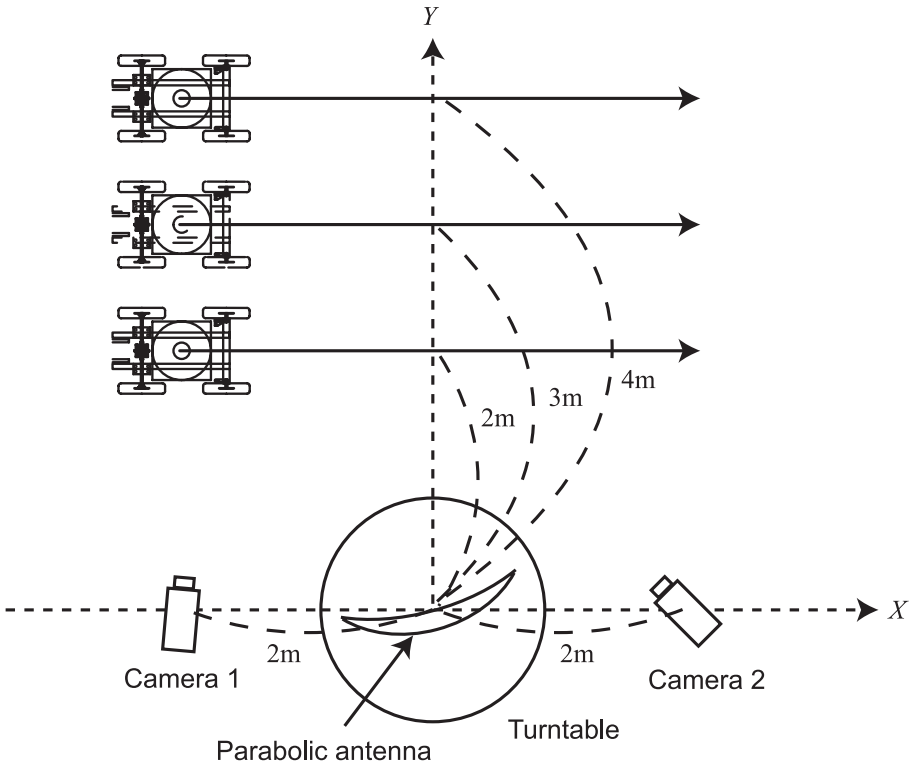


Fig. 4.9 Programmed Path (Straight Running)

4.2.7 Measured Items

The followings are the measurement items in this experiment.

(1) The estimated vehicle position
(2) The turntable angle
(3) The parabolic antenna depression angle
(4) Voltage of the vehicle motors (driving, steering, rectenna turntable, rectenna elevation)
(5) Current of the vehicle motors (driving, steering, rectenna turntable,

rectenna elevation)

(6) The receiving antenna angle

(7) The gyro sensor signal

## 4.3 Results and Discussion

In this section, results of the experiments using parabolic transmitting antenna and rotation control of the receiving rectenna panel on the vehicle are presented. The problems and the challenges of this system obtained from the results are also discussed.

### 4.3.1 Vehicle Path

Fig. 4.10, Fig. 4.11, and Fig. 4.12 show estimated running paths of the vehicle. These paths were calculated using the PC for image processing to detect the stripe marker on the vehicle.

In case of the path $y$ = 2 m, the vehicle ran straight on the programmed path. The difference between the detected path and the programmed path was less than about 10 cm. In this case, as shown in the following sections, the vehicle repeated 'go and stop' and this repetition was found in the graph. The vehicle speed was not constant as described later.

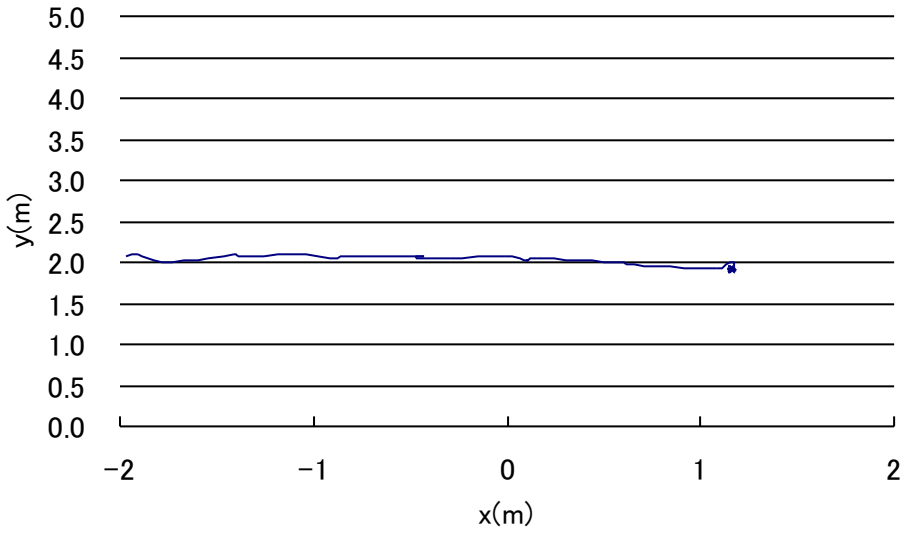


Fig. 4.10 Detected Position of the vehicle (Path: $y$ = 2 m)

In the case of the path $y$ = 3 m (Fig. 4.11), slight error between programmed and detected path was found. In the first part of the running, the vehicle ran to right a little and corrected its direction to left to move along the programmed path. In the final part of the running the vehicle path became slightly left. The jammed line of the final part of the path ($x$ = 1 m) is due to the movement of the cameras. The minimum control amount of the camera rotation angle was set to try to put the market in the center in the image in next image acquisition, in order not to lose the marker in the acquired image. This caused the rotation of the cameras even if the marker did not moved.

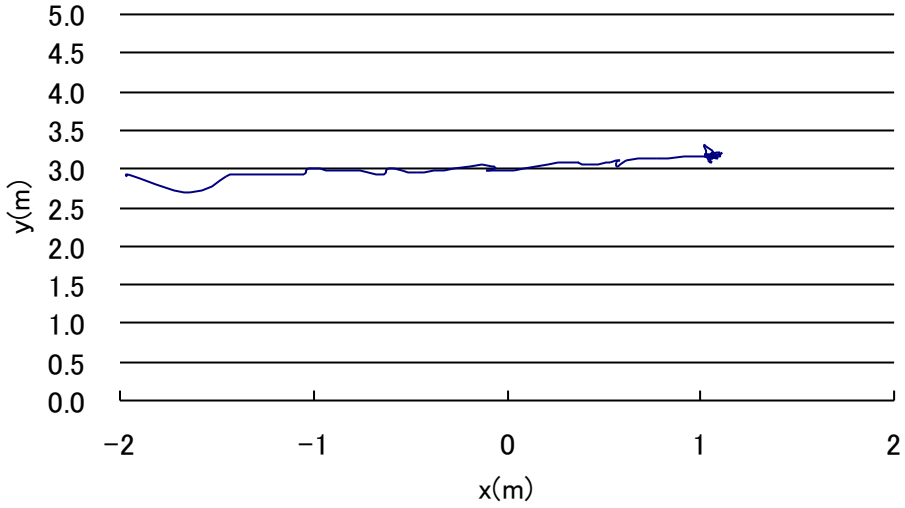


Fig.4.11 Detected Position of the vehicle (Path: $y$ = 3 m)

Zigzag patterns shown in Fig. 4.12 were derived from the detection error of the marker, the low speed of image processing, and the fact that the camera angle control was not adjusted properly. In the case of Fig. 4.12 ($y$ = 4 m), the distance between the vehicle and the cameras was long and this caused the decrease of the size of the marker in the acquired image. The decrease of the precision of the image detection was derived from this decrease of the marker size in the image. These errors were shown as zigzag patterns in Fig. 4.12, which were not the actual movement of the vehicle.

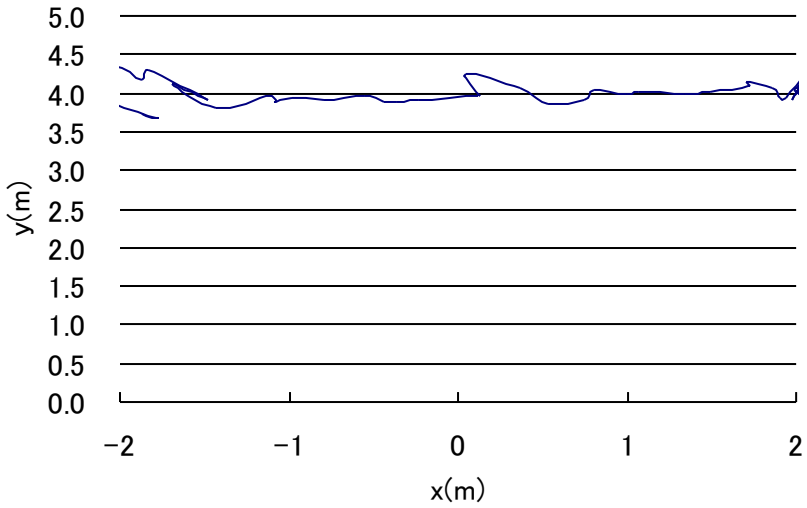


Fig. 4.12 Detected Position of the vehicle (Path: $y$ = 4 m)

4.3.2 Power Consumption of the Driving Motor

Fig. 4.13, Fig. 4.14, and Fig. 4.15 show power consumption results for the vehicle driving motor. The motor power consumption was calculated from the measured voltage and current of shunt registers, which are connected in series to the motors.

For the path y = 2 m, there were moments at which the vehicle speed increased, because of the enough reception of the microwave power. In those moments, the transmitting antenna was unable to follow the vehicle movement. Thereby, the received power decreased and the vehicle stopped. After the vehicle stopped, the transmitting antenna turned to the vehicle and the vehicle started again. The peaks in Fig. 4.13, Fig. 4.14, and Fig. 4.15 occurred for this reason.

The maximum power consumption of the vehicle driving motor was about 22 W, when the transmitting antenna directed just to the vehicle. When the tracking of the transmitting antenna was lost, the power consumption of the vehicle decreased to about 1 to 2 W which as not adequate to drive the vehicle.

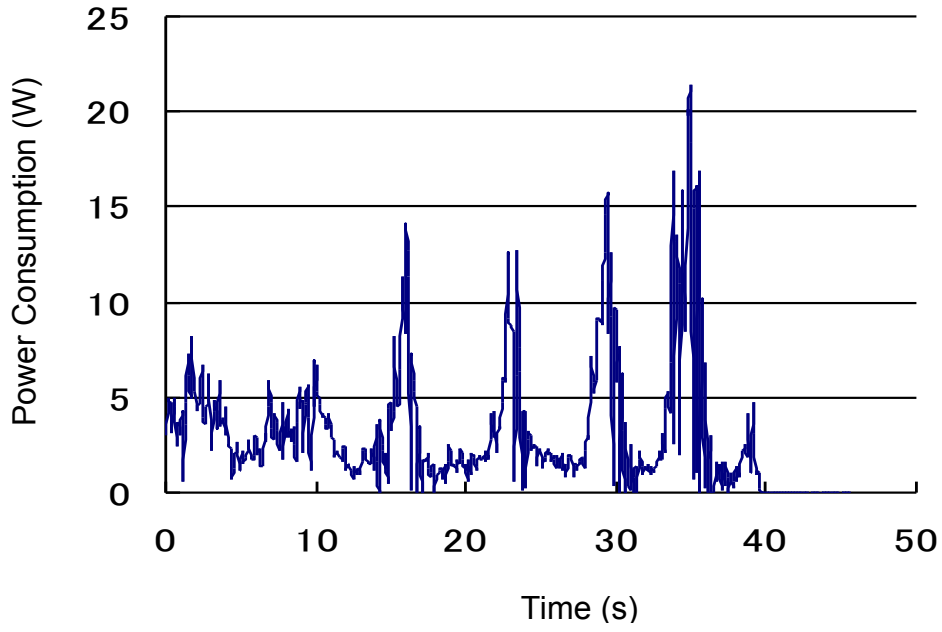


Fig. 4.13 Power Consumption of the Driving Motor (Path: $y$ = 2 m)

Fig. 4.14 shows the case of the path $y$ = 3 m. The received power decreased compared to the case of y = 2m, because of longer distance between the vehicle and the transmitter. In this graph, several peaks of the power consumption were found due to the reason as described above.

The maximum power consumption of the vehicle driving motor was about 14 W, when the transmitting antenna directed just to the vehicle. Due to the lower reception of the microwave power, it took longer time to run the same distance of the path. This was because the vehicle speed decreased and number of the repetition of 'go and stop' of the vehicle running increased.

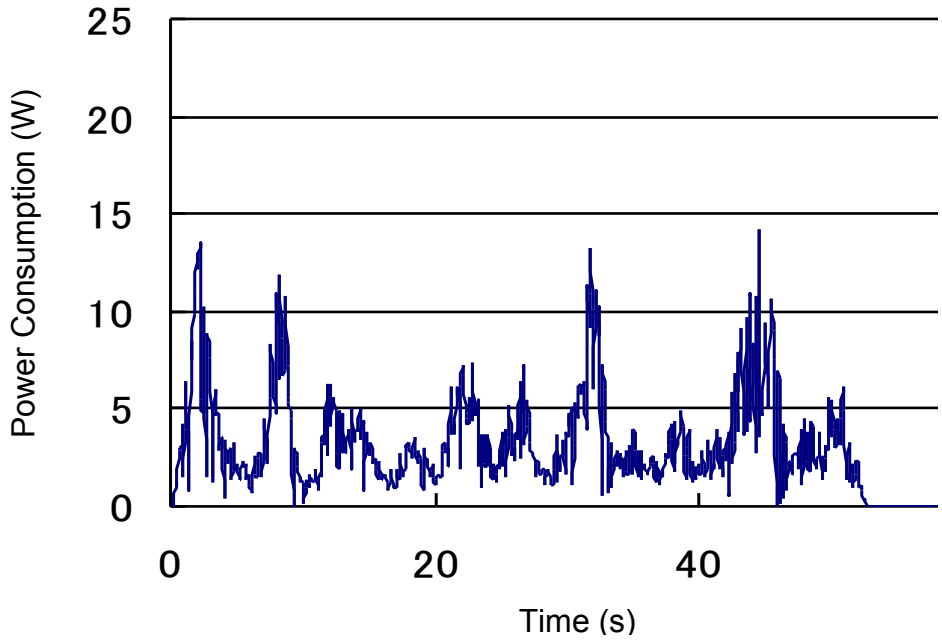


Fig. 4.14 Power Consumption of the Driving Motor (Path: $y$ = 3 m)

Fig. 4.15 shows the case of $y$ = 4 m. The received power decreased because of longer distance between the vehicle and the transmitter. Once the receiving rectenna panel turned to the correct direction as the vehicle ran, the microwave power supply became insufficient. When the power supply became inadequate, the vehicle was unable to turn the rectenna panel on it to receive the microwave power.

The maximum power consumption of the vehicle driving motor was about 10 W, and it took longer time to run the same distance of the path. The difference between the highest and the lowest power consumption decreased compared to the case of $y$ = 2 m and $y$ = 4 m. This was derived from the smaller amount of the control angle of the transmitting antenna when the distance between the vehicle and the transmitter increased. However, due to this longer distance, absolute power consumption the driving motor decreased compared to the case of $y$ = 2 m and $y$ = 4 m.

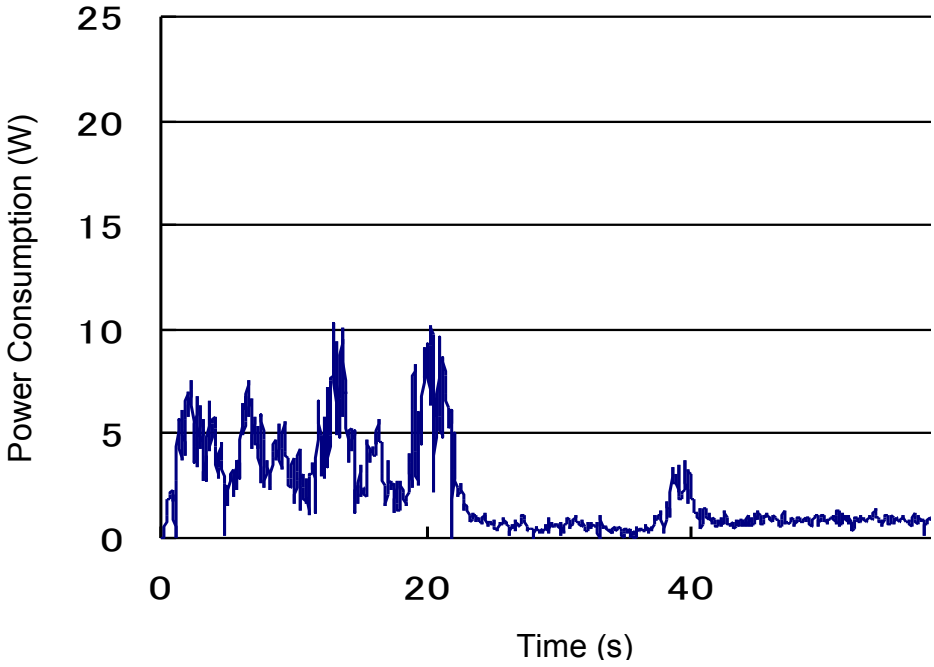


Fig. 4.15 Power Consumption of the Driving Motor (Path: $y$ = 4 m)

Comparing Fig. 4.13 , Fig. 4.14, and Fig. 4.15, maximum power reception decreased according to the greater distance between the transmitter and the vehicle because of the spreads of microwave from the antenna

### 4.3.3 Position Detection

Fig. 4.16, Fig. 4.17, and Fig. 4.18 present the rectenna angle on the vehicle and the power consumption of the motor of the rectenna panel turntable in the case of $y$ = 2 m, 3m, and 4m respectively. These graphs show that the receiving rectenna panel was controlled properly only when the power transmission to the vehicle increased. This was caused by the reason mentioned above.

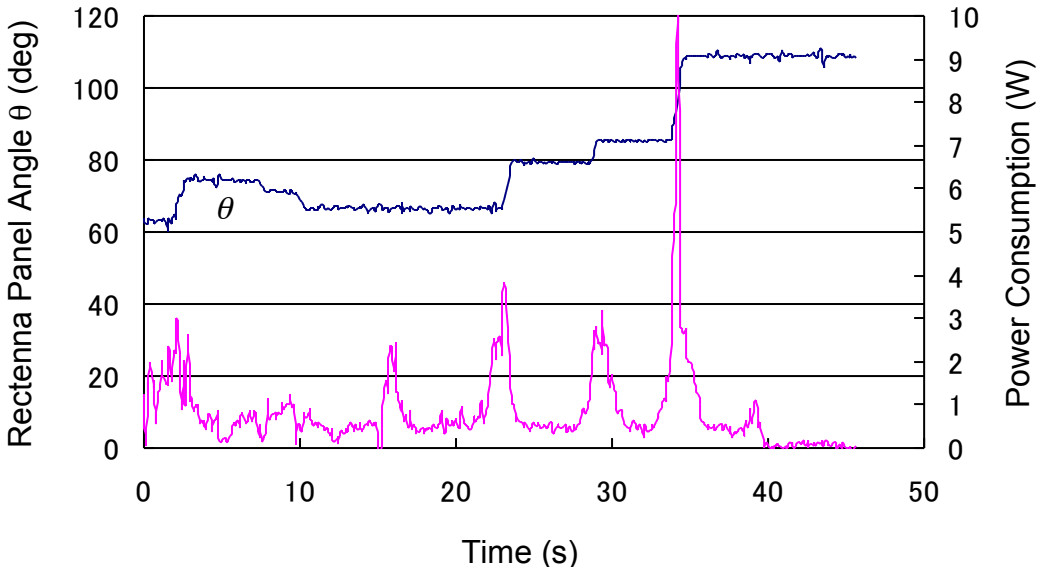


Fig. 4.16 Rectenna Panel Turntable Rotation Angle and Turntable Motor Power Consumption (Path: $y$ = 2 m)

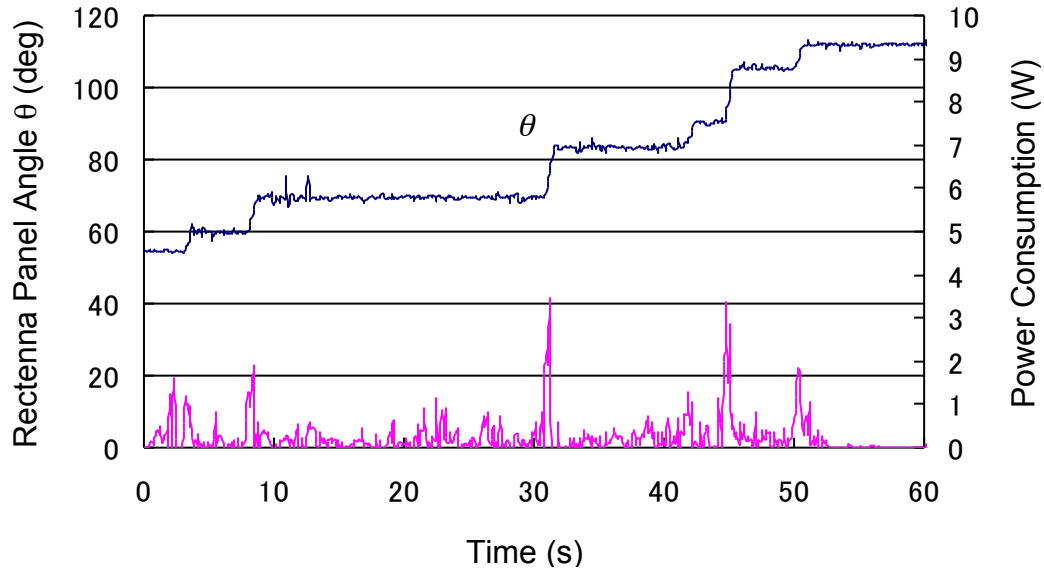


Fig. 4.17 Rectenna Panel Turntable Rotation Angle and Turntable Motor Power Consumption (Path: $y$ = 3 m)

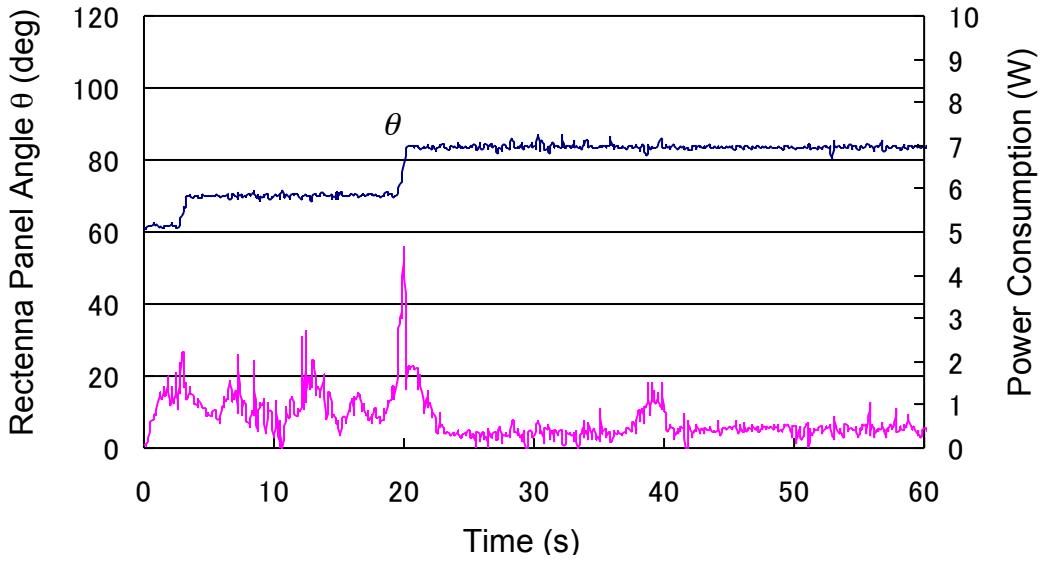


Fig. 4.18 Rectenna Panel Turntable Rotation Angle and Turntable Motor Power Consumption (Path: $y$ = 4 m)

The time of vehicle detection depends on the image processing speed of marker detection on the camera images. For each detection, control commands were sent to the transmitter turntable and rectenna turntable. The minimum time of detection was 0.34 s. The maximum time of detection was 2.11 s for the $y$ = 2 m distance case. The maximum rotation angle of the transmitter turntable was 8.04 deg/s. In the $y$ = 2 m case, transmitter can follow the vehicle at speeds of up to 0.14 m/s for the worst case. The vehicle showed running speed of 0.26 m/s with the microwave power supply. Consequently, the speed of the marker detection and transmission system was inadequate for the vehicle potential speed.

### 4.3.4 Total Power Consumption

Total power consumption of the vehicle in the case of 2 m is presented in Fig. 4.19. The magnetron output was 800 W and the maximum total power consumption of the vehicle was about 41 W. Consequently, the ratio of received power to the transmitted power was about 5%. This efficiency is still low. However, compared to the experiments using a horn antenna (Chapter 4 of this Thesis, Miyasaka et al. 2004, Miyasaka et al. 2005, Oida et al. 2004, Oida et al. 2007), the efficiency increased from

2% to 5%. This improvement was achieved due to the introduction of the parabolic transmitting antenna and the rotation control of the vehicle rectenna panel.

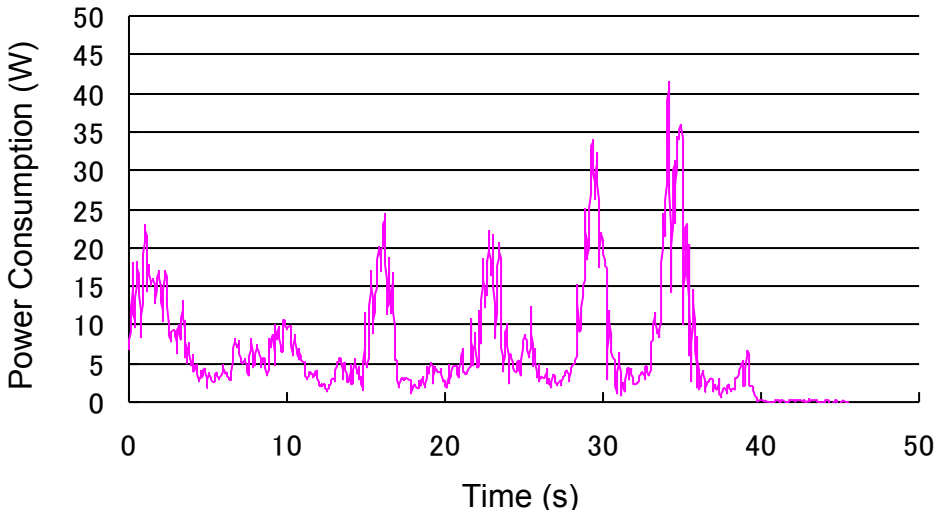


Fig. 4.19 Total Power Consumption of the Vehicle (Path: y = 2 m)

As described above, introduction of the larger rectenna panel, the parabolic transmitting antenna and the rotation control of the receiving rectenna panel improved the amount of microwave power transmission and its efficiency. By this improvement, the larger experimental vehicle was driven by microwave power transmission.

However, due to the inadequate response speed of the image processing (0.34–2.11 s for one detection) and the slow speed of the transmitter turntable (8.04 deg/s), the control speed of the transmitter turntable was inadequate for the potential running speed of the vehicle with microwave power supply. This inadequacy caused repeated running and stopping of the vehicle. Improvement of the control speed of the marker detection, camera rotation, transmitting turntable rotation, and the rectenna panel rotation is necessary to obtain the smooth running of the vehicle.

Nagano *et al.* reported the result of experiment using different microwave frequency, vehicle system, and conditions (Nagano *et al*., 2007). In that report, 5.8 GHz 100 W microwave and smaller rectennas were used for power transmission. A smaller vehicle that runs only along the arc shaped track was used and transmitting antenna was

installed at the center position of the arc. In this system, the distance between the transmitter and the receiving antenna was fixed and there was no need to control the direction angle of the receiving antenna, because the vehicle runs on the arc track and the rectenna was always directed to the center of the arc, i.e. the position where the transmitting antenna was installed. Under the condition of this report, the current capacity of the buffer battery that was installed on the vehicle reached from 0 to 80 Asec after the running of about 800 sec, and during the stop of the vehicle about 160 sec, the current capacity increased 60 Asec. The balance of the current capacity was always positive.

In this Nagano's experiment, a buffer battery and DC/DC converter circuit that enabled the constant load to the rectenna was introduced. The constant load to the rectenna enhances the efficiency of the power supply from the rectenna to the motor. Though this experiment was conducted under very different conditions, their results suggested the possibility of increase of the absolute value and the efficiency of the available electric power of the microwave power transmission to the running vehicle.

[References]

Miyasaka, J., A. Oida, H. Nakashima, K. Ohdoi, S. Yamada, M. Watanabe, H. Matsumoto, K. Hashimoto, N. Shinohara, and T. Mitani. 2004. Study on Mobility of Microwave-Driven Agricultural Vehicle - Orientation Control of Power Transmitter Using Image processing -.Technical Report of IEICE: SPS2003-14, 21-28.

Miyasaka, J., A. Oida, H. Nakashima, K. Ohdoi, M. Watanabe, H.
Miyanaga, H. Matsumoto, K. Hashimoto, N. Shinohara, and T. Mitani. 2005. Study on Control for Microwave-Driven Agricultural Vehicle and Effects of Microwave Exposure on Radish Seed Germination. Technical Report of IEICE: SPS2004-19.

Nagano, K., et al. Microwave Power Transmission Experiment Report to the Robot for the Work, Technical Report of IEICE SPA2006-22, 2007.

Oida, A., H. Nakashima, J. Miyasaka, K. Ohdoi, S. Yamada, M. Watanabe, H.

Matsumoto, K. Hashimoto, N. Shinohara, and T. Mitani. 2004. Development of No-Emission Vehicle by Means of Microwave Power Transmission. Proceedings of the Second International Symposium on Machinery and Mechatronics for Agriculture and Bio-systems Engineering, Kobe, Japan. CD-ROM.

Sasaki, M. 2005. Fundamental Study on Electric Drive for Agricultural Vehicle and Implement using Microwave Power Transmission Technology (Master Thesis, in Japanese), Laboratory of Agricultural Systems Engineering, Graduate School of Agriculture, Kyoto University.

# 5. Improvement of Vehicle with Rotating Rectennas

## 5.1 Improvement and Development of New System

In the chapter 4, the improvement of the microwave-driven vehicle was conducted introducing the rotating and elevating rectenna panel on the larger platform. The improvement of transmitting system was also made using a parabolic antenna with depression angle control.

The experiments described in the chapter 4 showed the possibility and applicability of microwave power transmission to the electric agricultural vehicle. However, due to the inadequate response speed of the image processing and the slow speed of the transmitter turntable, the tracking speed of the transmitter turntable was inadequate for the potential running speed of the vehicle with microwave power supply.

To improve the response speed of transmitter, a smaller transmission system with a horn antenna was introduced to the next experiment. To develop a right-weight transmitting system with quick response, a horn antenna was used, in spite of its dispersion of radiation. The vehicle was also improved using a smaller platform with quick rotating rectenna panel.

### 5.1.1 Vehicle with Rotating Rectenna

#### 1) Vehicle Platform

The experimental vehicle was developed based on a radio controlled model dump truck (TAMIYA Mammoth dump). This platform was the same with the model vehicle described in the chapter 4. On this vehicle, three motors are installed. A DC motor (Japan Servo DME37BB) is used for driving. A servo motor (Futaba Corporation S3003) is also equipped for steering. The rectenna panel is turned by a DC motor (Japan Servo DME37B8HPS).

#### 2) Rectenna Panel and Turntable

Twenty rectennas are placed on the rectenna panel (Fig. 5.1). These 20 rectennas are connected as a circuit of 5 parallels of 4 series. This panel is turned by a DC motor, thus wired connection cannot be used between the rectennas and the vehicle platform. To provide received electricity from the rectenna panel to the vehicle motors, a brush is

installed on the panel. This brush contacts to the electrode on the fixed axis on the vehicle that holds the rotating rectenna panel. This enables for the panel to rotate over 360 degrees.

Fig. 5.2 shows the vehicle platform and the rectenna panel on it.

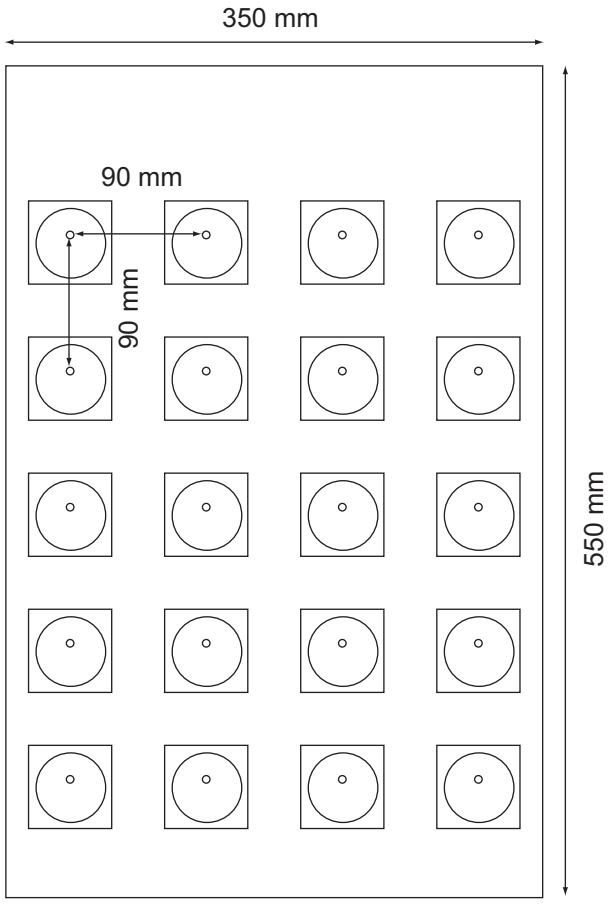


Fig. 5.1 Dimension of Rectenna Panel

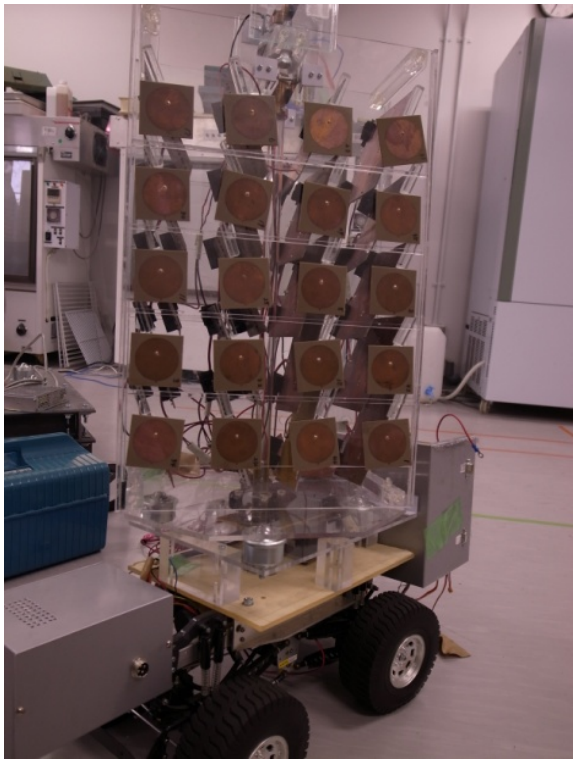

Fig. 5.2 Vehicle Platform and Rectenna Panel

3) Microcomputer Controller and Inner Measurement System

Three microcontrollers and two DC motor drivers are used in the controller circuit. These microcontrollers are connected with $I^2C$ bus, which enables to communicate among the microcontrollers. The first microcontroller (PIC 1 in Fig. 5.3) receives data of vehicle position and attitude from outside PC which detects these data by image processing with two color cameras. This PIC 1 measures pulse of a rotary encoder on a vehicle wheel and the voltage of a potentiometer fixed on the rotating axis of the rectenna panel. PIC 1 functions as the master of the $I^2C$ in this circuit. PIC 1 calculates control amounts using data from PC and from the inner sensors and sends commands to other two PICs via $I^2C$.

PIC 2 in Fig. 5.3 generates pulses for two DC motors which drive the vehicle wheels and the rectenna turntable. Rotation speed of these motors is controlled by PWM, which is determined by the commands from PIC 1. PIC 2 also measures voltage and current data of two DC motors by A/D conversion. This PIC 2 sends these data to the PC via RS-232C wired-communication along with the data of pulse encoder and rotary

potentiometer measured by PIC 1. PIC 3 generates pulses for steering servomotor according to commands from PIC 1. Voltage and current data of two DC motors are also measured by a data logger which is directly connected to the two DC motor driver circuits.

In front of the vehicle, dummy loads of the motor driver were installed in a metal box. The control circuits were installed in another metal box put at rear of the vehicle (Fig. 5.2).

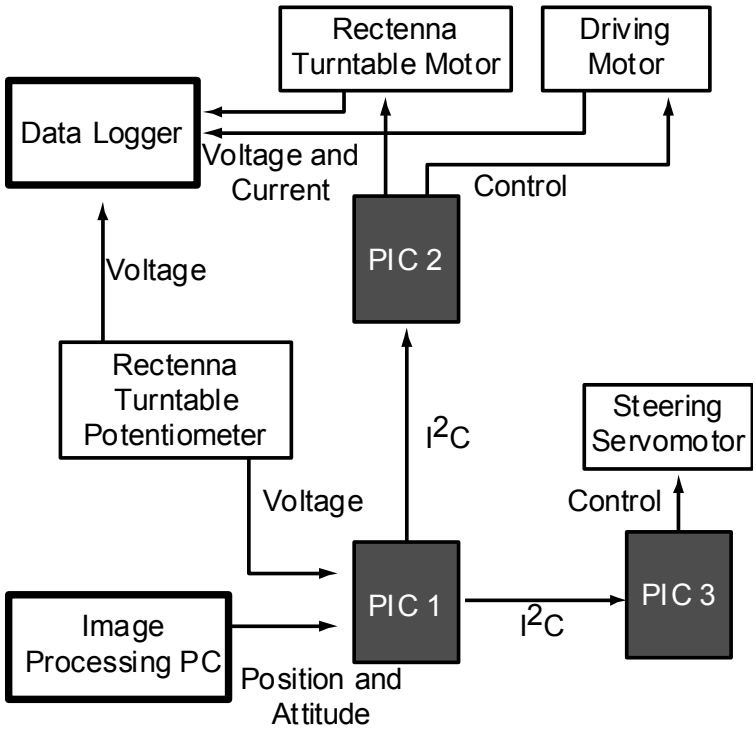


Fig. 5.3 Diagram of Microcontroller, Motor, and Measurement of the Vehicle

5.1.2 Transmitting System (Turntable, Antenna, and Magnetron)

1) Turntable and Stepper Motor Controlled by PC

Vehicle position and attitude are detected by the PC using image processing. The PC acquire images from two pan tilt zoom cameras (SONY EVI-D30). The PC sends commands to the transmitter turntable controller. It also sends the position and attitude data to the model vehicle via wired RS-232C. For more details of the detection system, refer to Nakagawa et al. 2008 and Nakagawa et al. 2009.

2) Horn Antenna and Magnetron

A new turntable was developed to install the transmitting horn antenna. This turn table rotates by a stepper motor controlled by the PC via the motor controller (Oriental Motor, XG9200T-G) and the motor driver(Oriental Motor, ASD13A-A). Commands are sent from the PC to the motor controller through parallel I/O board (INTERFACE, PCI-2726) on the PC.

On this turntable, a magnetron, a transformer, waveguides, a directional coupler, and a horn antenna are installed. A power sensor is connected to the directional coupler to measure output power from the magnetron. Output microwave power can be adjusted by voltage control to the DC power supply to the magnetron. As described above, a horn antenna was introduced to obtain quicker response of turntable with right-weight.

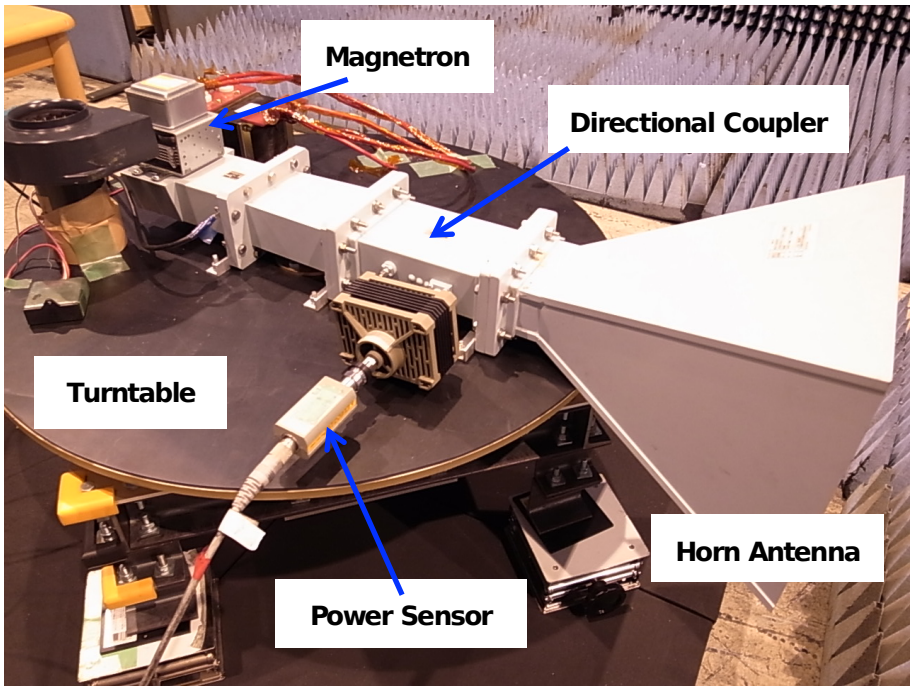


Fig. 5.4 Magnetron and Horn Antenna on New Turntable

5.1.4 Wired Communication between Microcomputer and PC

Wired communication was used to send the information on vehicle position and attitude from outside PC. The PC detects these data by image processing with two color

cameras and sends them to the vehicle on RS-232C communication cable between the PC and the vehicle. The vehicle attitude was detected by image processing of the color marker installed on the vehicle (Nakagawa et al. 2008 and Nakagawa et al. 2009).

The vehicle controller calculates the appropriate rotation angle of the rectenna turntable from these data to direct the rectenna panel to the transmitting horn antenna.

### 5.1.5 Measured Items

Microwave power output was measured by a power meter (Agilent Technologies E44198-2) and a power sensor (Agilent Technologies 8481B) which was connected to the directional coupler.

For the examination of receiving power according to the angles of transmitter and receiver antenna (mentioned later), another power sensor (8481B) was connected to a patch antenna.

Received microwave power during running by DC supply was estimated by measuring voltage between both ends of a dummy load connected to rectenna output.

Voltages and currents of the driving motor and the rectenna panel turntable motor were measured by inner PIC microcontroller A/D conversion input and also by a data logger (Keyence NR-HA08, NR-500) connected to instrumentation amplifier circuit (ANALOG DEVICES AD623A). Rotation angle of the rectenna turntable was also measured by PIC A/D conversion and Keyence data logger.

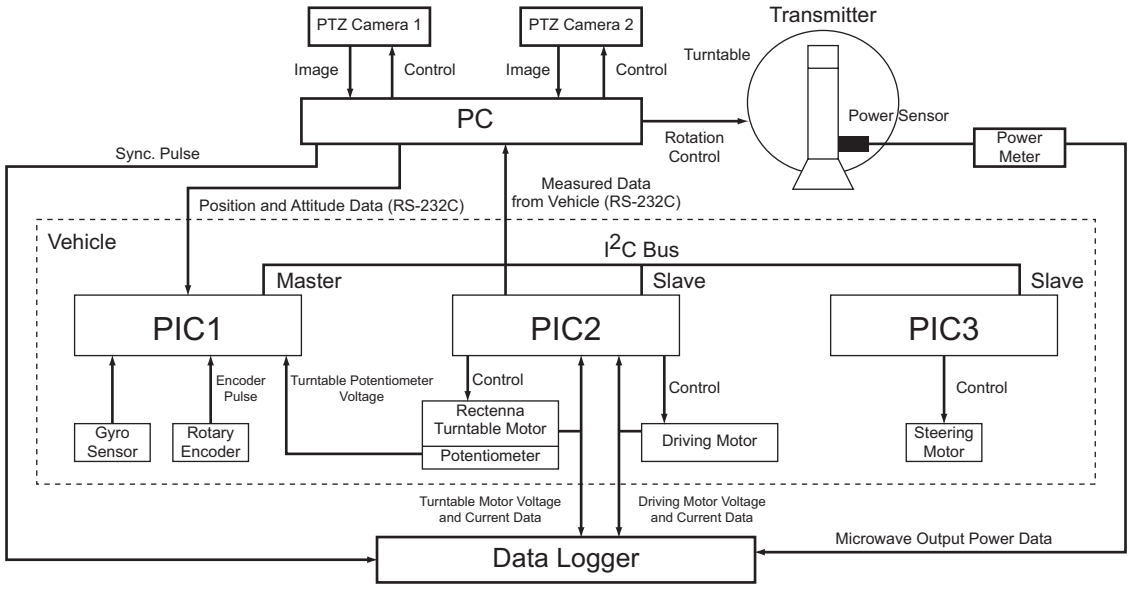


Fig. 5.5 Total System of the Experiment

## 5.2 Experiments

### 5.2.1 Characteristics of Transmitting and Receiving Antenna

1) Distance and Rotation Angle

To set the target accuracy of rotation angles of both transmitter and receiver antennas, received power of a patch antenna was measured by changing the rotation angle of both antennas. Receiving patch antenna connected to a power sensor is fixed on a GP-IB controlled turntable. The distance between the rotation centers of the horn antenna and patch antenna was set to 2 m, 3 m, and 4 m. The actual distances between the horn and patch antenna were 1.35 m, 2.35 m, and 3.35 m. The height of the both antenna from the floor was 65 cm.

For the experiment of measurement by rotating the transmitting horn antenna, angles were set from -30 deg. to +30 deg. by 5 deg. step. For the experiment by rotating the receiving patch antenna, the angles were set from -90 deg. to +90 deg. by 5 deg. step.

Fig. 5.6 shows the placement and the angles of the both antenna. Fig. 5.7 shows the photos of the horn antenna and the patch antenna.

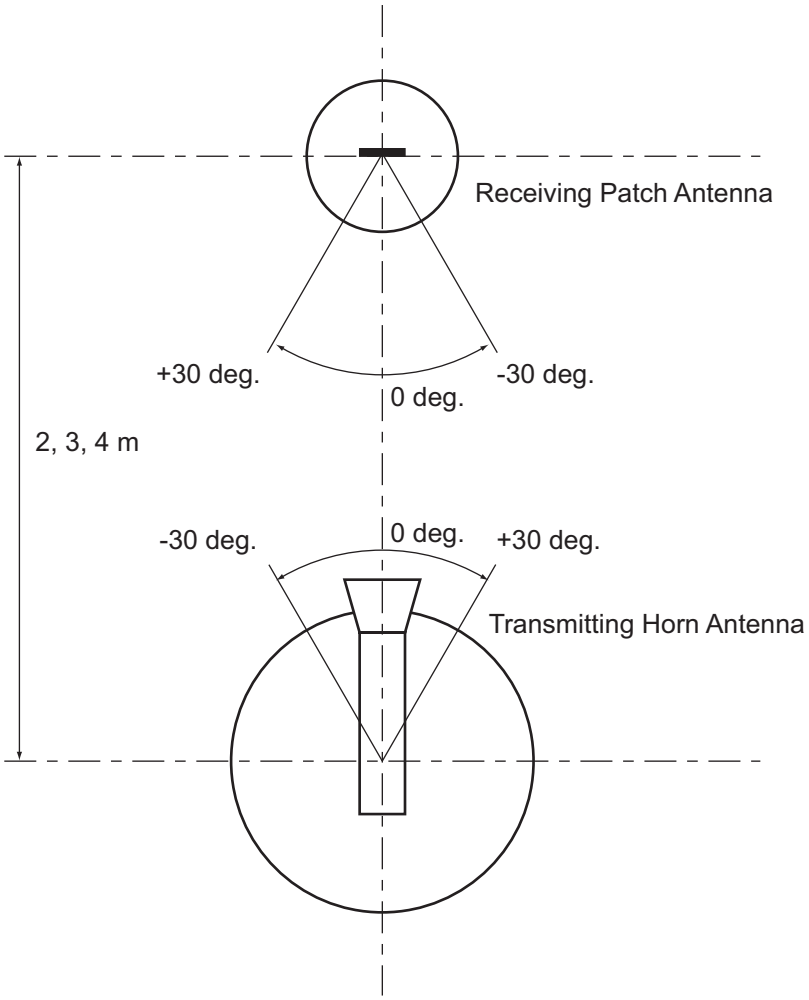


Fig. 5.6 Placement and Angles of the both Antenna

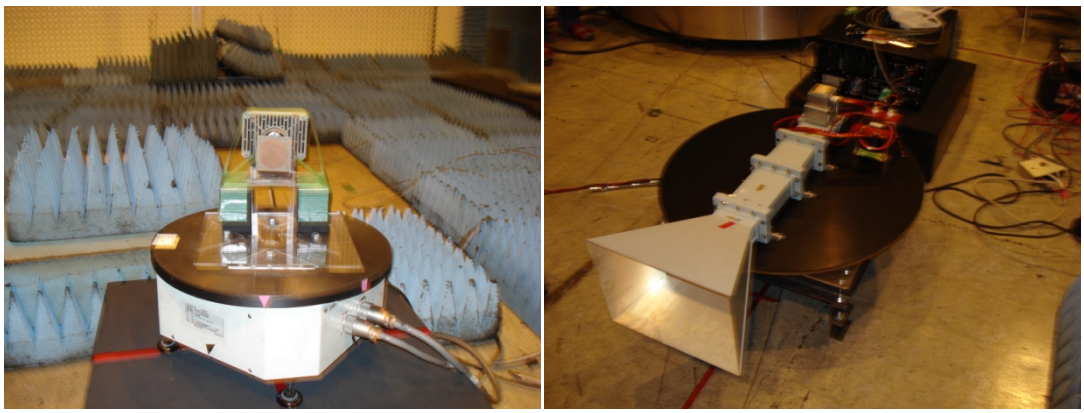

(a) Receiving Patch Antenna (b) Transmitting Horn antenna

Fig. 5.7 Patch Antenna and Horn Antenna

2) Transmitted and Received Microwave Power

The output power of microwave was set to 800 W. The output power from the horn antenna was measured by a power sensor (Agilent Technologies, 8481B) with a attenuator and a power meter (Agilent Technologies E44198-2). The received power of the patch antenna was also measured by the same power sensor, attenuator, and power meter. These measured power were recorded by a data logger (Keyence, NR-HA08) and a PC.

5.2.2 Control of Rectenna Panel

Response of the rectenna panel turntable on the vehicle was measured by giving the target angle of the panel from the controlling PC. The target angles were set to 30, 90, 120 150 deg. (positive direction) and 210, 240, 270, 300 deg. (negative direction). The duty ratio of the current pulse to the driving motor was set to 20 %.

In case of full speed rotation, rotating speed of angle was also measured by setting the duty ration of the current pulse as 100 %.

5.2.3 Measurement of Receiving Power during Running with DC Power Supply

To estimate received microwave power under normal condition of the vehicle running and control, experiments with external DC power supply were conducted. Dummy load resistance was connected to the rectenna output to measure received microwave power while the vehicle was running with the DC power supply to ensure normal running and rectenna panel control. In these experiments, microwave output power was set to about 250 W.

5.2.4 Running with Microwave Power

Experiments of running with received microwave power were conducted to examine the behavior of the vehicle with only the transmitted microwave power except the battery power supply for the microcontroller circuits. The rectenna output was connected to the vehicle motor power supply inputs. In these experiments, microwave output power was set to about 800 W.

5.2.5 Path Settings

Path settings for the experiments of running both with DC power supply and with microwave power were shown in Fig. 5.8 and Fig. 5.9. Seven straight-line paths and one circular path were programmed in the microcontroller. These paths were set to examine the power transmitting and receiving characteristics in various situation of running.

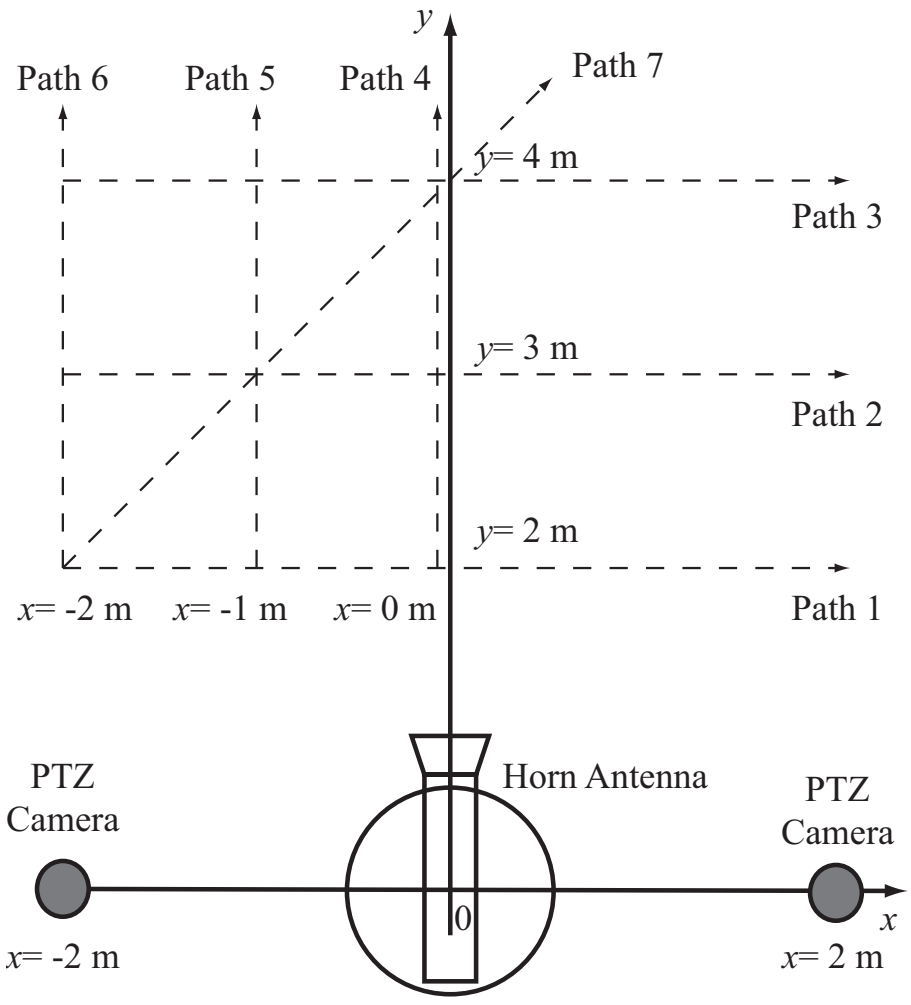


Fig. 5.8 Path Setting (Straight Path)

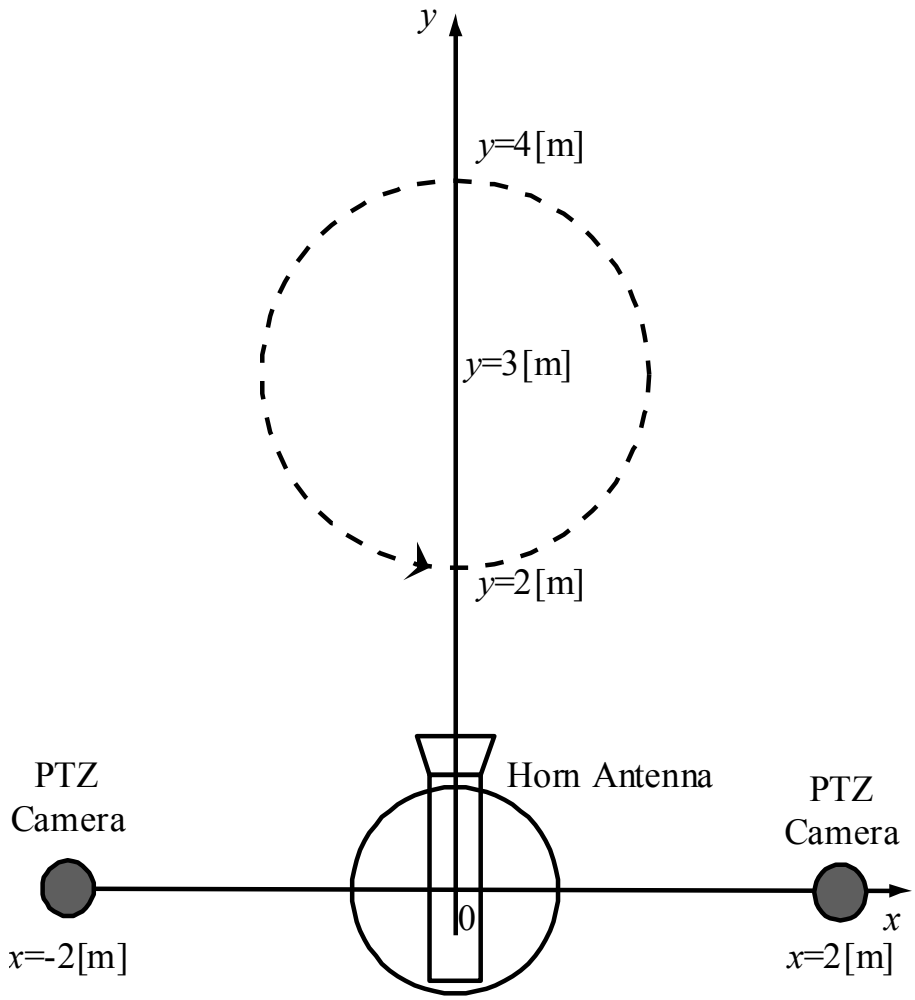


Fig. 5.9 Path Setting (Circular Path)

## 5.3 Results and Discussion

The experiments were conducted at the METLAB, Research Institute for Sustainable Humanosphere, Kyoto University. The system was installed in the anechoic chamber.

### 5.3.1 Receive Power according to Distance and Rotation Angle

To obtain less than 5 % of loss in both transmitting and receiving, The following results were measured to evaluate the required angular error of rotation of the horn antenna and the receiving rectenna.

(1) Receiving (Rectenna Angle)

Fig. 5.10 shows received microwave power from fixed (0 deg.) transmitter horn antenna at the distance of 2, 3, and 4 m when receiver antenna turned at every 5 deg. between -90 and +90 deg. Full width at half maximum of the received power is approximately 80 deg.

Fig. 5.11 shows the ratio of received power to maximum value for each distance. Power loss of receiver is considered less than 5% when the declination of receiver angle is less than 10 deg. According to this result, the target declination of receiver antenna angle was set at less than 10 deg.

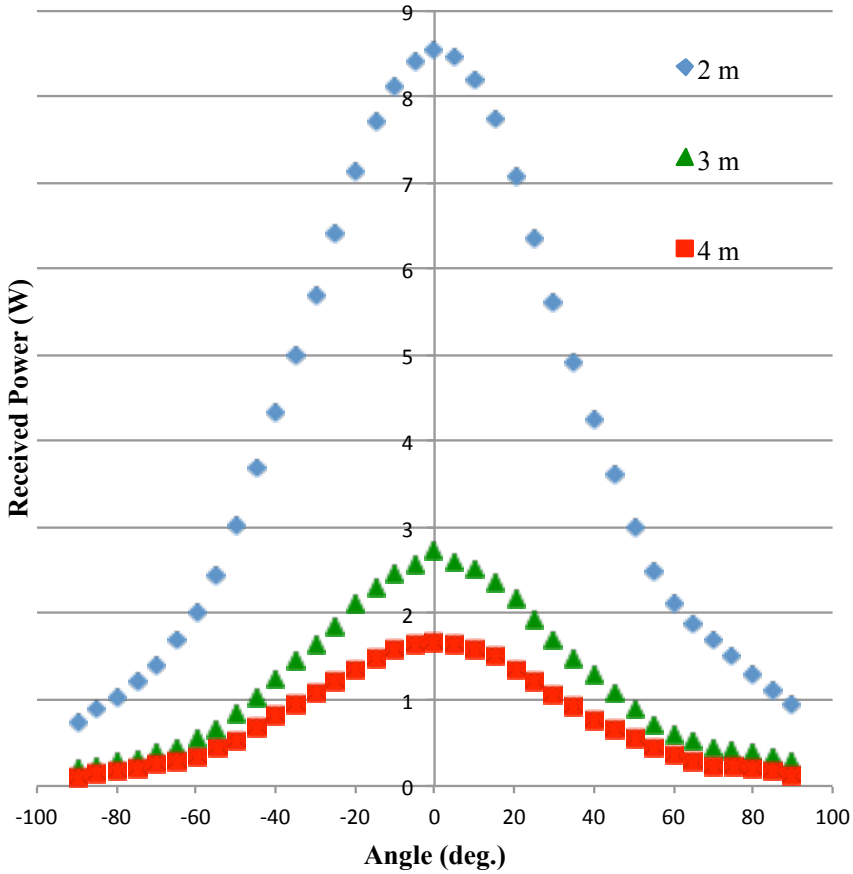


Fig. 5.10 Received Power and Patch Antenna Angle

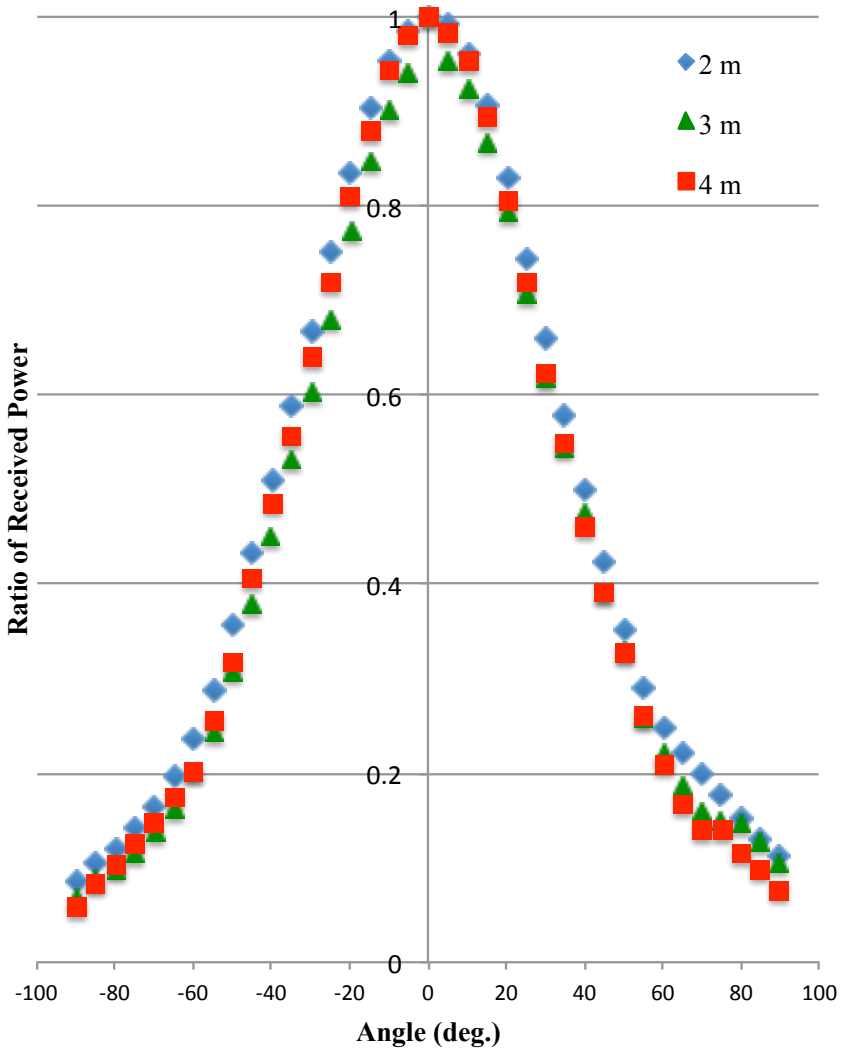


Fig. 5.11 Ratio of Received Power and Patch Antenna Angle

(2) Transmitting (Horn Antenna Angle)

Fig. 5.12 shows received microwave power of fixed (0 deg.) receiver antenna when rotating the transmitter horn antenna by 5 deg. between -30 to + 30 degree. This is derived from the characteristics of the horn antenna and full width at half maximum is approximately 18 (-10 to + 8) degree.

Fig. 5.13 shows the ratio of received power to maximum value for each distance. To obtain the power loss less than 5%, angle error of the transmitter should be within ± 5 degree.

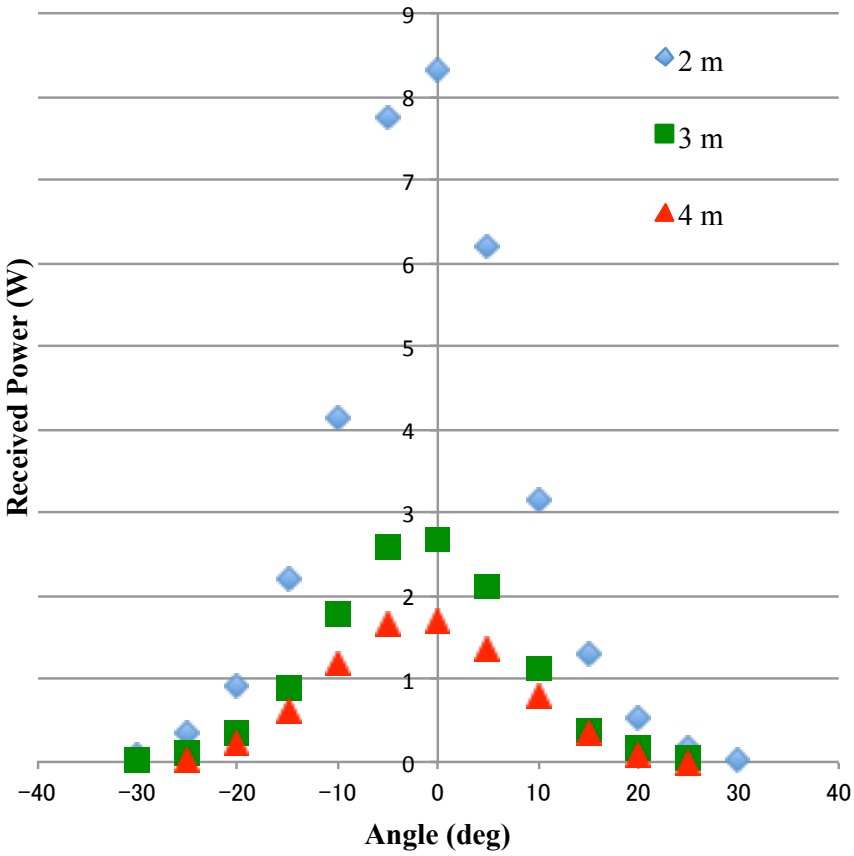


Fig. 5.12 Received Power and Horn Antenna Angle

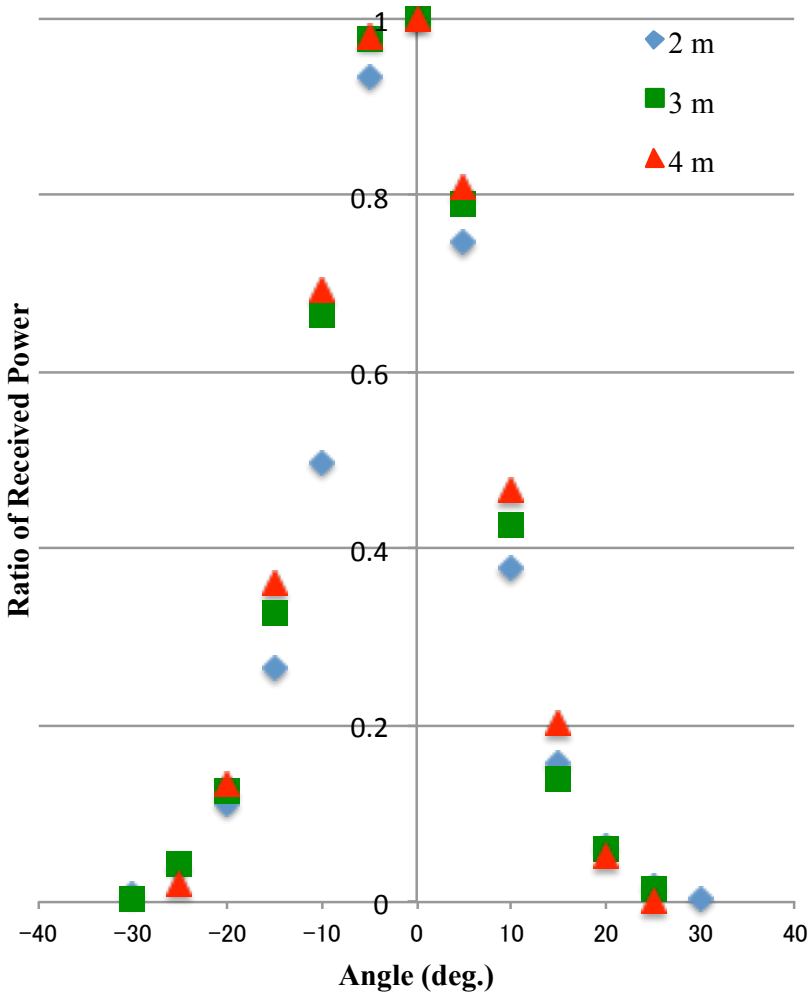


Fig. 5.13 Ratio of Received Power and Horn Antenna Angle

5.3.2 Control of Rectenna Panel

Rotation angle of the rectenna panel turntable on the vehicle by giving the target angle of 30, 90, 120 150 deg. (positive direction) is shown in Fig. 5.14. Rotation angle by giving the target angle of 210, 240, 270, 300 deg. (negative direction) is shown in Fig. 5.15. As mentioned above, the duty ratio of the current pulse to the driving motor was set to 20 %.

Maximum about 10 deg. of error from target angle was observed. This error satisfies the target declination of receiver antenna angle (less than 10%) described in 5.3.1 (1).

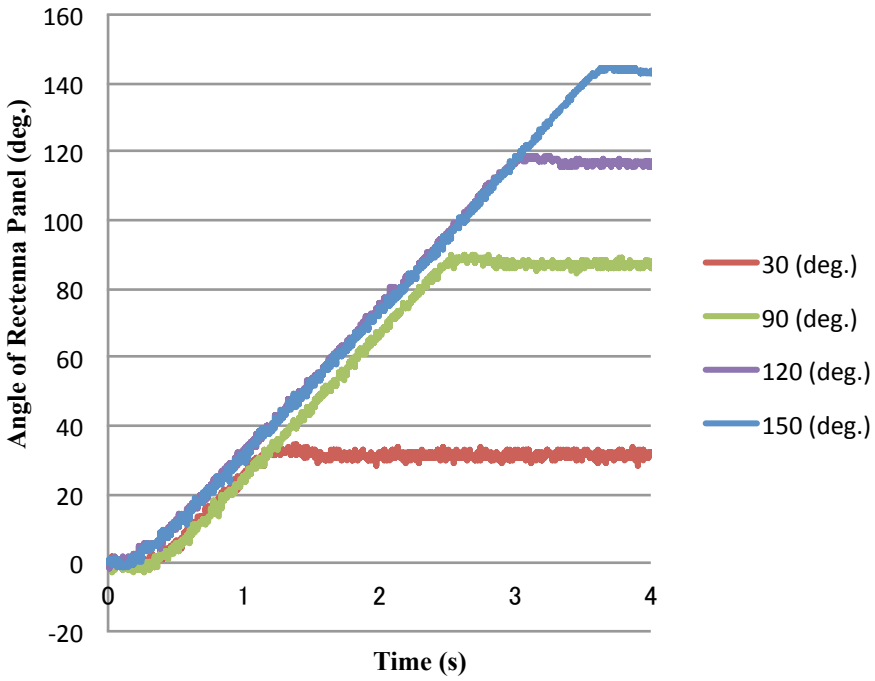


Fig. 5.14 Rotation of Rectenna Panel (Positive Target Angle)

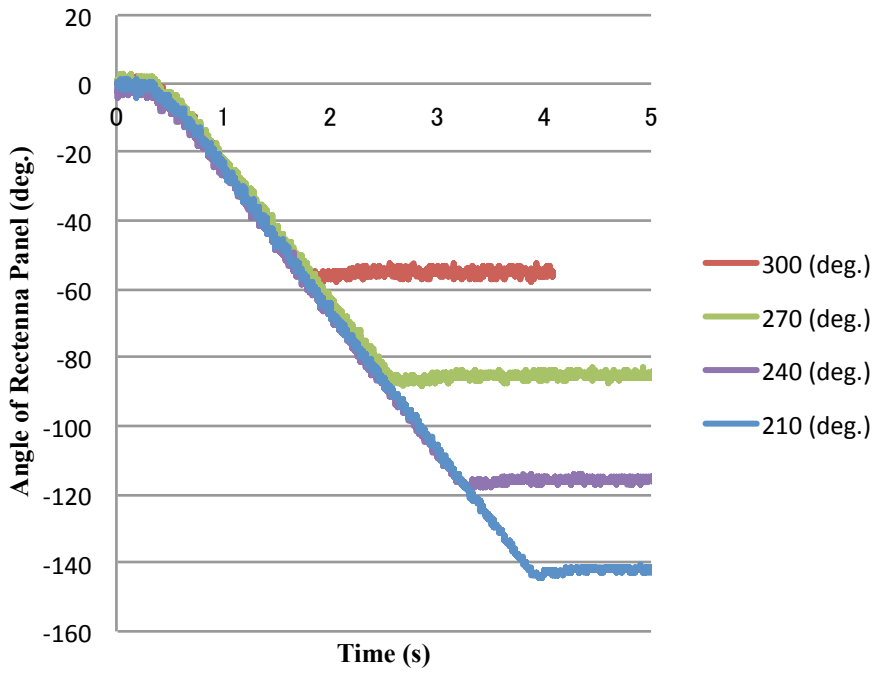


Fig. 5.15 Rotation of Rectenna Panel (Negative Target Angle)

Rotation angle in case of full speed rotation by setting the duty ration of the current pulse as 100 % is shown in Fig. 5.16. According to this result, the maximum rotation speed of the rectenna panel was estimated as 117.9 deg./sec.

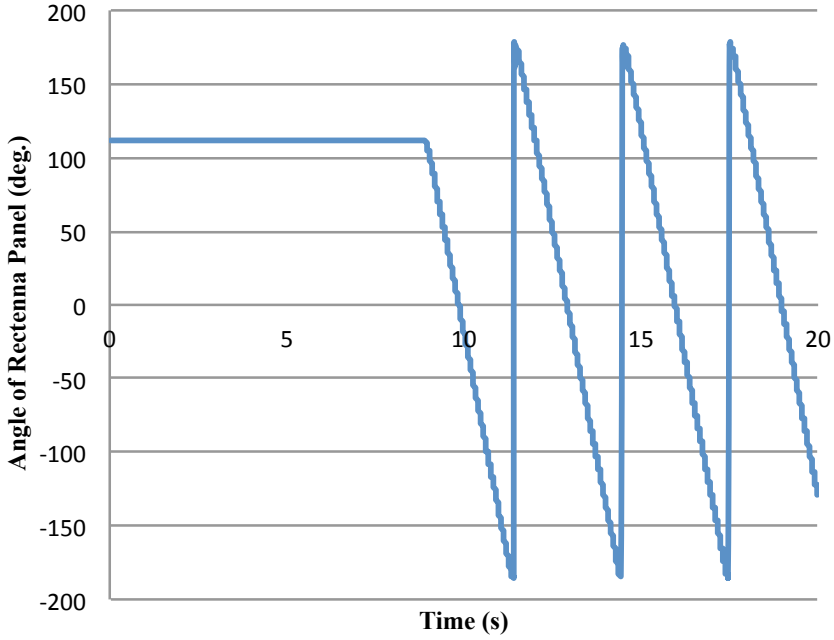


Fig. 5.16 Rotation Angle of Rectenna panel at Maximum Rotation Speed

5.3.3 Received Microwave Power and Angular Error during Running with DC Power Supply

Results of the experiments with external DC power supply are as follows. In these experiments, necessary power for vehicle was provided from DC power supply. Received microwave power by the rectenna panel was measured and consumed by the dummy loads. Fig. 5.17 is a photo of transmitting turntable and the experimental vehicle.

In the first part of this section, results of received power and angular error are shown. In the second part, results of received power and power consumption of the vehicle motors are shown. Note that the power consumption of the vehicle motors means the power consumption of vehicle driving motor and rectenna panel turntable motor that was provided by outer DC power supply.

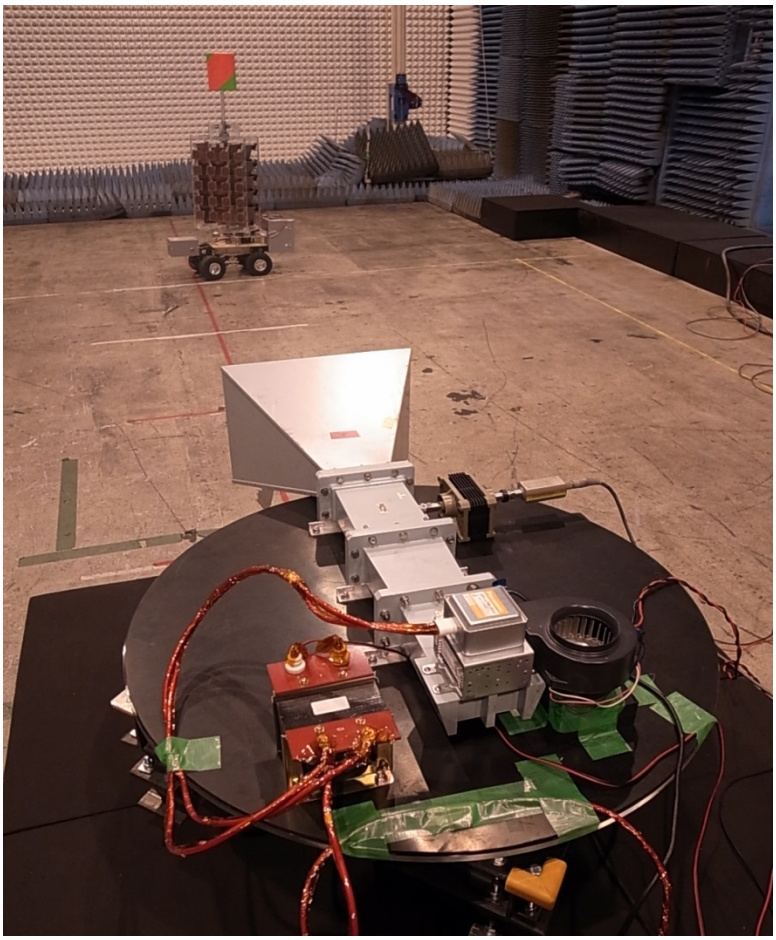

Fig. 5.17 Transmitting Turntable and Experimental Vehicle

1) Received Microwave Power and Angular Error

Experiments of seven straight-line paths were conducted. Followings are the results of each path.

a. Path 1

Estimated path by image processing and camera angles is shown in Fig. 5.18. The programmed path was straight line. However, the estimated actual path was not straight. The reason of it could be the backlash of steering gear and the steering control was not able to detect it and correct it.

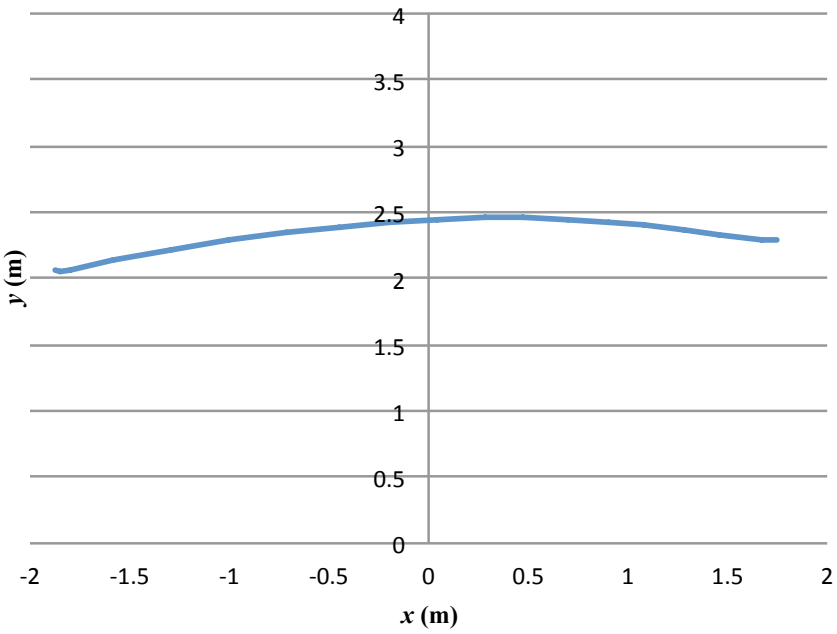


Fig. 5.18 Estimated Path (Path 1)

Fig. 5.29 shows the distance between the transmitting horn antenna and the vehicle. Received power of the rectenna panel is also shown. The red markers present the acquisition timing of vehicle position data from the outside image processing PC to the running vehicle.

The reason of the fluctuation of the received power is the slow data acquisition. According to the graph, received power increased just after the data acquisition. This means that the controller adjusted the rectenna panel angle according to the previously acquired position data. The interval of the data acquisition corresponds to the interval of rectenna panel control. To obtain quick response of rectenna panel angle control, short interval of data acquisition is necessary.

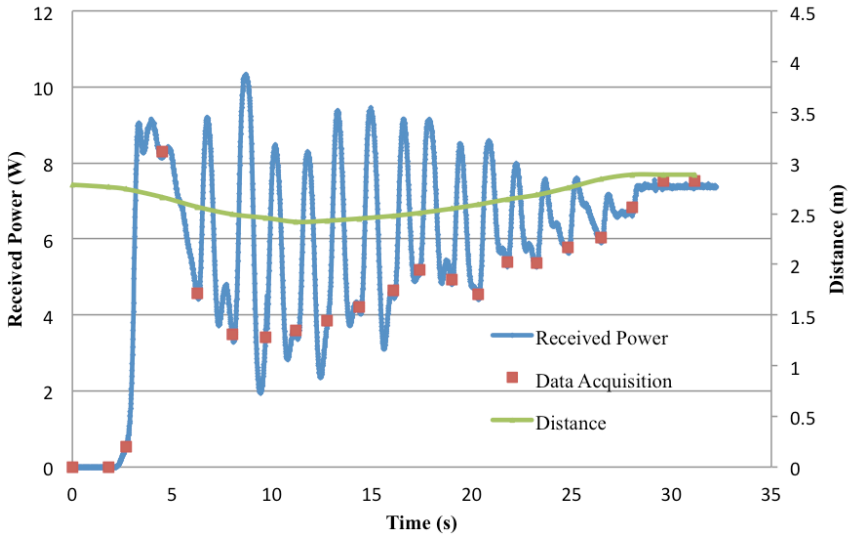


Fig. 5.19 Received Power and Distance (Path 1)

Fig. 5.20 show the received power and the error angle of rectenna panel rotation from the target angle. Fig. 5.21 shows the target angle and actual angle of the rectenna panel. In some case, error more than 10 degree was observed. This does not satisfy the target control error of the rectenna panel. As mentioned above, quick interval of data acquisition is required to decrease the error angle.

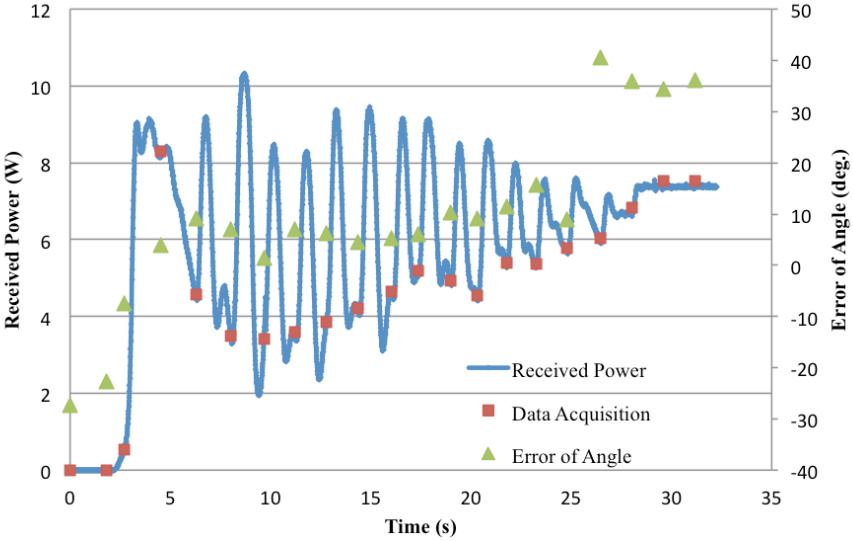


Fig. 5.20 Received Power and Error of Angle (Path 1)

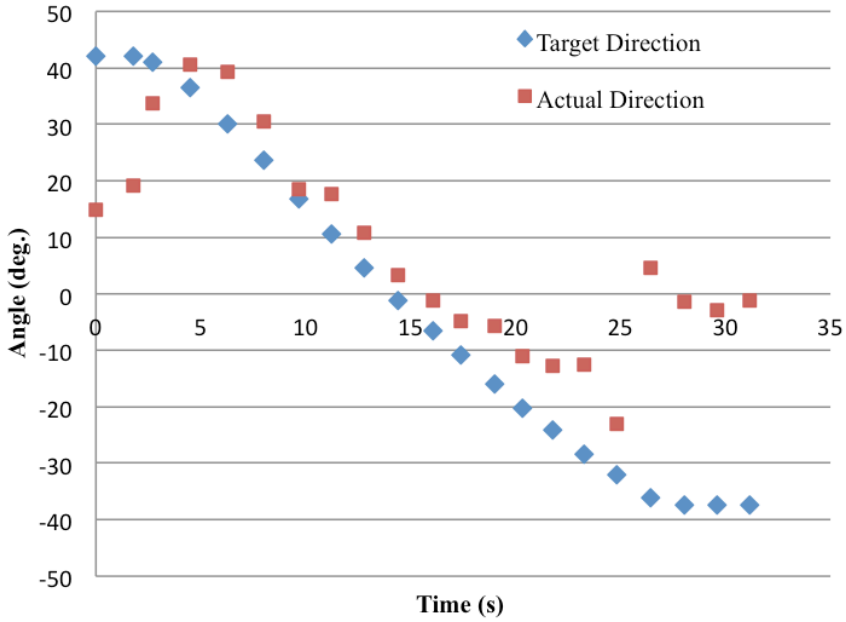


Fig. 5.21 Target Direction and Actual Direction of Rectenna Panel (Path 1)

In the experiments of path 2 and path 3, the same tendency was observed. The followings are the results of path 2 and path 3 (Fig. 5.22 to Fig. 5.29).

b. Path 2

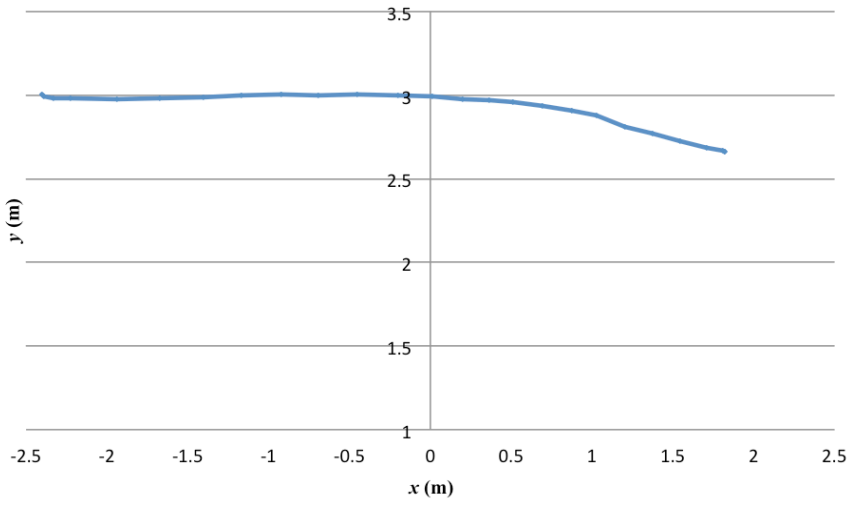


Fig. 5.22 Estimated Path (Path 2)

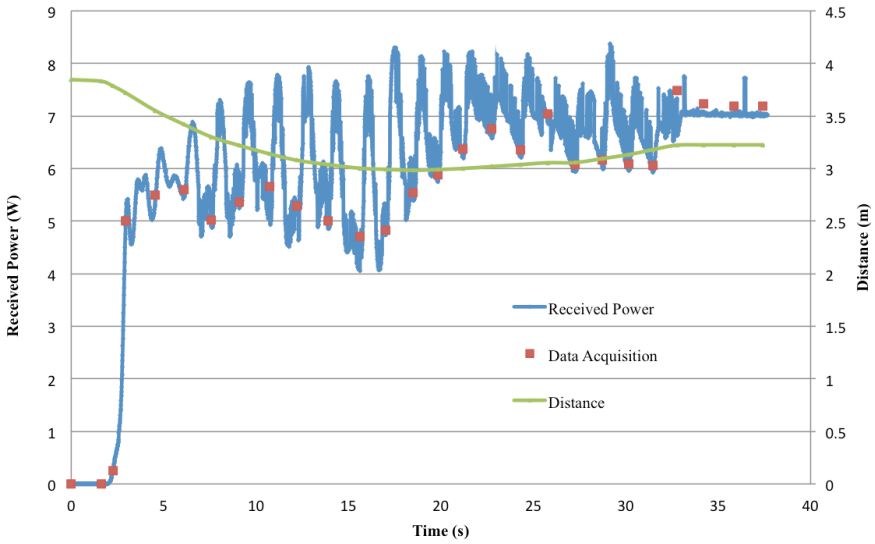


Fig. 5.23 Received Power and Distance (Path 2)

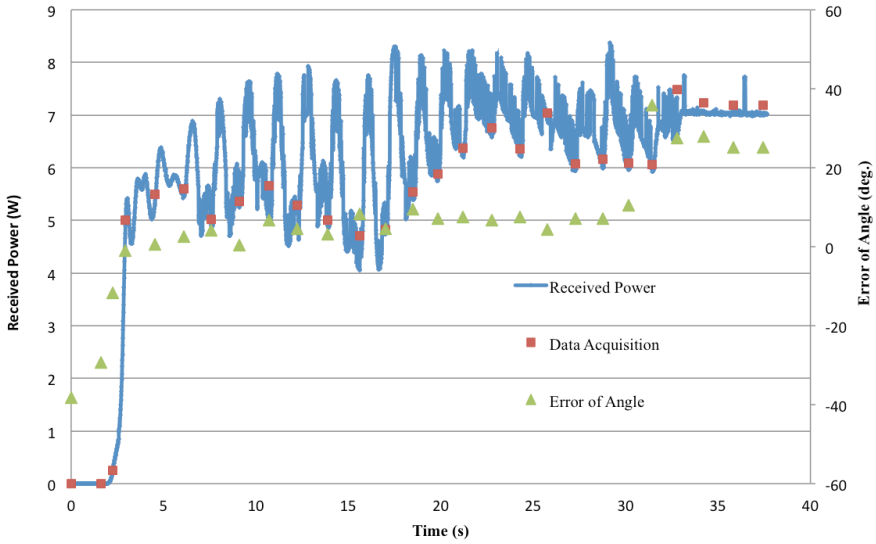


Fig. 5.24 Received Power and Error of Angle (Path 2)

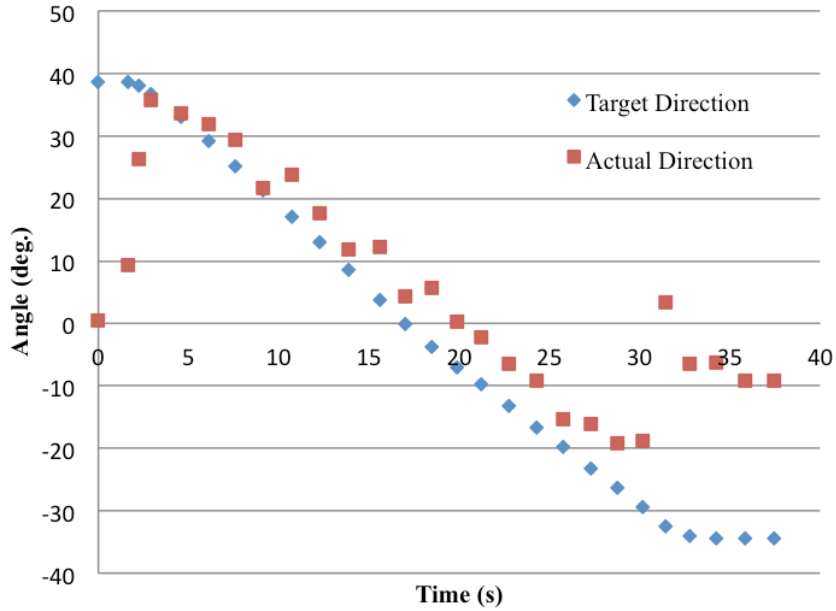


Fig. 5.25 Target Direction and Actual Direction of Rectenna Panel (Path 2)

c. Path 3

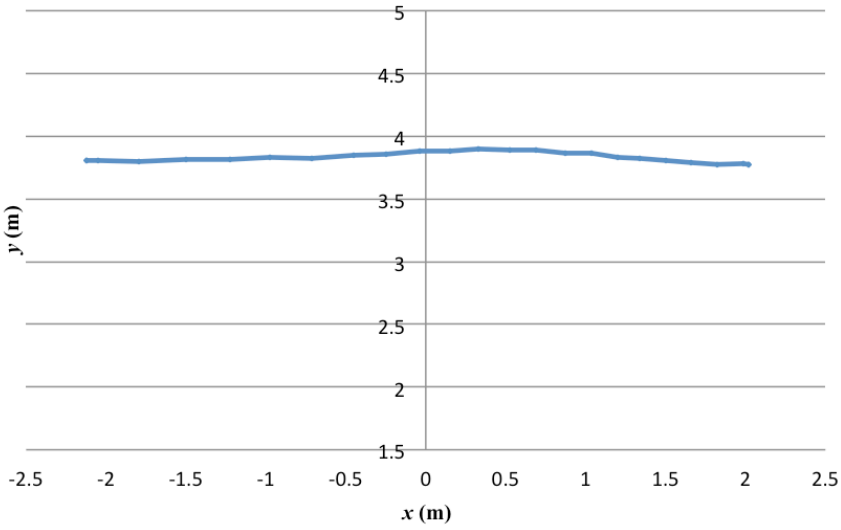


Fig. 5.26 Estimated Path (Path 3)

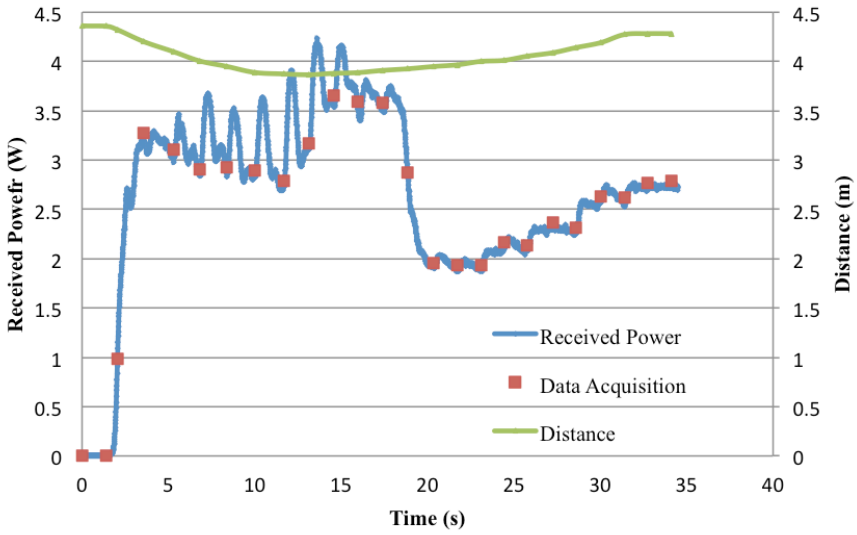


Fig. 5.27 Received Power and Distance (Path 3)

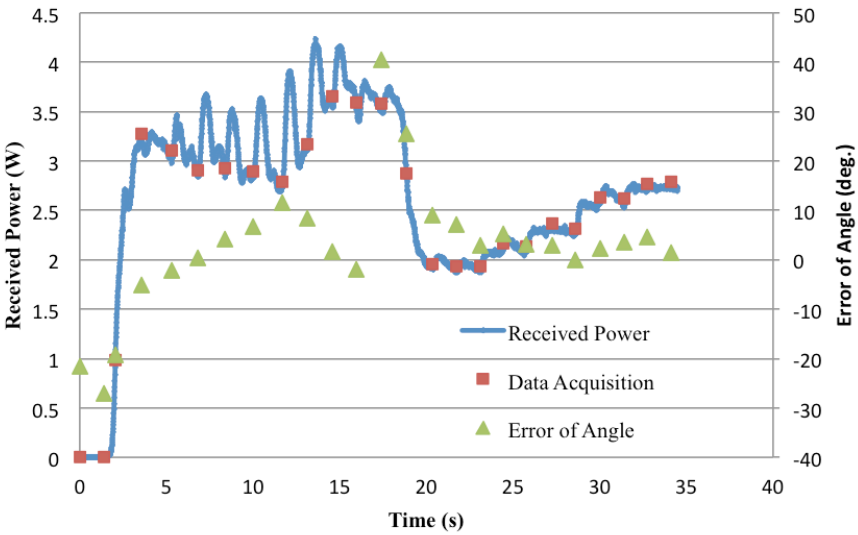


Fig. 5.28 Received Power and Error of Angle (Path 3)

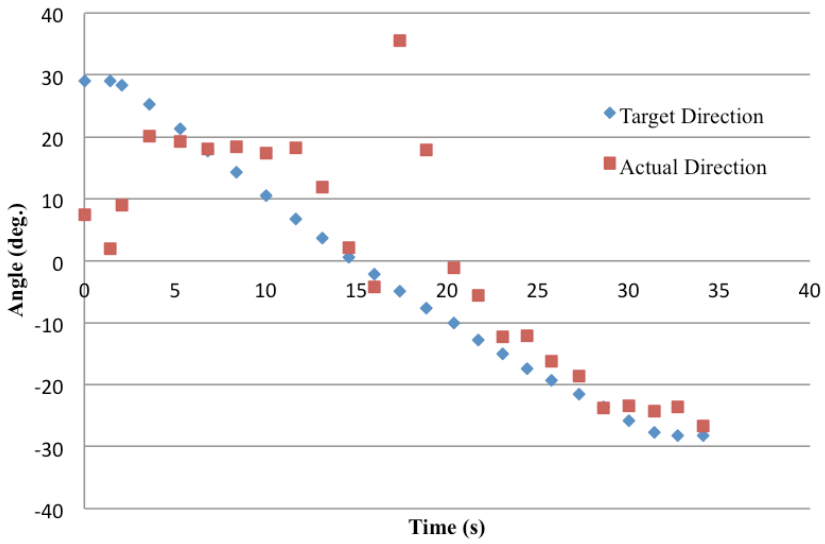


Fig. 5.29 Target Direction and Actual Direction of Rectenna Panel (Path 3)

The results of experiments of path 4, 5, and 6 are as follows (Fig. 5.30 to Fig. 5.41). Programmed paths in these experiments were y-axis direction, while paths 1 to 3 were x-axis direction. According to the path direction of the experiments, no fluctuation was observed, which appeared in the experiments of path 1 to 3. However, the received power quickly decreased as the distance increased.

Angular error of the rectenna panel showed the same tendency with the path 1 to 3. The long interval of position data acquisition inhibited
quick response of the rotation control of the rectenna panel.

d. Path 4

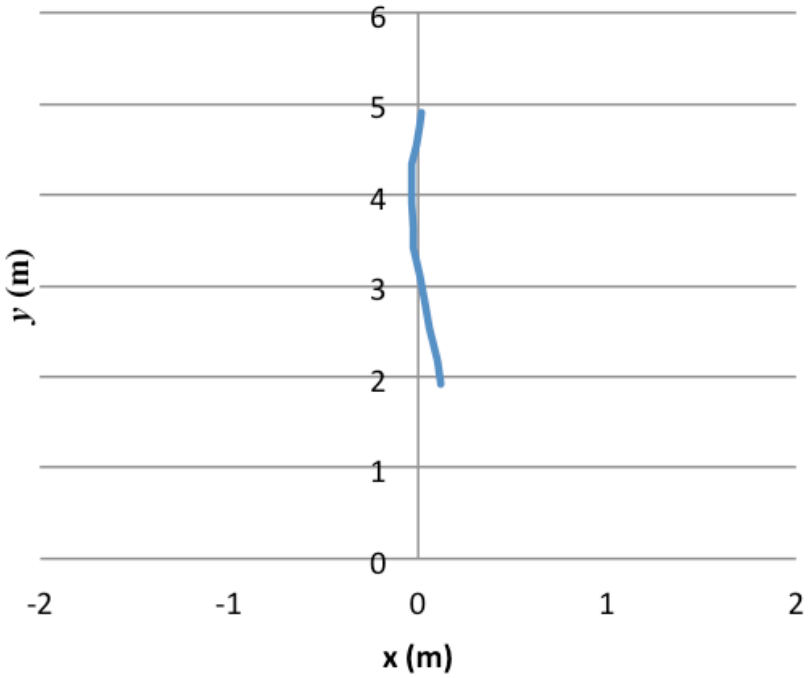


Fig. 5.30 Estimated Path (Path 4)

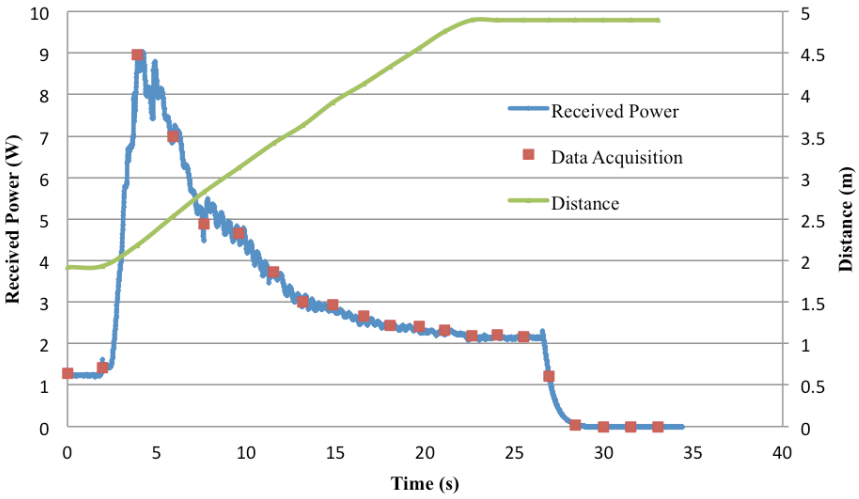


Fig. 5.31 Received Power and Distance (Path 4)

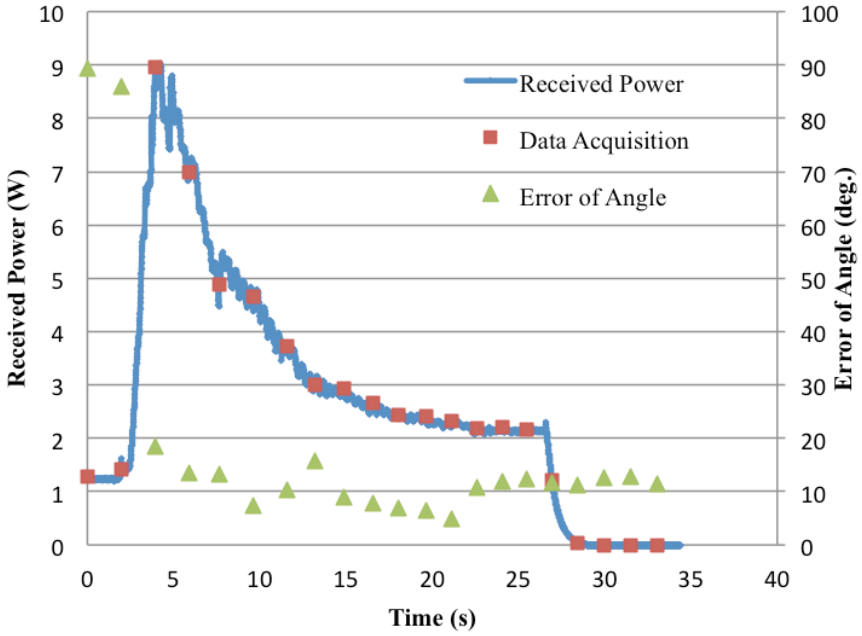


Fig. 5.32 Received Power and Error of Angle (Path 4)

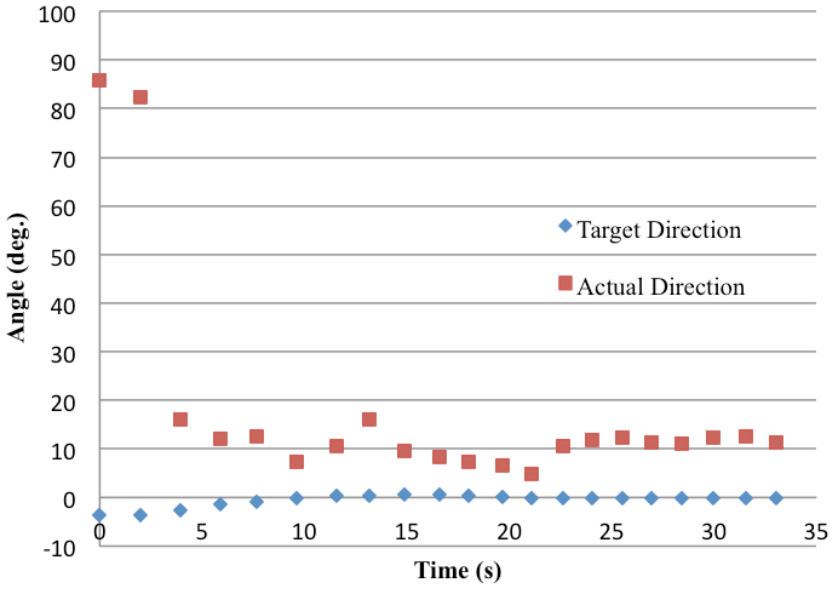


Fig. 5.33 Target Direction and Actual Direction of Rectenna Panel (Path 4)

e. Path 5

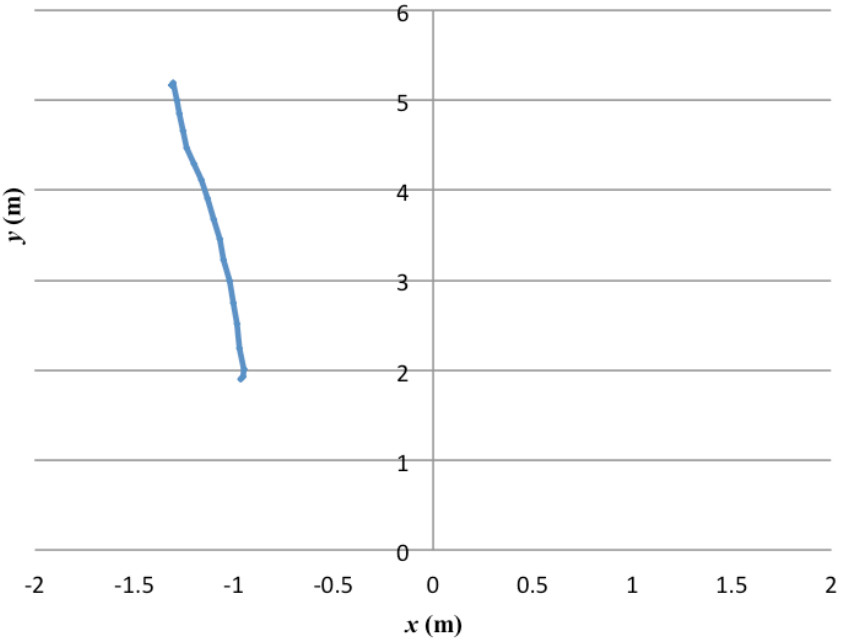


Fig. 5.34 Estimated Path (Path 5)

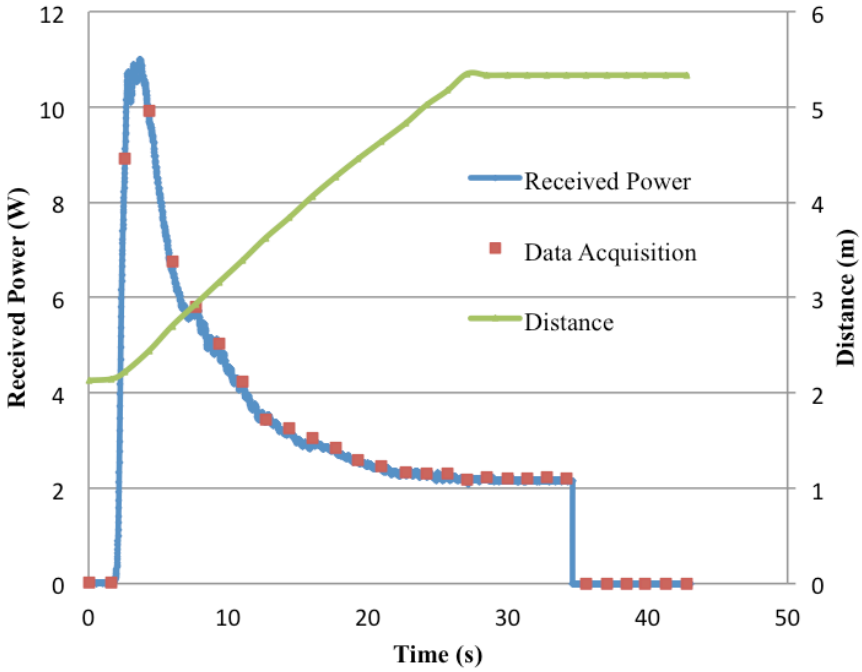


Fig. 5.35 Received Power and Distance (Path 5)

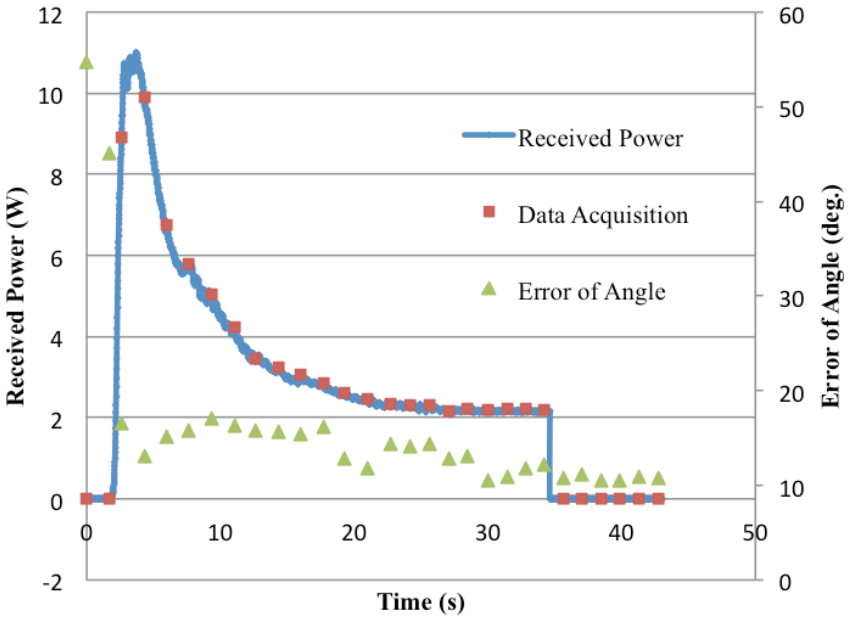


Fig. 5.36 Received Power and Error of Angle (Path 5)

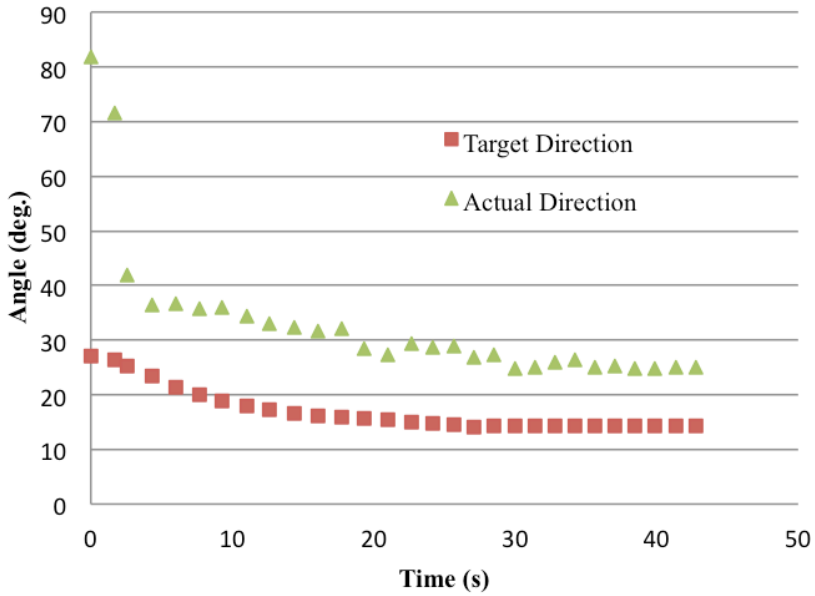


Fig. 5.37 Target Direction and Actual Direction of Rectenna Panel (Path 5)

f. Path 6

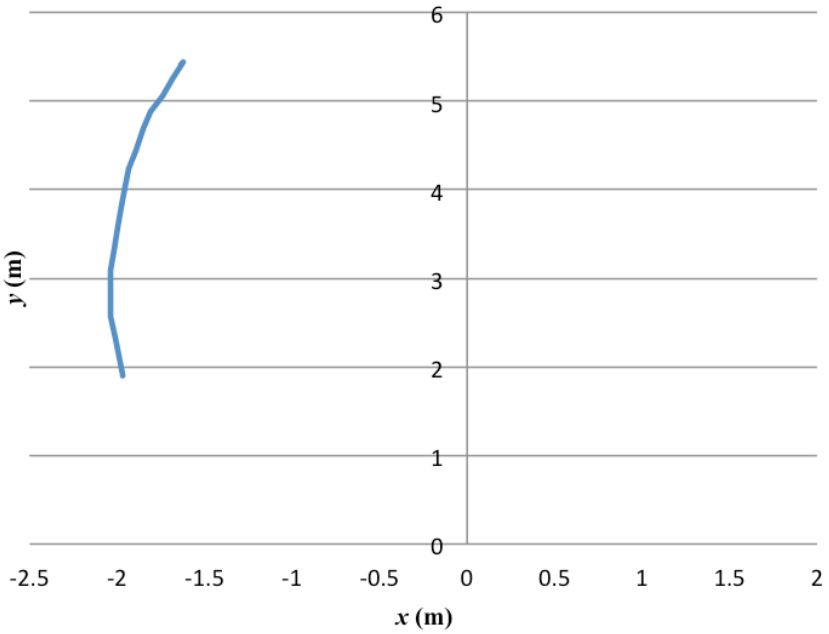


Fig. 5.38 Estimated Path (Path 6)

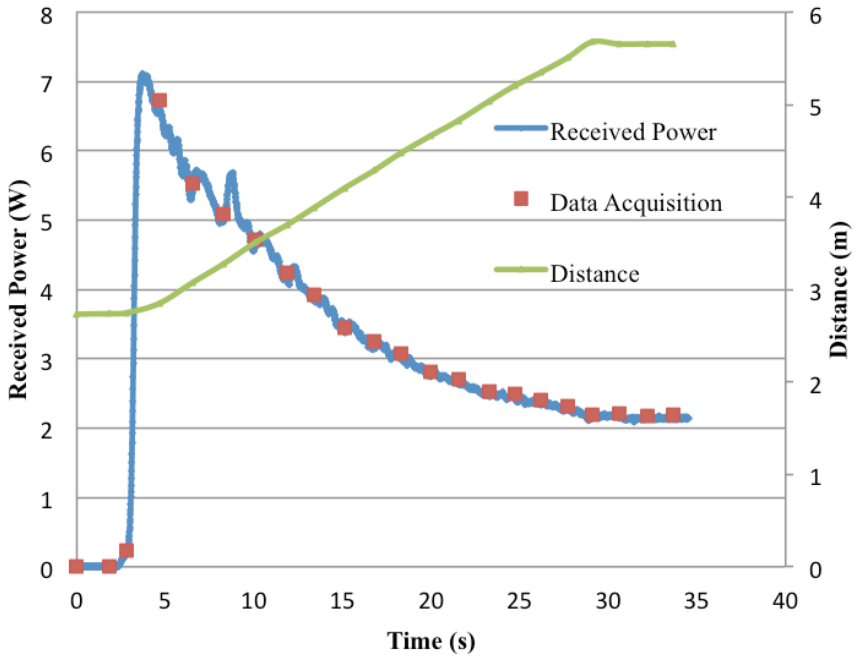


Fig. 5.39 Received Power and Distance (Path 6)

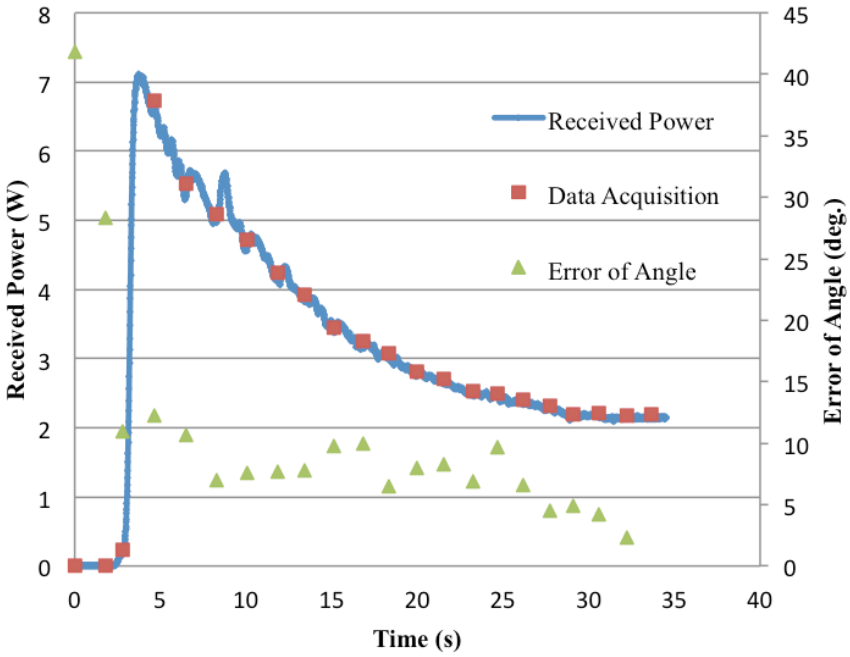


Fig. 5.40 Received Power and Error of Angle (Path 6)

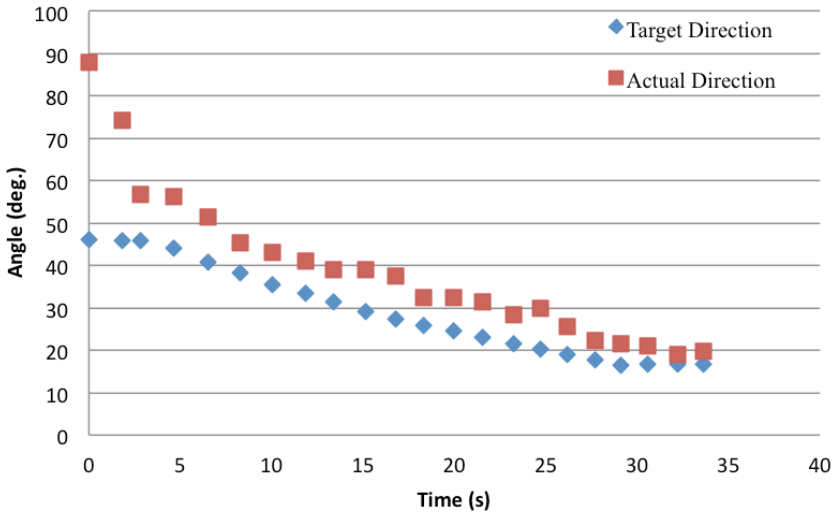


Fig. 5.41 Target Direction and Actual Direction of Rectenna Panel (Path 6)

g. Path 7

The results of path 7 were shown in Fig. 5.42 to Fig. 5.45. This path 7 has the characteristics of the combination of x-axis direction movement and y-axis direction movement. Both fluctuation and quick decrease of received power was observed.

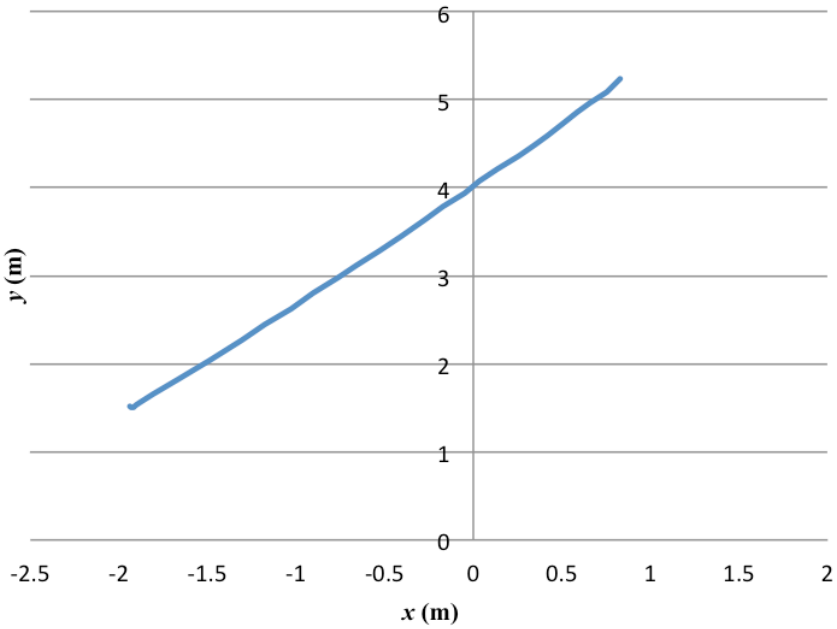


Fig. 5.42 Estimated Path (Path 7)

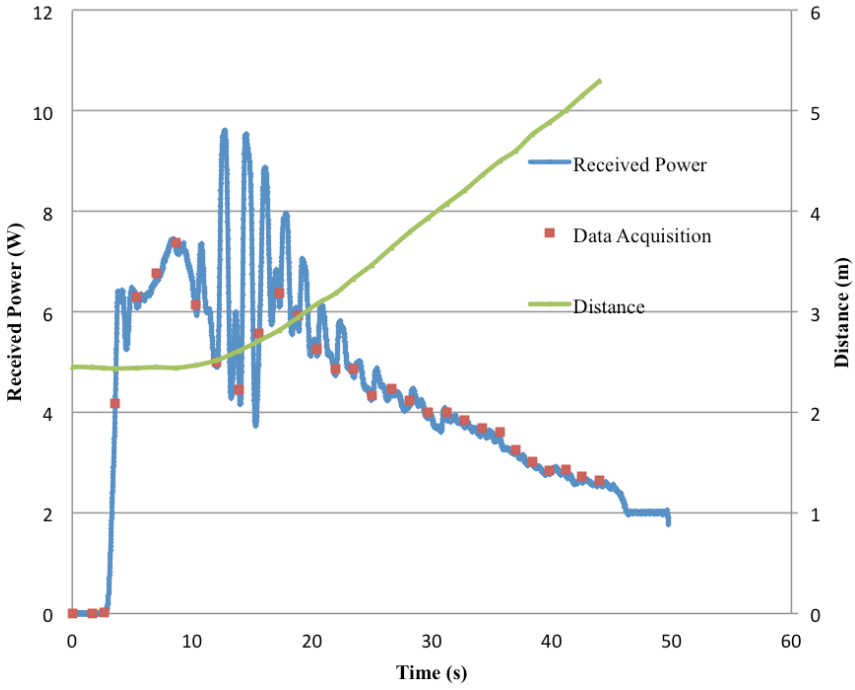

Fig. 5.43 Received Power and Distance (Path 7)

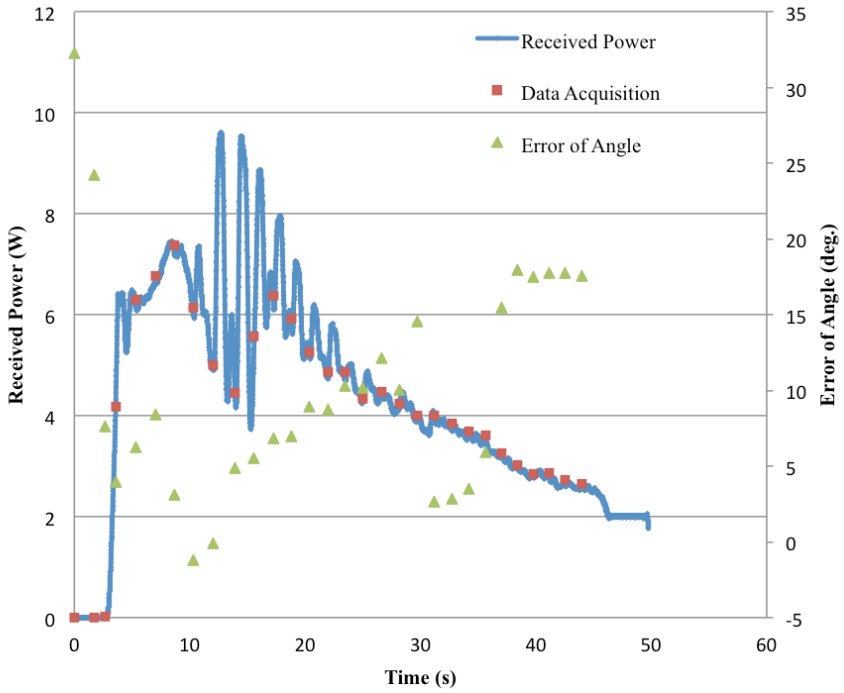


Fig. 5.44 Received Power and Error of Angle (Path 7)

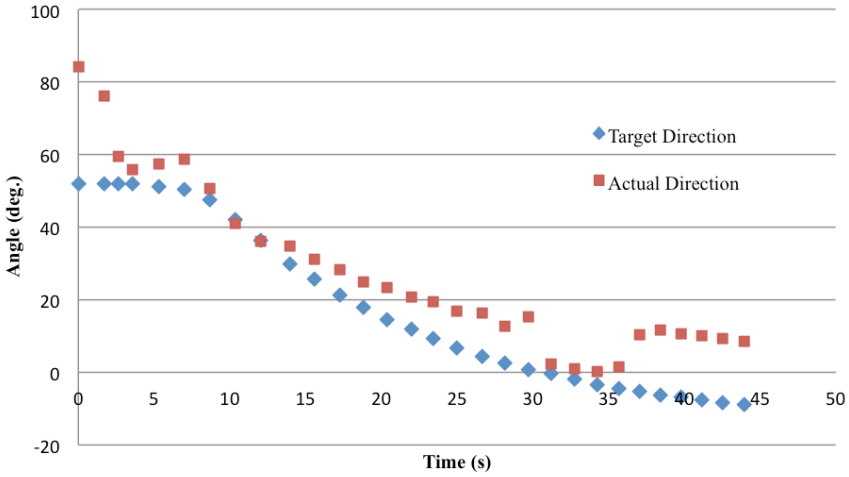


Fig. 5.45 Target Direction and Actual Direction

of Rectenna Panel (Path 7)

2) Received Microwave Power and Motor Power Consumption

To compare received power and vehicle power consumption, the following results were obtained. Experiments of these results were different from the ones in the previous section. Additional measurement of voltage and current of the driving motor and the turntable motor was introduced.

Fig. 5.46 shows the estimated path of path 2. Fig. 5.47 shows the received power and the power consumption of the driving motor and the turntable motor. This graph presents that when the received power was decreased, required power for running exceeded the actual receiver microwave power.

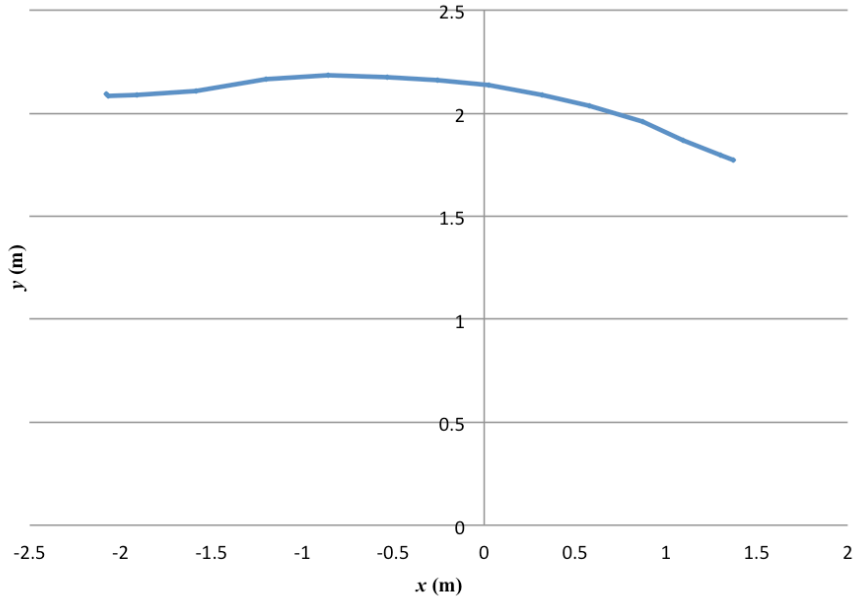


Fig. 5.46 Estimated Path (Path 2)

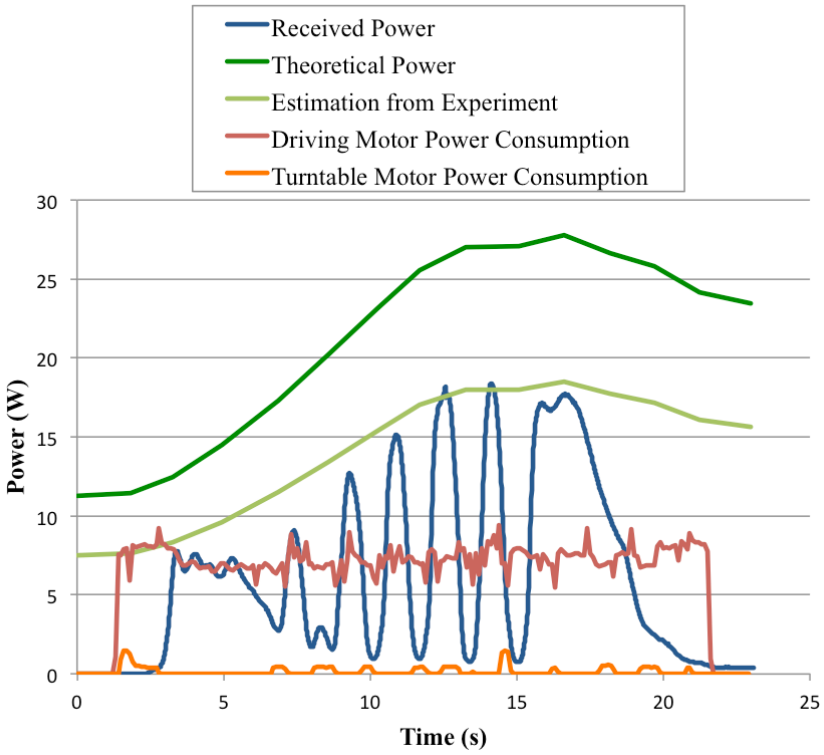


Fig. 5.47 Received Power and Power Consumption (Path 2)

In Fig. 5.47, theoretical power reception and estimated maximum power reception from experiment are also shown. The green curve represents theoretical reception power of 20 rectennas calculated from Friis' transmission formula (Eq. 5.1).

$$P_r = \left(\frac{\lambda}{4\pi L}\right)^2 G_t \, G_r \, P_o \tag{5.1}$$

where $P_r$ [W]: received power, l (m): wave length, $L$ (m): distance between transmitting and receiving antennas, $G_t$: gain of transmitting antenna, $G_r$: gain of receiving antenna, $P_o$ (W): output power. In this calculation l = 0.122 m, $G_t$ = 17 dB (≒ 50.1), $G_r$ = 6 dB (≒ 3.98).

The light green curve shows estimated (calculated) reception power ($P_e$ (W)) of 20 rectennas calculated from Friis' transmission formula and the results of unit test of one patch antenna and the horn antenna.

$$P_e = C\left(\frac{\lambda}{4\pi L}\right)^2 G_t \; G_r \; P_o \tag{5.2}$$

The coefficient *C* is calculated from the patch antenna unit test and is determined as 0.665. This estimated power from the unit test draws nearly an envelope of the actual received power. From this estimated power (envelope), if the tracking response of the transmitting horn antenna and receiving rectenna panel is adequate, the rectennas can provide enough power to the driving and turntable motors.

Fig. 5.48 and Fig. 5.49 show the result of circular path for the same items with the above results. In Fig. 5.49, the power consumption of the driving motor exceeded the theoretical received power. This means that, for this circular path, provided microwave power will not be adequate to drive the vehicle. To cope with this problem, microwave output power has to be increased.

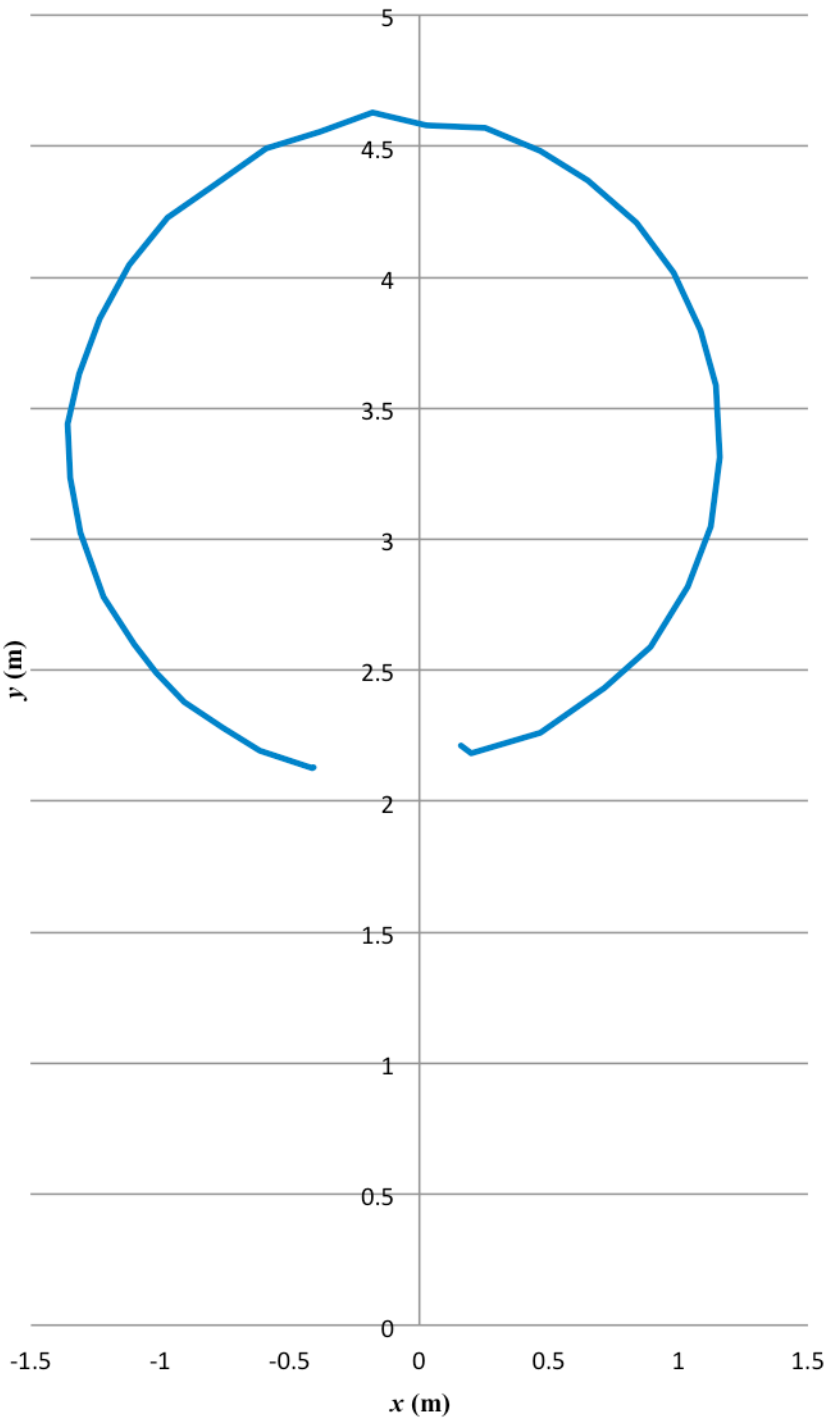


Fig. 5.48 Estimated Path (Circular Path)

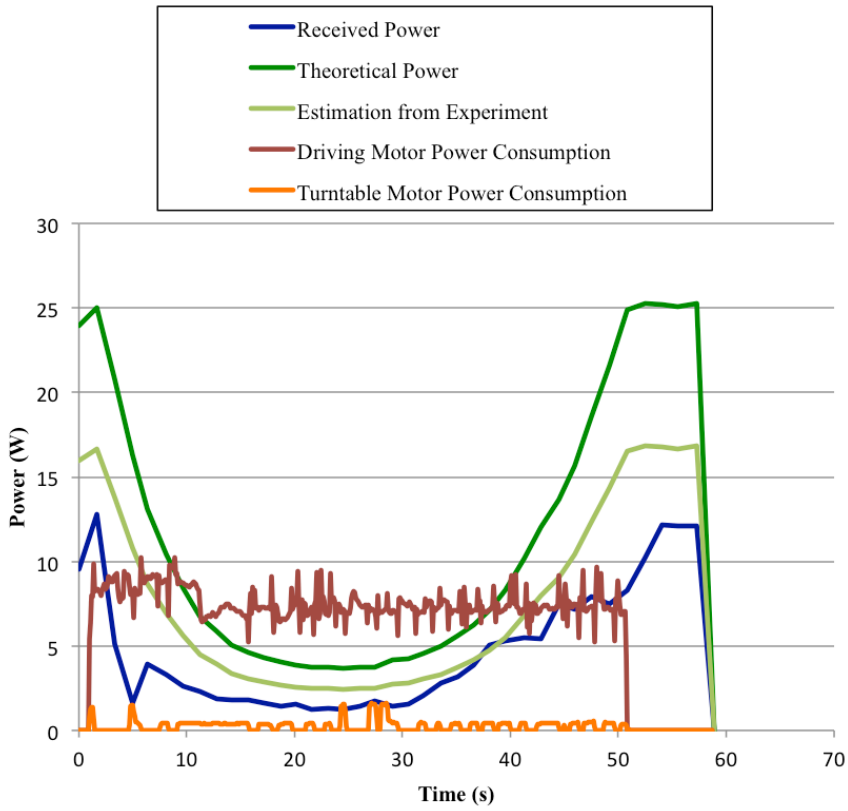


Fig. 5.49 Received Power and Power Consumption (Circular Path)

5.3.4 Path and Power Consumption during Microwave-Driven Running

Experiments of microwave driven running were only conducted for path 4 and path 5, because the microwave power reception in other paths was not enough to control and drive the vehicle.

Fig. 5.50 and Fig. 5.51 are the results of path 4. Due to the shortage of the received power, which was shown in the experiments with the external DC power supply, vehicle ran only about 1 m for the path 4 ($x$ = 0 m). The transmitted power was 800 W in this experiment. Estimating from the point where the vehicle stopped, the distance between the vehicle and the transmitter was about 2.8 m and calculated received total power was 18.1 W. To run the vehicle, constant reception of more than this value was needed.

Fig. 5.52 and Fig. 5.53 are the results of path 5. The same tendency as described above was observed. Shortage of the starting torque of the driving motor is possibly the cause of this result. The mass and the running resistance of the vehicle need to be reduced. More patch antennas are also required to supply adequate power for the

starting torque of the vehicle driving motor.

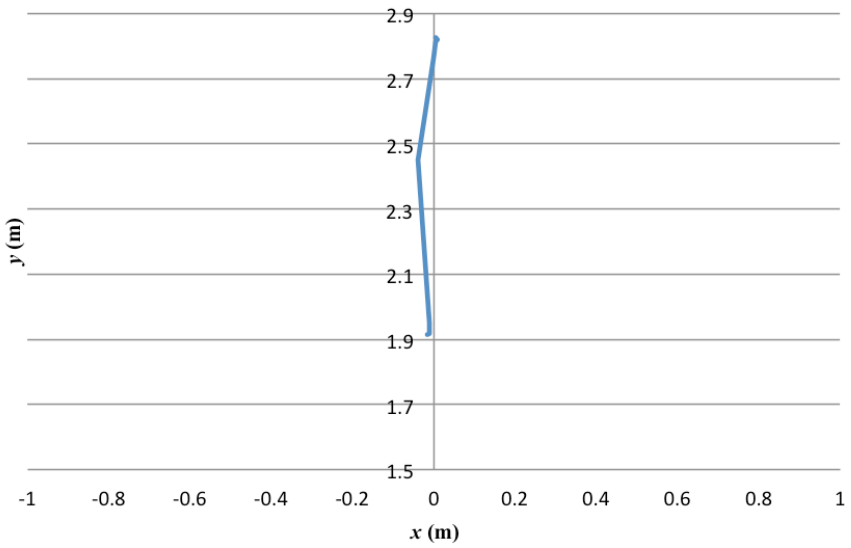


Fig. 5.50 Estimated Path (Path 4)

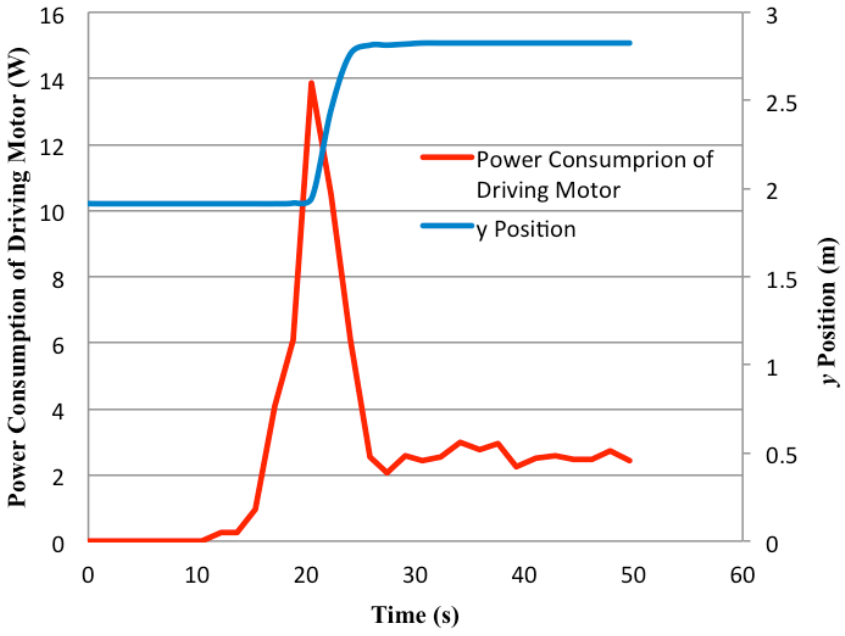


Fig. 5.51 Output Power and Power Consumption (Path 4)

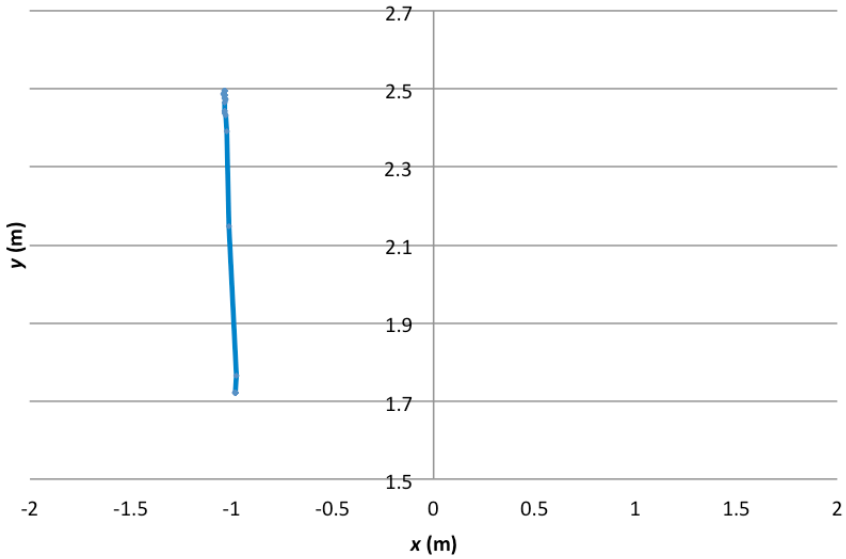


Fig. 5.52 Estimated Path (Path 5)

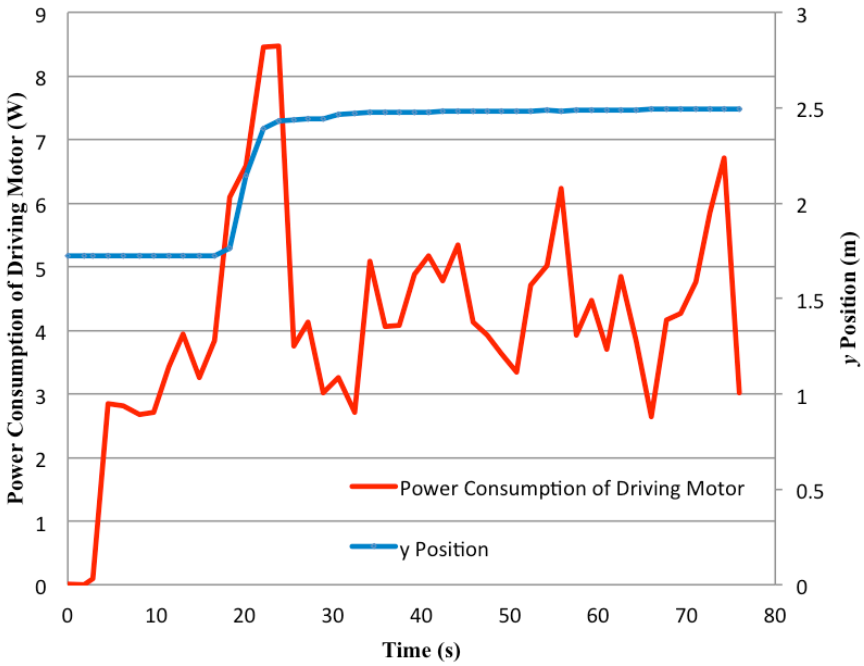


Fig. 5.53 Output Power and Power Consumption (Path 5)

Compared to previously mentioned report in Chapter 4 (Nagano *et al.*, 2007), the results showed relatively higher instability of power transmission and higher fluctuation

of received power due to the low responsibility of the controls of transmitting and receiving antennas. In Nagano's report, a smaller vehicle ran only along the arc shaped track and the distance between the transmitter and the vehicle was kept always the same. In addition to that, the receiving antenna on the vehicle was always faced to the transmitter because of the running truck with arc shape. This enabled the stable transmission and reception of microwave power and the balance of the current capacity was always positive.

Fig. 5.54 shows the ideal receivable power in the field from theoretical equations (Eq. 5.1 and 5.2), transmitting power and number of rectenna under the condition of path 4. From this graph, at 4 m distance, about 18 W power was available.

Fig. 5.55 shows the actual receivable power considering energy loss and efficiency. Fig. 5.56 shows the comparison between ideal and actual available power and distance. From this graph, at 4 m distance, maximum available power was about 12 W. Required power of the vehicle must be les than 12 W from this result.

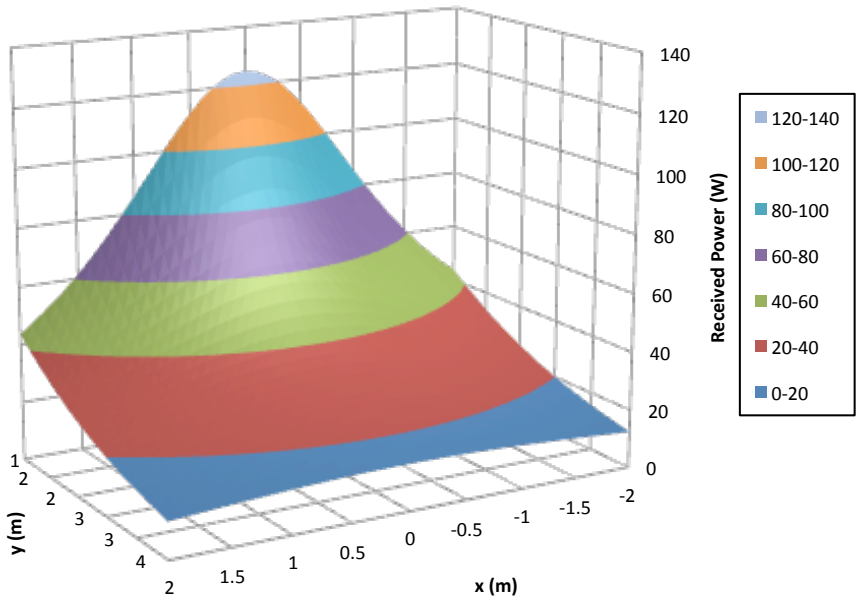


Fig. 5.54 Ideal Power Distribution in the Field

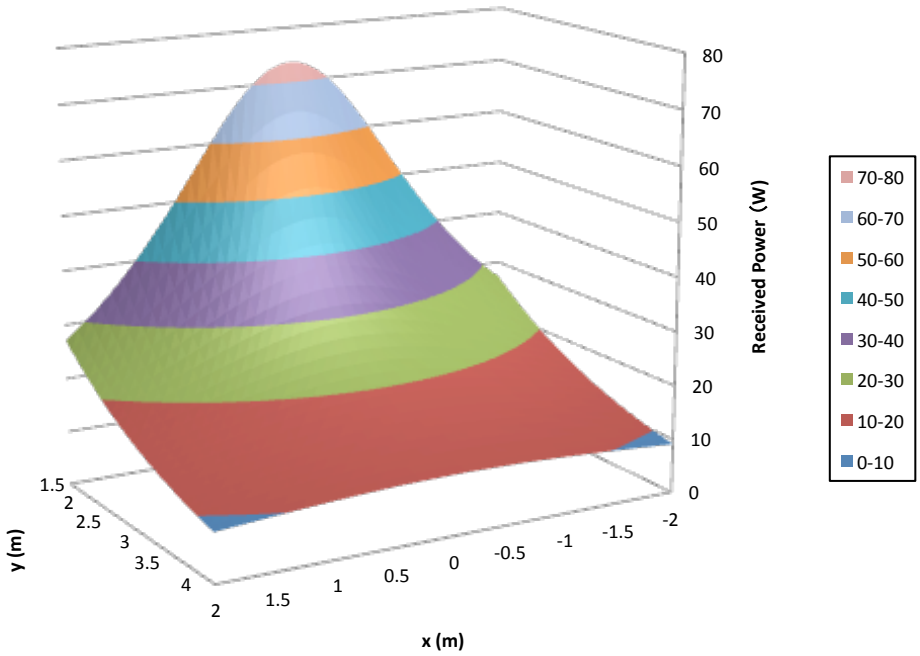


Fig. 5.55 Estimated Actual Available Power Distribution in the Field

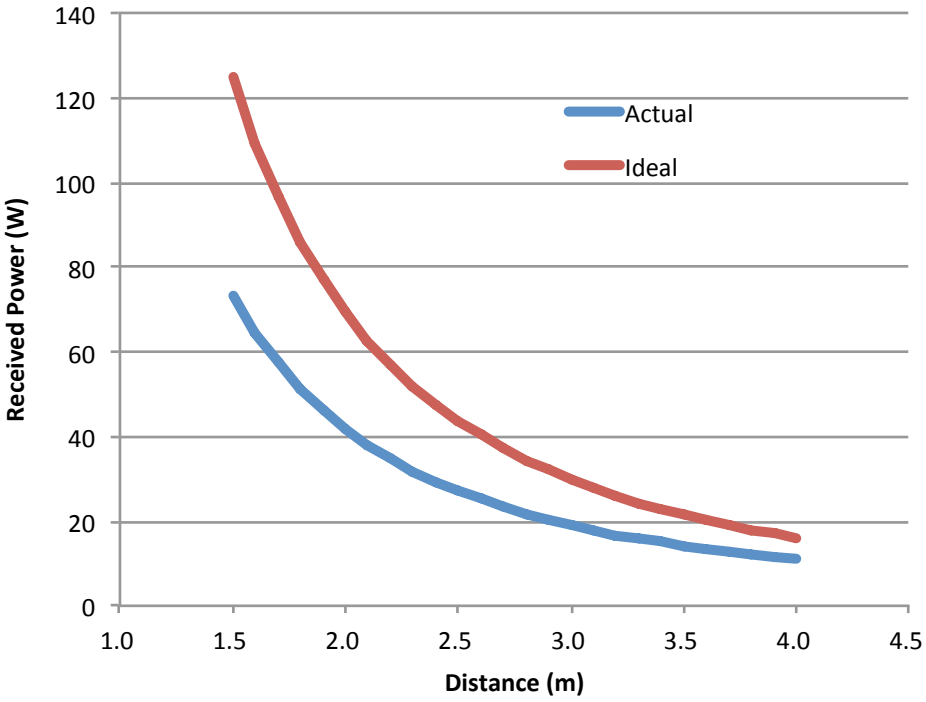


Fig. 5.56 Relation between Distance and Received Power

[References]

Nagano, K., et al. Microwave Power Transmission Experiment Report to the Robot for the Work, Technical Report of IEICE SPA2006-22, 2007.

Nakagawa, S., Y. Yamanaka, K. Ohdoi, J. Miyasaka, H. Nakashima. 2008. Development of an Electric Vehicle by Microwave Power Transmission - Detection of Vehicle's Position using Image Processing. Technical Report of IEICE: SPS2007-21.

Nakagawa, S., Y. Yamanaka, K. Ohdoi, J. Miyasaka, K. Hashimoto, N. SHinohara, T. Mitani. 2009. Development of an Electric Vehicle by Microwave Power Transmission – Fundamental Experiments for Angle Control of Transmission and Receiving Antenna -. Technical Report of IEICE: SPS2008-12.

# 6. Effects of Microwave on Plants

Considering of microwave power transmission in agriculture, effects of microwave on crop must be examined carefully, because the effects are not fully understood.

Various studies on effects of short-time exposure of microwave to plants were conducted. Chen *et al*. reported increase of activities of enzymes (amylase, transaminase, and proteinase) and biophoton emission in *I. Indigotica* cotyledon after exposure to 2.45 GHz, 1.26 $mW/mm^2$ microwave for 8 seconds (Chen *et al*., 2005). Diminution of chlorophyll A and B, and carotenes after exposure of 10.75 GHz, 1 $mW/cm^2$ microwave for 1, 2, 4, and 12 hours on 14 days old Maize (*Zea mays* L.) was also reported (Ursache *et al*., 2009). Roux *et al*. reported rapid molecular response, such as changes of in abundance of stress-related transcripts, *calmodulin-N6*, *cmbp*, and *pin2* in tomato plants caused by 900 MHz, 40 $Vm^{-1}$ and 5 $Vm^{-1}$ microwave exposure for 10 min (Roux *et al*., 2006). They also reported that low amplitude (5 $Vm^{-1}$), short duration (10 min) of 900 MHz EMF evoked the accumulation of *bZIP* mRNA (Vian *et al*., 2006). These studies indicated the effects of microwave to biochemical reactions in plant body.

As a related study of SPS, Skiles conducted experiment of long-term 2.45 GHz microwave exposure (7 weeks) on alfalfa (*Medicago sativa*, L.). The intensities of microwave were weak (0.5-1.2 $mW/cm^2$) and no significant differences of chlorophyll content by SPAD measurement, fresh weight, and dry weight were observed (Skiles, 2006).

Using the same frequency of 2.45 GHz, Jonas exposed relatively high amplitude (600 W) of pulsed microwave with 16 and 60Hz pulses for short time to *Momosa pudica* L. and obtained the change of circadian response by measuring of petiolar folding and recovery (Jonas, 1979). $Ca^{++}$, $K^+$, and $Na^+$ transportation was also discussed in the paper. Jonas also exposed short-period pulsed microwave (600 W) to *Zea mays* L. and obtained the result that the maize seedlings were the most resistant when irradiated at sunrise and the least resistant at sunset (Jonas, 1983). The significant production of carotenes and anthocyanins in plants irradiated at noon was also reported in the paper.

Shmutz *et al*. reported the results of exposure of 2.45 GHz microwave to young spruce and beech trees in field plots. Power flux densities ranged from 0.007 to 300 $W/m^2$, which depends on the location and continuous exposure period was 3.5 years. No visual symptoms of damage were observed during the whole period. During the first 2

years, negative relationship between power flux density and foliar concentrations of calcium and sulfur in beech trees was found. However, in the third year these effects were not found (Shmutz *et al*., 1996).

The papers mentioned above reported inner plant changes under short-term pulsed microwave of high intensity, or long-term or extra long-term exposure of low intensity continuous microwave that resulted inner substance change and no outer changes. However, there is a possibility that differences of outer figure caused by inner biochemical changes may take long time and disappear after a certain period. Short-term and extra long-term differences may be hidden by disturbance from environment or homeostasis. In addition to the exposure time, intensity of microwave can be an important factor. Necessary level of intensity to cause the changes of plant growth is not determined.

To determine the effects on outer figure on plants, experiments in strictly controlled environment should be conducted. In this chapter, two studies of microwave effects on plants are described. One is a study on 2.45 GHz microwave effects on the germination of *Spinacia oleracea*. The other is a study on effects of long-term exposure of microwave at certain intensity levels effects on growth of *Spinacia oleracea* in soil under controlled environments of growth chamber. In both studies, growth measurement of plants after exposure of microwave was conducted to determine the existence of the effects.

## 6.1 Effects on Germination Stage

### 6.1.1 Distinction between Thermal and Non-Thermal Effect

Direct measurement of temperature inside plant body under ongoing growth is not easy because sensors inserted into the plants might affect the growth. To obtain non-destructive experiments, measurement of temperature characteristic of plant growth was introduced. If the effect is thermal, the curve of the relation between temperature and growth will shift horizontally under microwave exposure (Fig. 6.1) because the real temperature of the plants will be higher than atmospheric temperature, while the curve will shift vertically, if the effect is non-thermal, which will cause simple increase or decrease of growth at each temperature (Fig. 6.2). There could be the combination of

these two effects, which cause the both horizontal and vertical shift of the temperature characteristic.

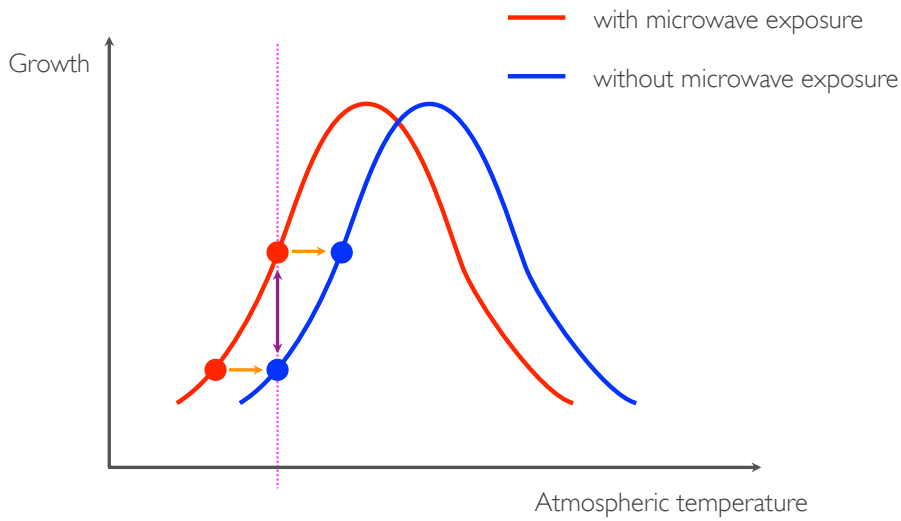


Fig.6.1 Thermal Effect on Growth

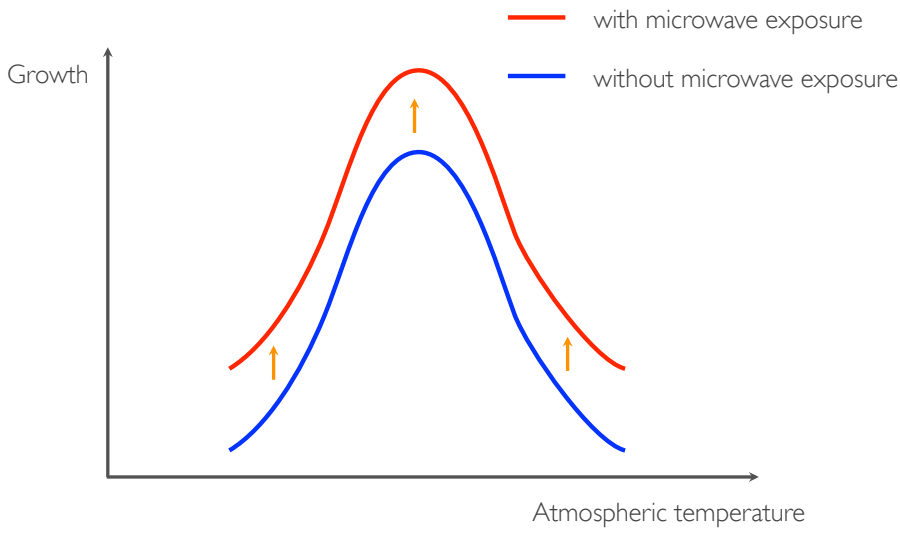


Fig.6.2 Non-Thermal Effect on Growth

### 6.1.2 Materials and Methods

1) Seeds and Germination Beds

Germination beds were made from vinyl chloride pipes. The diameter of the beds is 45 mm and the height is 60 mm. The top of the beds is covered by fiber glass mesh (18x14 mesh size). The sidewall of the beds has holes, which ensure water flow under the mesh (Fig. 6.3). Total 20 germination beds were used for each experiment.

Spinach naked seeds ('Try', Takii & Co., Ltd) were selected for this study. Naked process removes the shell of the seeds and enhances the germination rate. Fifty seeds were placed on the mesh of each bed. Thus, total 1000 seeds were sowed for one experiment.

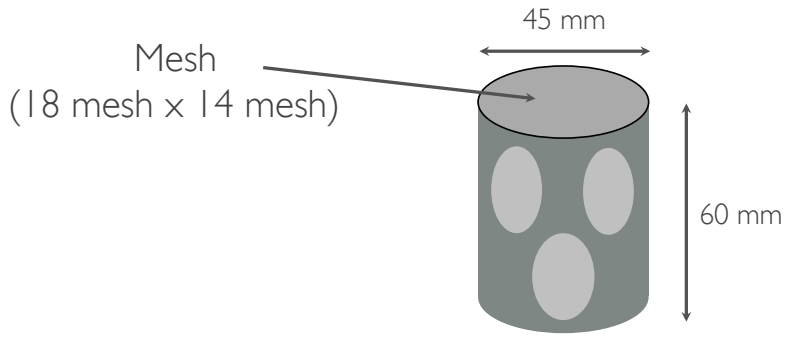


Fig. 6.3 Germination Bed

2) Growth Chamber

Twenty germination beds with 50 spinach seeds for each were placed in a water container (Fig.6.4). Depth of water was kept the same as the height of germination beds by constant water feed and overflow. An aspirator was installed to stir the water to eliminate uneven of water temperature. The water container was placed in a growth chamber (Takayama NS360), inside of which was covered with microwave absorber (Fig. 6.6, Fig. 6.7). Inside atmospheric temperature was controlled within ±1.0°C. Fluctuation of water temperature was within ±0.3°C. Water temperature showed from (preset temperature - 0.5) to preset temperature + 4.0) °C according to preset temperature. Fig. 6.5 shows a photo of the germination beds with seeds in the water container.

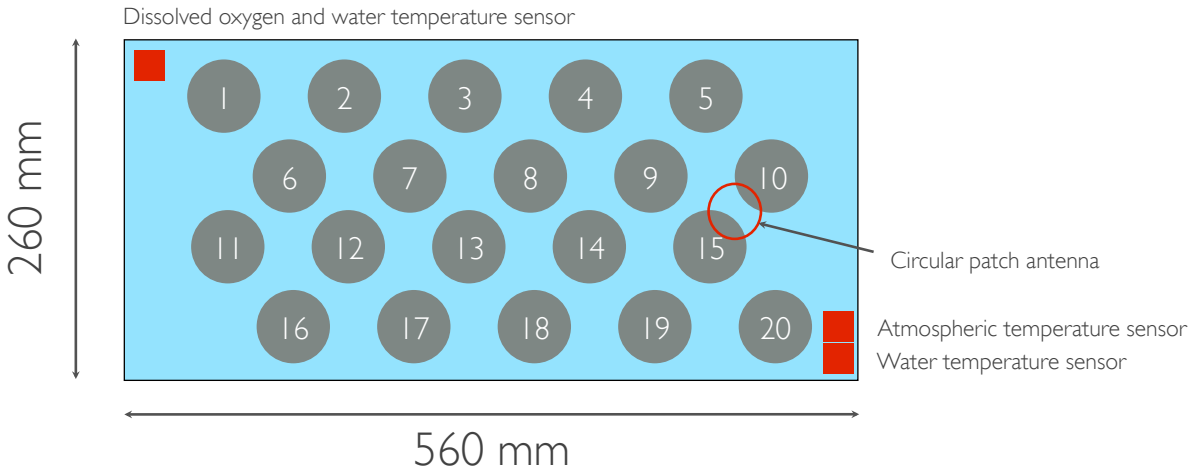


Fig. 6.4 Germination Beds in Water Container

Fig. 6.5 Seeds and Germination Beds in Water Container

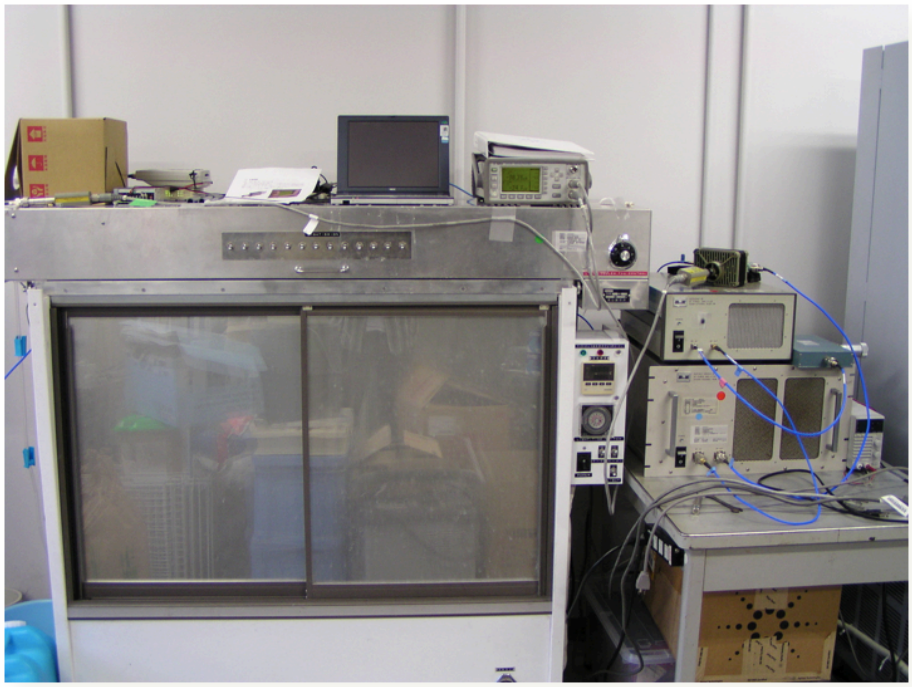

Fig. 6.6 Growth Chamber

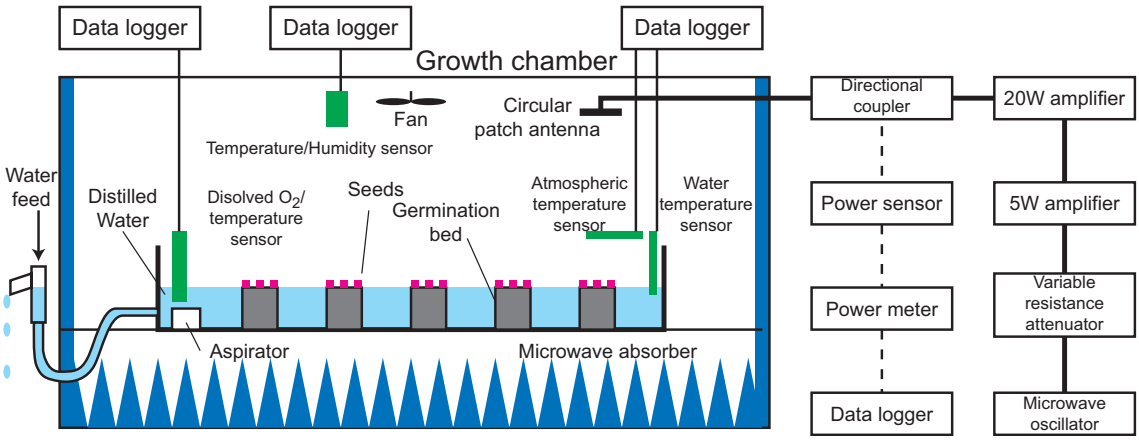


Fig. 6.7 Total System of Experiment

3) Microwave Exposure System

Microwave generated by an oscillator (Tokyo Keiki Inc. TSVF-NB-F2400M-01) was adjusted using a variable resistance attenuator (Nihon Kosyuha Co., Ltd. AT-NJ-801) and amplified through 5W amplifier (R & K Co., Ltd. A250HP-R) and 20W amplifier (R & K Co., Ltd. A2040-4643-R). Microwave was split by a directional coupler (SPC

Electric Corporation 5D906) and was sent to a circular patch antenna installed on the ceiling of the chamber and to a power sensor.

Fig. 6.7 shows the diagram of the chamber and the measurement equipment.

4) Measurement Method

Atmospheric temperature, humidity and water temperature were measured and logged by TR-71Ui and TR-72Ui (T & D Corporation). Dissolved oxygen was also measured by DO-17SD (Sato) because dissolved oxygen in water affects seed germination. Microwave output through the directional coupler was measured by a power sensor (Agilent Technologies, 8481B) and a power meter (Agilent Technologies, E4419B) and logged by an A/D converter and a notebook PC. After experiments, individuals of germinated seeds were scanned by an image scanner (Canon, Canoscan8200F) and stored as bitmap files in a PC. Plant growth was automatically measured by processing the bitmap images using software written in C language on Microsoft Visual Studio 2010.

Automatically measured items of plant growth were perimeter and area of roots. From the perimeter and the area, the following pseudo volume $V$ ($mm^3$) was calculated, using the Equation 6.1. This $V$ is considered to present virtual volume of a root.

$$V = \pi \left( \frac{1}{2} \frac{area}{\frac{perimeter}{2}} \right)^2 \left( \frac{perimeter}{2} \right) = \frac{\pi}{2} \frac{(area)^2}{perimeter} \qquad (6.1)$$

6.1.3 Experiments

At each location of a germination bed, microwave power density was measured before starting the experiments. The container with water was placed and the growth chamber was activated. After couple of hours of temperature stabilization period, 20 germination beds with 50 seeds were placed in the water and water level was adjusted. After 96 hours of germination period, individuals were scanned with resolution of 1200 dpi and saved as bitmap files. From these image files perimeter, area, and virtual volume (calculated from perimeter and area) were measured using an original image processing software. Table 6.1 shows the experimental conditions.

Table 6.1 Experimental Conditions

| | |
|---|---|
| Spinach cultivar | Try (Takii Co., Ltd.) |
| Number of seeds for one experiment | 1000 |
| Number of seeds for one bed | 50 |
| Number of germination bed | 20 |
| Experimental period (hour) | 96 |
| Preset temperature (°C) | 12, 20, 30, 35 |
| Light condition | Dark condition |
| Nourishing solution | Distilled water |
| Microwave power density ($mW/cm^2$) | 0.0, 0.4 - 8.1 |

### 6.1.4 Results

1) Temperature, Humidity and Dissolved Oxygen

During the experiment, atmospheric and water temperature, temperature and humidity near ceiling, and dissolved oxygen were measured. Table 6.2 shows the measured value of these items. In Table 6.2, 'm' in the left column means 'with microwave exposure. Values of dissolved oxygen of 12ºC with out microwave exposure and 35ºC with microwave exposure are missing because of the trouble of the dissolved oxygen meter.

Table 6.2 Temperature, Humidity and Dissolved Oxygen

| | Temperature around seed bed | | Temperature near ceiling | | Dissolved $O_2$ and water temperature | |
|---|---|---|---|---|---|---|
| | Atmospheric (ºC) | Water (ºC) | Atmospheric (ºC) | Humidity( %) | dissolved $O_2$ (mg/L) | Water (ºC) |
| 12 ºC | 12.48 | 11.79 | 12.49 | 68.83 | | |
| m, 12 ºC | 12.67 | 11.43 | 11.97 | 67.55 | 9.85 | 11.55 |
| 20 ºC | 19.92 | 18.56 | 20.11 | 69.18 | 7.56 | 18.59 |
| m, 20 ºC | 21.08 | 19.15 | 20.60 | 67.77 | 7.49 | 19.18 |
| 30 ºC | 29.35 | 26.20 | 29.18 | 65.71 | 6.46 | 26.05 |
| m, 30 ºC | 30.14 | 26.88 | 29.31 | 67.49 | 6.20 | 29.99 |
| 35 ºC | 33.59 | 29.48 | 33.97 | 57.33 | 5.89 | 29.64 |
| m, 35 ºC | 34.24 | 29.90 | 34.00 | 58.22 | | |

2) Microwave Power Density

Estimated microwave power density at each point of the germination beds is shown in Table 6.3. These density were calculated from the measure value before the experiments and measured output power of microwave during the experiments.

Table 6.3 Microwave Power Density

| | Microwave Power Density ($mW/cm^2$) | | | |
|---|---|---|---|---|
| Germination Bed No. | 12ºC | 20ºC | 30ºC | 35ºC |
| 1 | 0.39 | 0.40 | 0.41 | 0.39 |
| 2 | 0.53 | 0.53 | 0.55 | 0.53 |
| 3 | 1.21 | 1.22 | 1.26 | 1.22 |
| 4 | 3.71 | 3.75 | 3.85 | 3.72 |
| 5 | 6.99 | 7.07 | 7.26 | 7.02 |
| 6 | 0.85 | 0.86 | 0.89 | 0.86 |
| 7 | 1.38 | 1.40 | 1.44 | 1.39 |
| 8 | 3.27 | 3.31 | 3.40 | 3.29 |
| 9 | 6.35 | 6.42 | 6.59 | 6.37 |
| 10 | 7.97 | 8.06 | 8.28 | 8.01 |
| 11 | 0.87 | 0.88 | 0.90 | 0.87 |
| 12 | 1.68 | 1.70 | 1.74 | 1.69 |
| 13 | 2.57 | 2.60 | 2.67 | 2.59 |
| 14 | 5.32 | 5.38 | 5.52 | 5.34 |
| 15 | 7.91 | 8.00 | 8.21 | 7.95 |
| 16 | 0.75 | 0.76 | 0.78 | 0.75 |
| 17 | 1.74 | 1.76 | 1.81 | 1.75 |
| 18 | 2.49 | 2.52 | 2.59 | 2.51 |
| 19 | 4.88 | 4.94 | 5.07 | 4.91 |
| 20 | 7.27 | 7.35 | 7.55 | 7.30 |

3) Spinach Roots and Scanned Images

After 96 hours of growth roots on the germination beds were taken and scanned by the image scanner. Fig 6.8 shows the seeds after 96 hours' germination and Fig. 6.9 shows examples of scanned root image with and without microwave exposure.

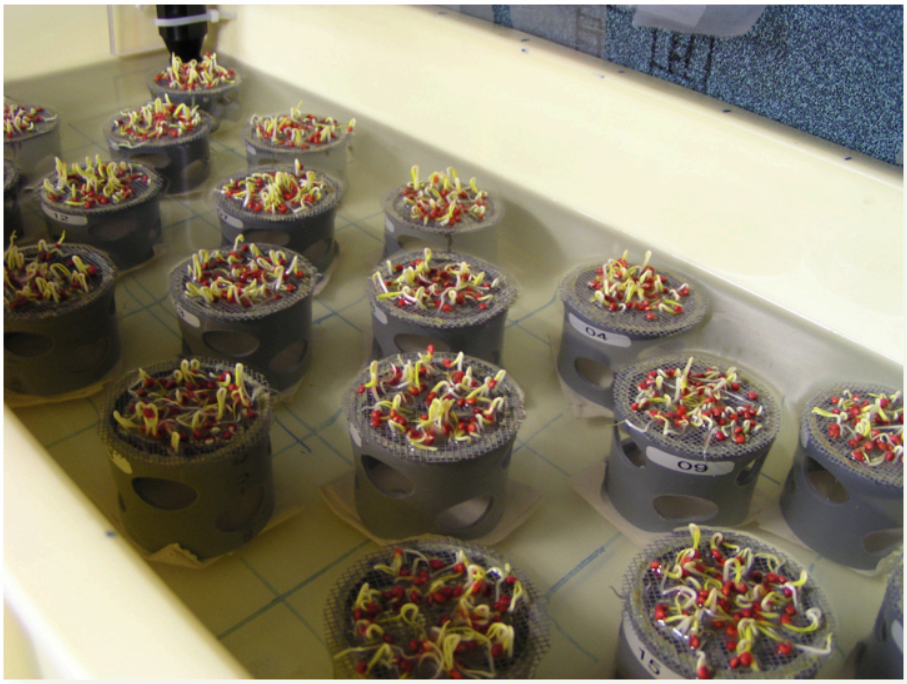

Fig. 6.8 Seeds after Germination

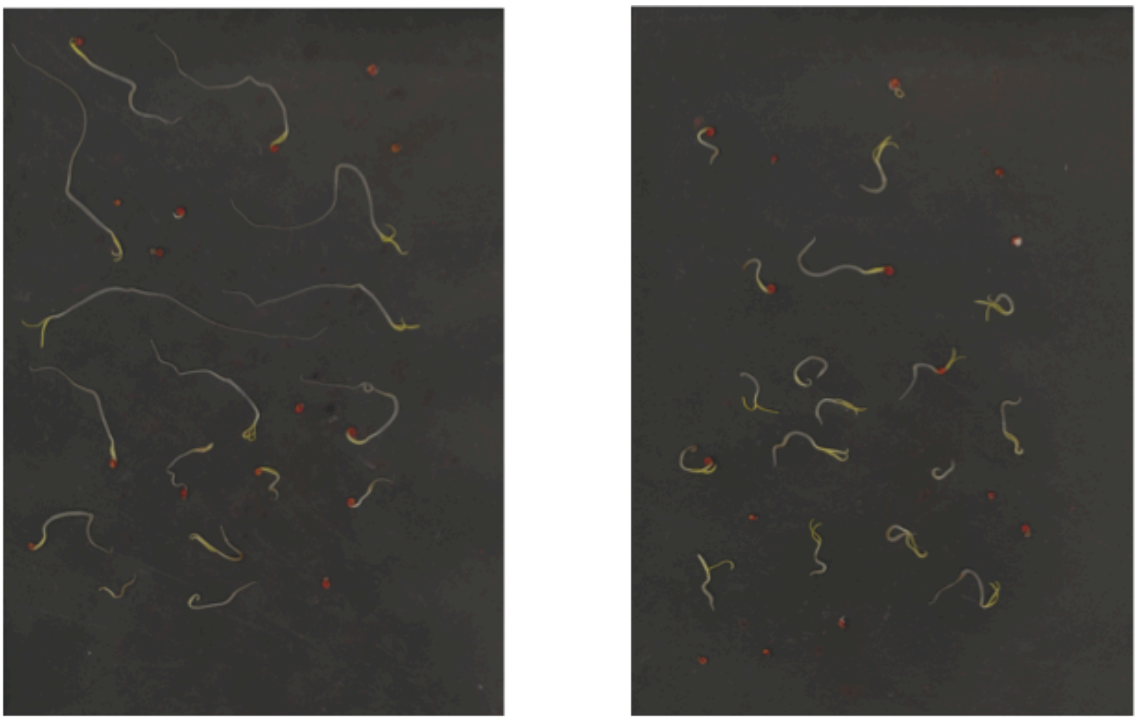

(a) With Microwave Exposure (b) Without Microwave Exposure

Fig. 6.9 Example of Scanned Root Image (35°C)

4) Dry Matter

Comparison between dry matter of seed before experiment and dry matter of plant body after germination was conducted. Fig. 6.10 shows the decreased dry matter after experiments.

In microwave exposure plots, for all temperatures, decrease of dry matter was larger than control plots. During the experiment, plants were not fertilized and no light was lit. Thus, in the experiment plots, more consumption of nutrition in seed was observed compared to the control plots. This suggests larger growth of microwave exposure plots.

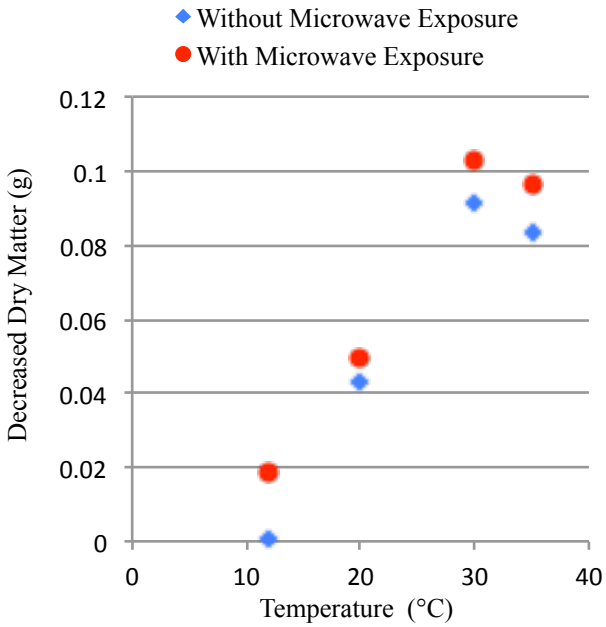


Fig. 6.10 Decreased Dry Matter

5) Temperature and Growth

Fig. 6.11, 6.12, and 6.13 show the relationship between temperature and growth of roots (mean area, mean perimeter, and mean *V*). From these graphs, clear distinction between thermal and non-thermal effect was not obtained because these graphs do not show the similar tendency as Fig. 6.1 or Fig. 6.2. However, except 30ºC, these graphs show the similar tendency with non-thermal pattern of Fig. 6.2.

Analysis of variance (ANOVA) at the 5 % level of significance was conducted between control and experiment plots of the same temperature. Except area and *V* of 30ºC, all showed the significant difference. These results suggest the existence of

non-thermal effect of microwave on plant growth.

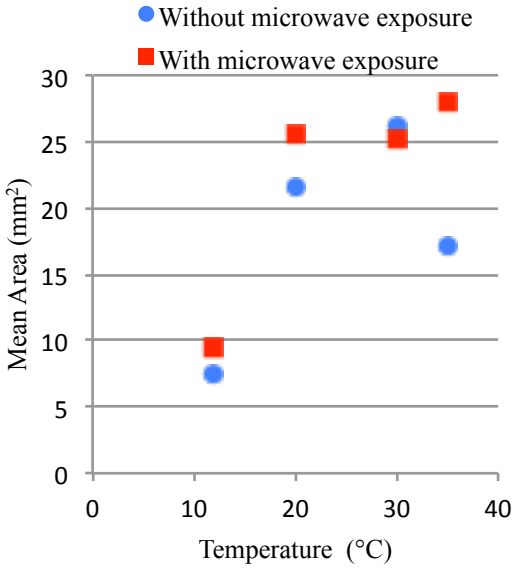


Fig. 6.11 Mean Area and Temperature

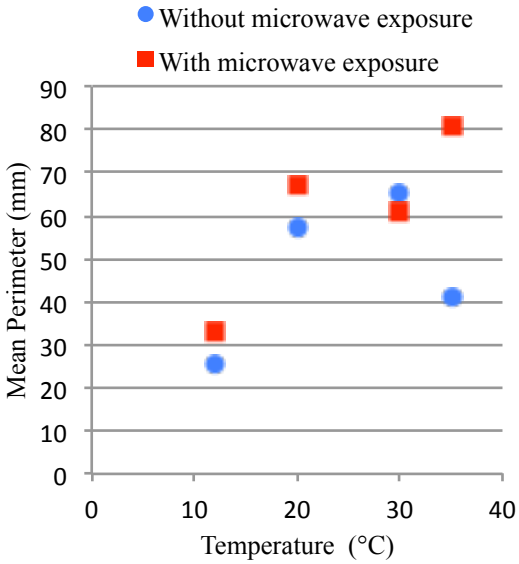


Fig. 6.12 Mean Perimeter and Temperature

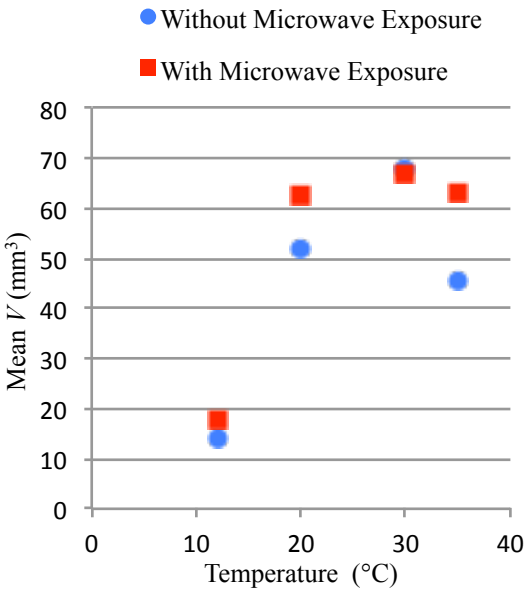


Fig. 6.13 Mean *V* and Temperature

6) Distribution of Measured Value

Fig. 6.14, 6.15, and 6.16 show the distribution of each measured value for all samples in both control and experiment plots. Between control and experiment plot, different distributions were observed. However, no abnormal pattern of distribution was found. These results are not adequate to provide enough information for discussion of thermal and non-thermal effects.

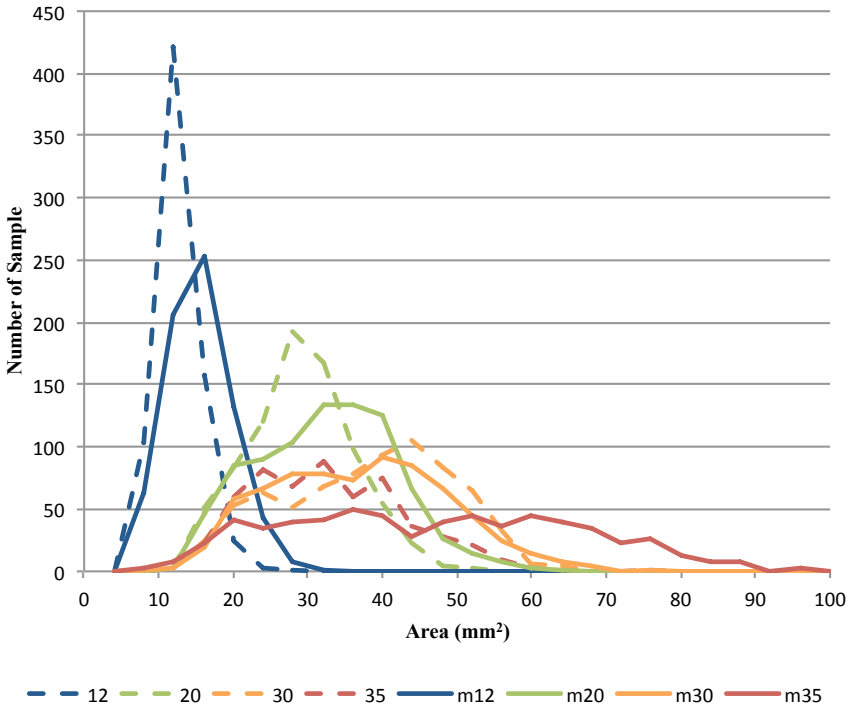


Fig. 6.14 Distribution of Area

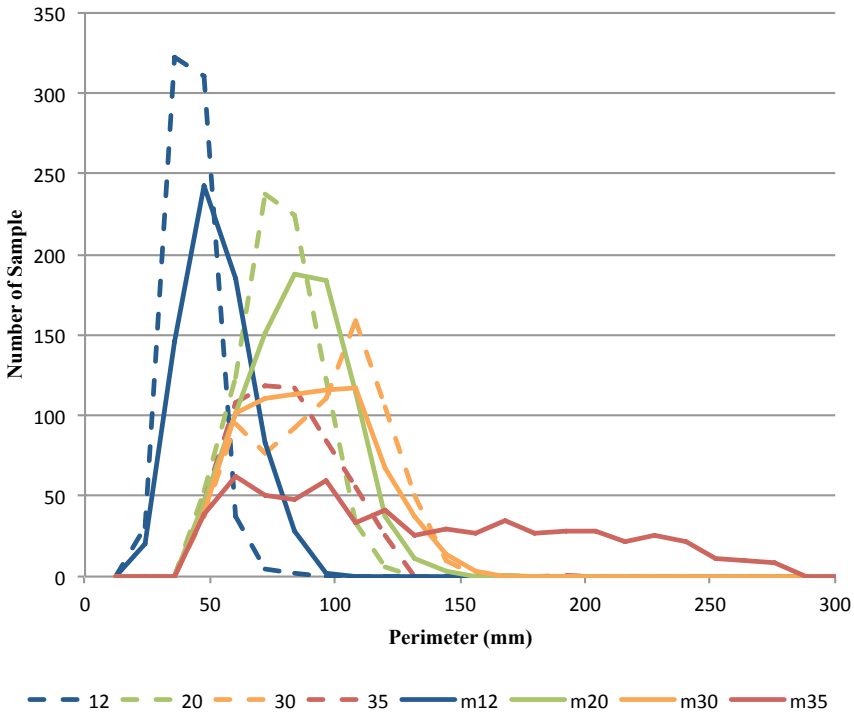


Fig. 6.15 Distribution of Perimeter

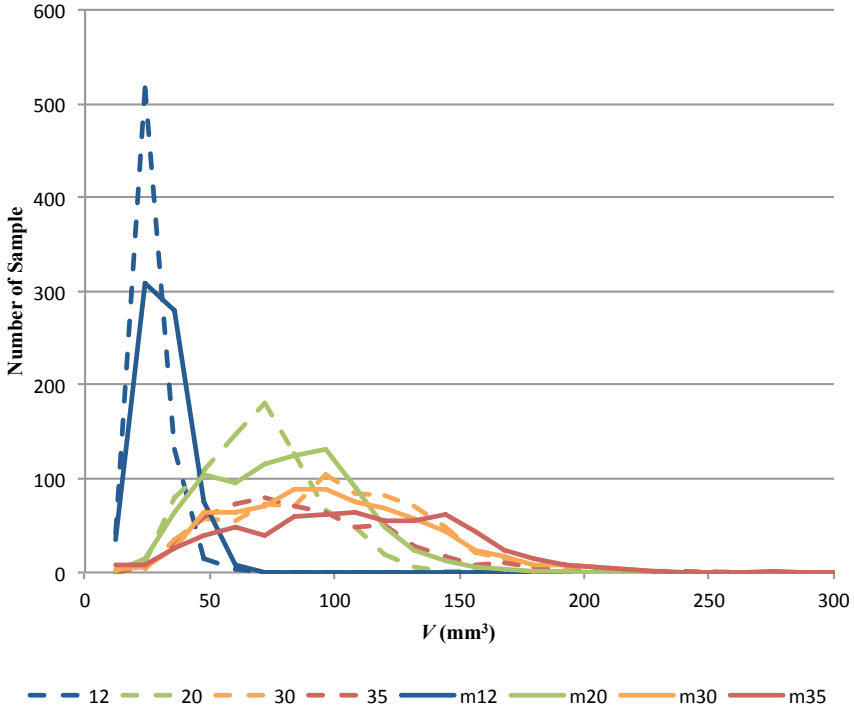


Fig. 6.16 Distribution of *V*

7) Power Density and Growth

Relations between growth and microwave power density for each germination beds are shown in Fig. 6.17, 6.18, and 6.19. In the experiments with microwave exposure, correlation cannot be shown in these graphs. However, difference between values without exposure (0.0 mW/cm$^2$) and those with exposure is shown in these graphs, which indicated the significance mentioned above.

If temperature changed according to power density, growth amount might differ, which is derived from thermal effect. However there is no correlation between growth and power density. If these results were derived from thermal effect and water temperature was kept equally by the aspirator, significance mentioned above cannot be explained. This suggests the existence of non-thermal effect of microwave, though it was not shown clearly.

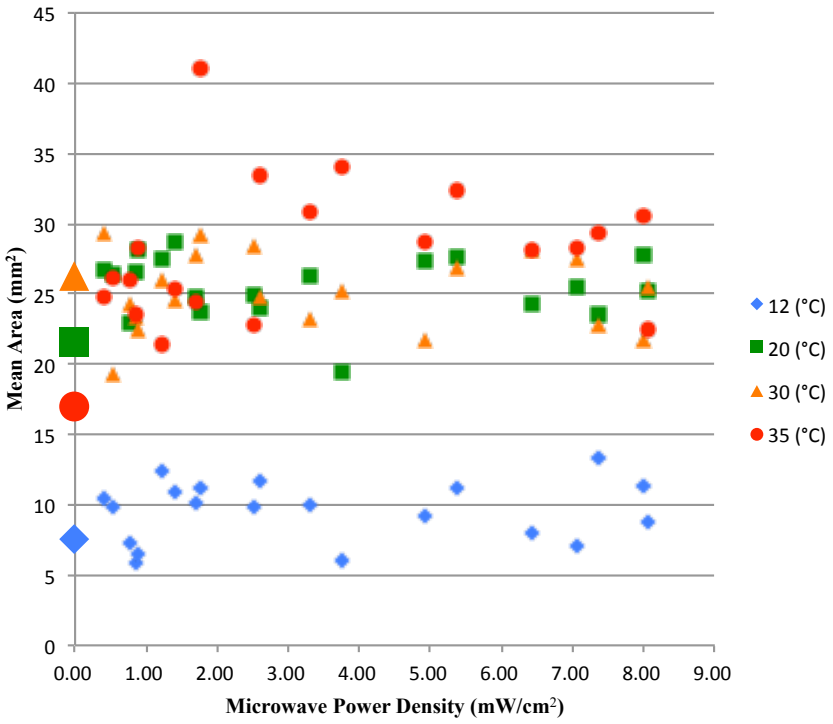


Fig. 6.17 Mean Area and Power Density

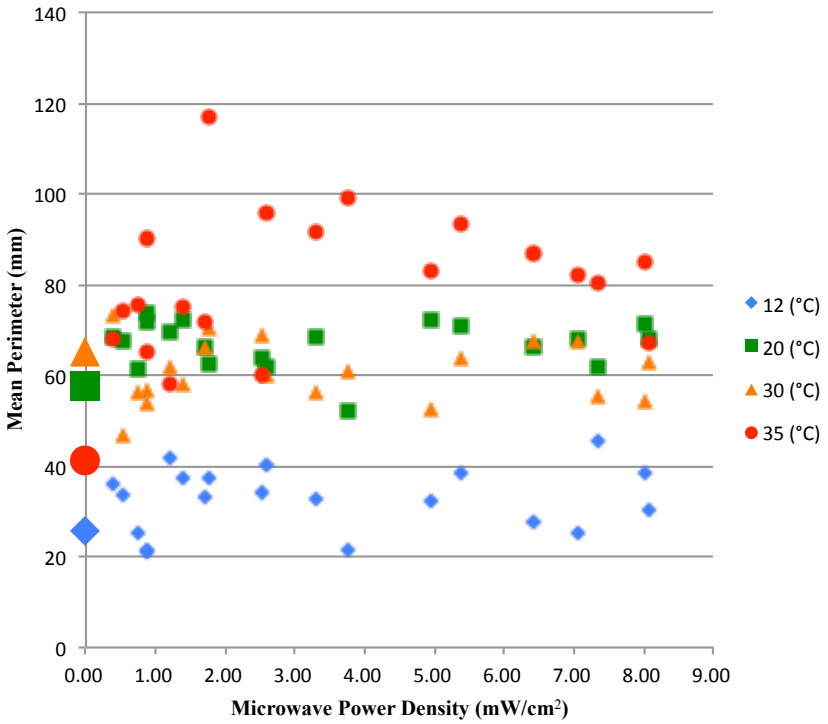


Fig. 6.18 Mean Perimeter and Power Density

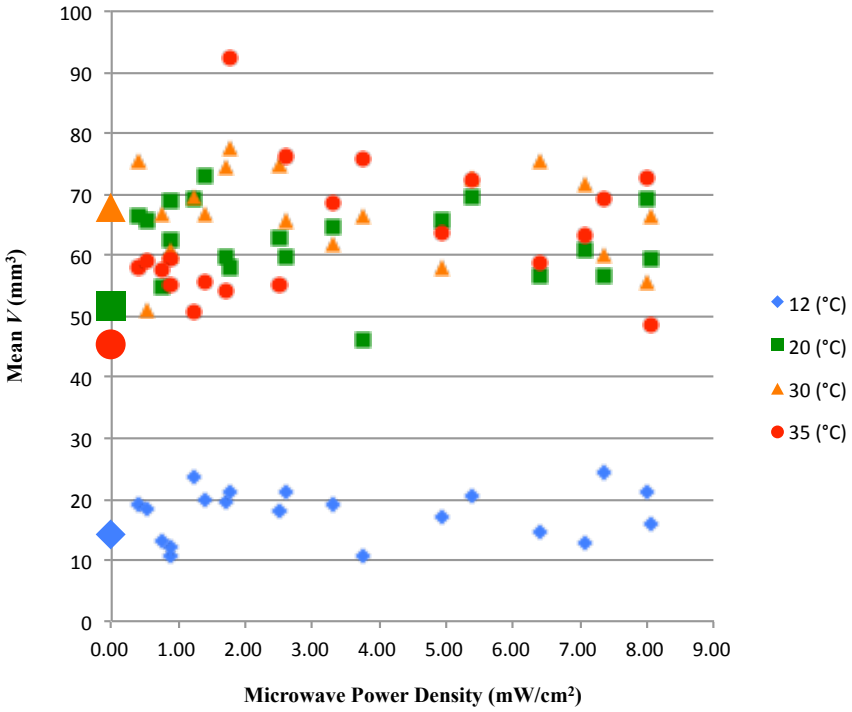


Fig. 6.19 Mean *V* and Power Density

## 6.2 Long-Term Effects on Growth of Spinach

In the previous section (6.1 Effects on Germination Stage), short-term (96 hours, germination stage) experiments were conducted. To estimate effects of microwave on plant growth in further stage, long-term experiments were conducted. The experiments were conducted to determine the effects on outer figure on plants exposed with microwave in long-term at certain intensity levels in strictly controlled environment. In this section, effects of long-term exposure of 2.45 GHz microwave on growth of *Spinacia oleracea* in soil under controlled environments of growth chamber were examined, which were not conducted in our previous study. Leaf area and weight were measured to determine the existence of the effects.

### 6.2.1 Materials

1) Plant

*Spinacia oleracea* L. cv Try (Takii & Co., Ltd) was chosen as experimental seed. Ten growth pots with 500g soil (Takii raising culture soil) were prepared and watered initially with 700ml water. Five seeds for each pot were sown at the depth of 3cm.

2) Growth Chamber and Microwave Generator

Ten pots were placed in a growth chamber (Takayama NS360). On the ceiling of the chamber, a circular patch antenna was installed to emit microwave on plants.

Microwave was generated by an oscillator (TSVF-NB-F2400M-01; Tokyo Keiki Inc.) and was adjusted using a variable resistance attenuator (AT-NJ-801; Nihon Kosyuha Co., Ltd.). Adjusted microwave was amplified through 5W amplifier (A250HP-R; R & K Co., Ltd.) and 20W amplifier (A2040-4643-R; R & K Co., Ltd.). Amplified microwave was split by a directional coupler (5D906; SPC Electric Corporation) and was sent to a circular patch antenna in the chamber and to a power sensor.

3) Measurement Equipment

Atmospheric temperature was measured and logged by TR-71Ui (T & D Corporation). Humidity was measured and logged by and TR-72Ui (T & D Corporation).

Microwave output through the directional coupler was measured by a power sensor (8481B; Agilent Technologies) and a power meter (E4419B; Agilent Technologies) and logged by an A/D converter and a notebook PC. In second 3 weeks experiment, microwave power was logged by another data logger (Memory Hilogger LR8430; HIOKI E. E. Corporation). After experiments, individuals of germinated seeds were scanned by an image scanner (Canoscan8200F ; Canon Inc.) and stored as bitmap files in a PC. Plant growth was automatically measured by using image processing software, ImageJ.

Fig. 6.20 and Fig. 6.21 depict the chamber and equipment.

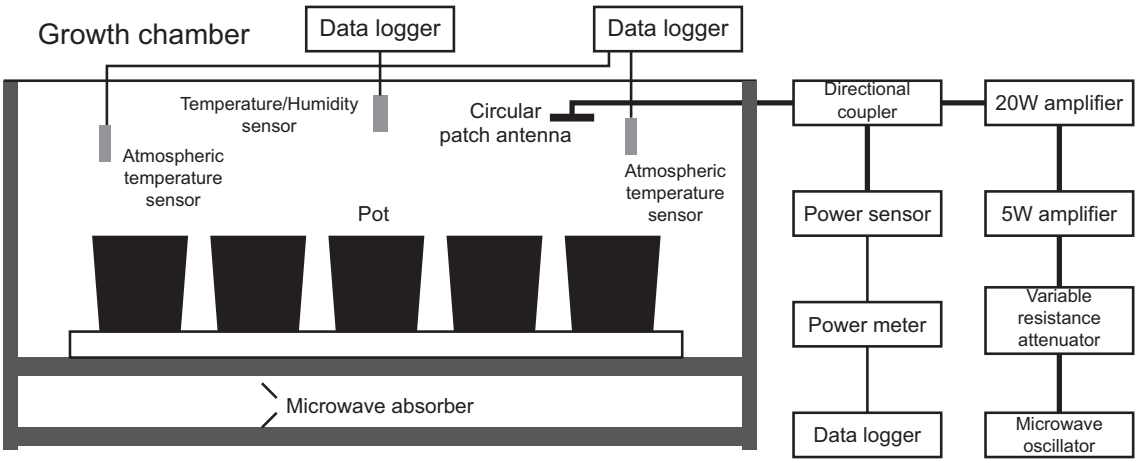


Fig.6.20 Chamber, Sensors, and Microwave Generator

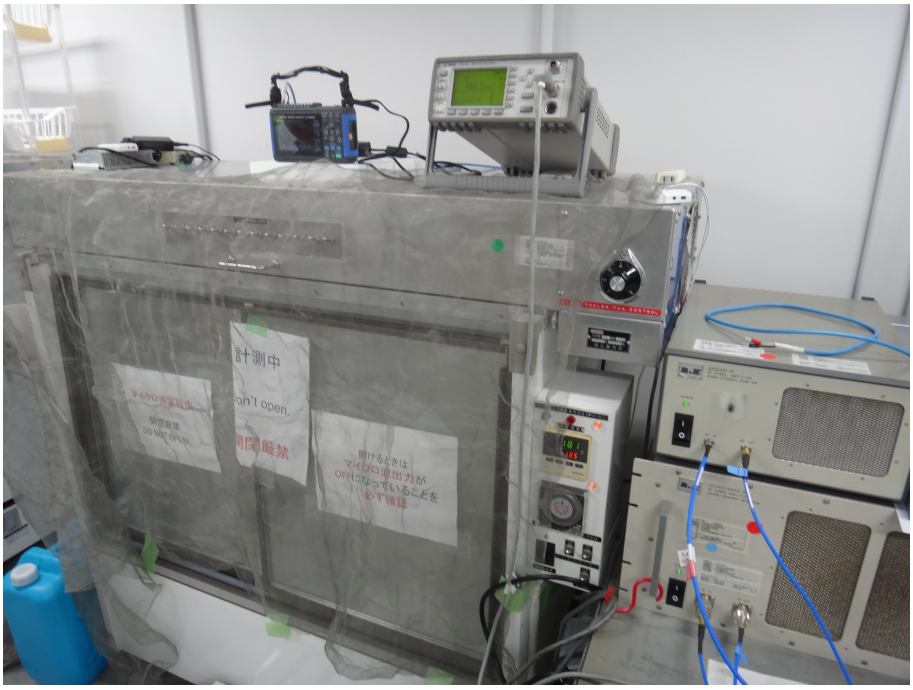


Fig.6.21 Growth Chamber

6.2.2 Method

1) Plant Growth

Ten pots were placed in the chamber as shown in Fig. 6.22. Temperature setting was 18.5 °C. This setting made the mean atmospheric about 20 °C. The light/dark photoperiod was set to 14:10h. Plants were grown in this condition for 1, 3, and 5 weeks in experimental and control plots.

In 1 week experiment, all 5 plans per one pot was measured. In 3 and 5 weeks experiment, one plant per pot was left and other 4 plants were removed after 5 or 6 days from sowing. Pots were watered when total weight became less than 900 g, so that total weight becomes 1000 g.

One plot has 10 pots for both control and experimental plot. For 1 week experiment, 3 control plots and 3 experimental plots were tested. Total number of individuals of 1 week experiment was 115 in control plot and 119 in experimental plot. For 3 weeks experiment, 2 control plots and 2 experimental plots were tested. Total number of individuals was 20 for each plot. One control plot and one experimental plot were tested

in 5 weeks experiment. Total number of individuals of 5 weeks experiment was 10 for each plot.

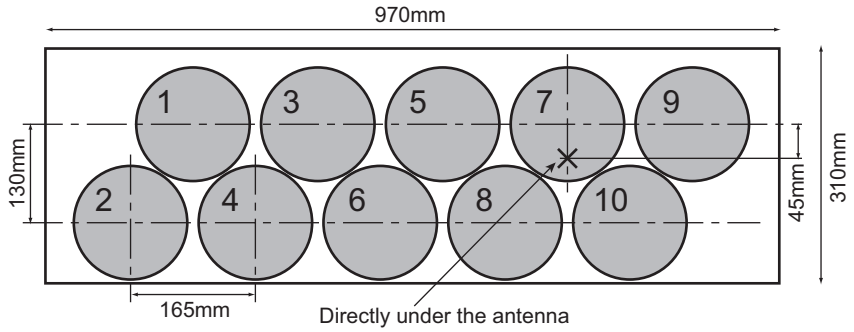


Fig.6.22 Placement of Pots

2) Microwave Exposure

In Experimental plot, microwave was emitted from the circular patch antenna. Total output power to the antenna was set to around 18 W by adjusting the variable resistance attenuator in order not to exceed the maximum output of the amplifier.

Table 6.4 shows the estimated power density of microwave exposure at each center point on soil surface level of pot. These estimated values were obtained from initial measurement of power density at height of soil surface level and mean microwave output during each experiment. Under the circular antenna showed the higher power density.

Table 6.4 Power Density Distribution in Chamber

| Pot No. | 1 week | | | 3 weeks | | 5 weeks |
|---|---|---|---|---|---|---|
| | No. 1 | No. 2 | No. 3 | No. 1 | No. 2 | |
| 1 | 0.38 | 0.42 | 0.39 | 0.39 | 0.39 | 0.39 |
| 2 | 0.16 | 0.18 | 0.16 | 0.16 | 0.16 | 0.16 |
| 3 | 0.58 | 0.64 | 0.60 | 0.59 | 0.59 | 0.60 |
| 4 | 0.28 | 0.31 | 0.29 | 0.29 | 0.29 | 0.29 |
| 5 | 3.05 | 3.41 | 3.18 | 3.13 | 3.15 | 3.19 |
| 6 | 1.02 | 1.14 | 1.06 | 1.04 | 1.05 | 1.07 |
| 7 | 8.00 | 8.93 | 8.34 | 8.19 | 8.24 | 8.35 |
| 8 | 5.39 | 6.01 | 5.62 | 5.51 | 5.55 | 5.62 |
| 9 | 3.71 | 4.14 | 3.87 | 3.80 | 3.82 | 3.87 |
| 10 | 5.23 | 5.84 | 5.46 | 5.36 | 5.39 | 5.46 |

Unit: $mW/cm^2$

3) Measurement

Atmospheric temperature and humidity were measured through the experimental period every 5 minutes. Total microwave output was also measured and logged every 1 second by using the equipment as mentioned above.

After growth of each plot, fresh and dry matter weight, and leaf area was measured. Dry weight was measured after drying in 80 °C for 72 hours.

Leaves were cut from the stem and scanned by the image scanner into Bitmap format files. Leaf area was measured using ImageJ software.

Fig. 6.23 depicts the initial state of the chamber.

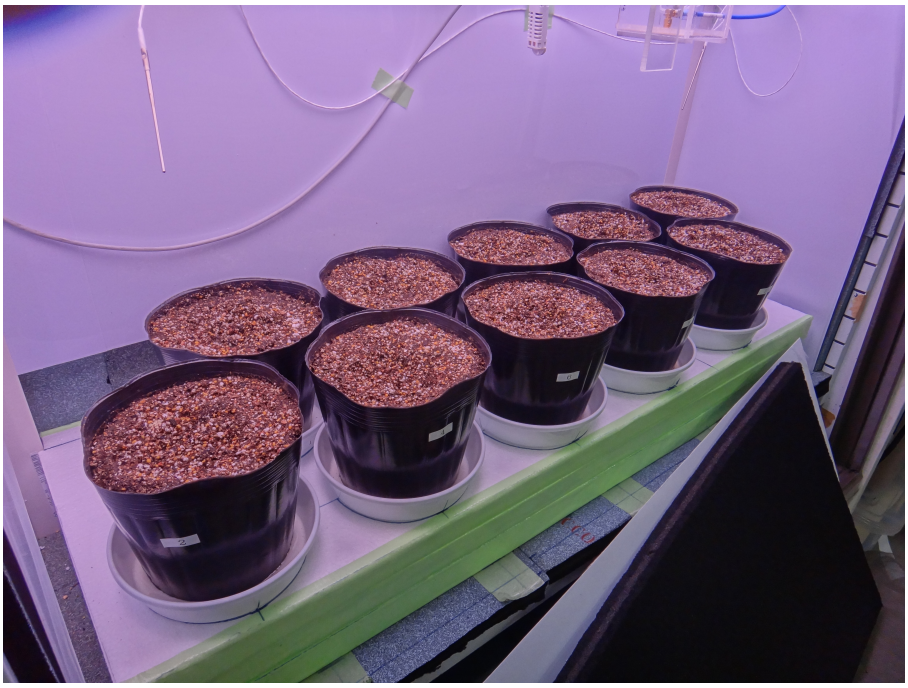

Fig. 6.23 Chamber and Pots

### 6.2.3 Results

1) Microwave Output

Fig. 6.24 shows an example of total microwave output in 3 weeks experimental plot. The output power fluctuated as shown in the graph. Mean output power in each plot was shown in Table 6.5. When watering, microwave was turned off, which is shown as sudden drops (vertical lines) of microwave output.

Fluctuation of microwave output is synchronized to the light/dark photoperiod. There is a possibility that the lights affected the microwave output. However, the reason is unidentified. These experiments were conducted under the long-term exposure of microwave and the effects can be discussed using mainly the mean microwave output.

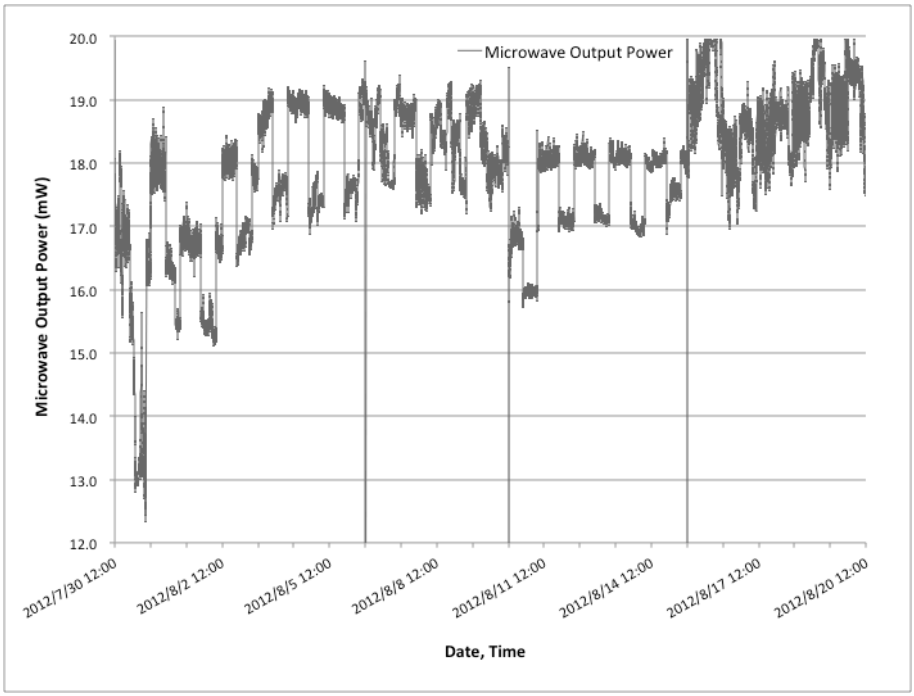


Fig. 6.24 Example of Microwave Output (3 Weeks, with Microwave, No.2)

Table 6.5 Mean Total Microwave Output

| Period | Mean Microwave Output (W) |
|---|---|
| 1 week No. 1 | 17.33 |
| 1 week No. 2 | 19.34 |
| 1 week No. 3 | 18.07 |
| 3 weeks No.1 | 17.74 |
| 3 weeks No. 2 | 17.85 |
| 5 weeks | 18.09 |

2) Temperature and Humidity

Fig. 6.25 shows an example of temperature fluctuation and Fig. 6.26 shows that of humidity. Temperature and humidity fluctuated according to activations of cooler, heater and light.

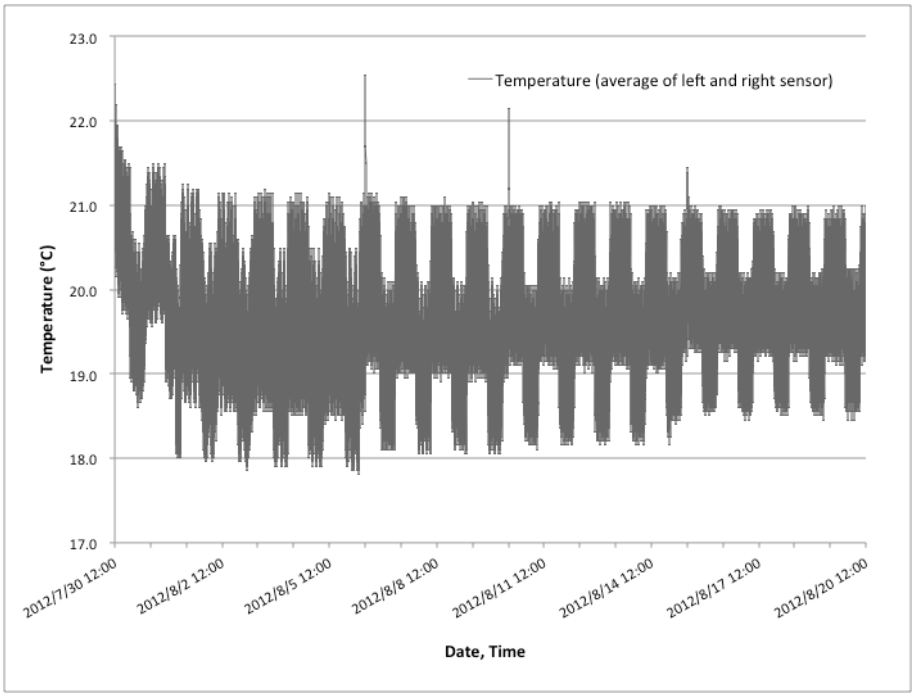


Fig. 6.25 Temperature in Chamber (3 Weeks, with Microwave, No.2)

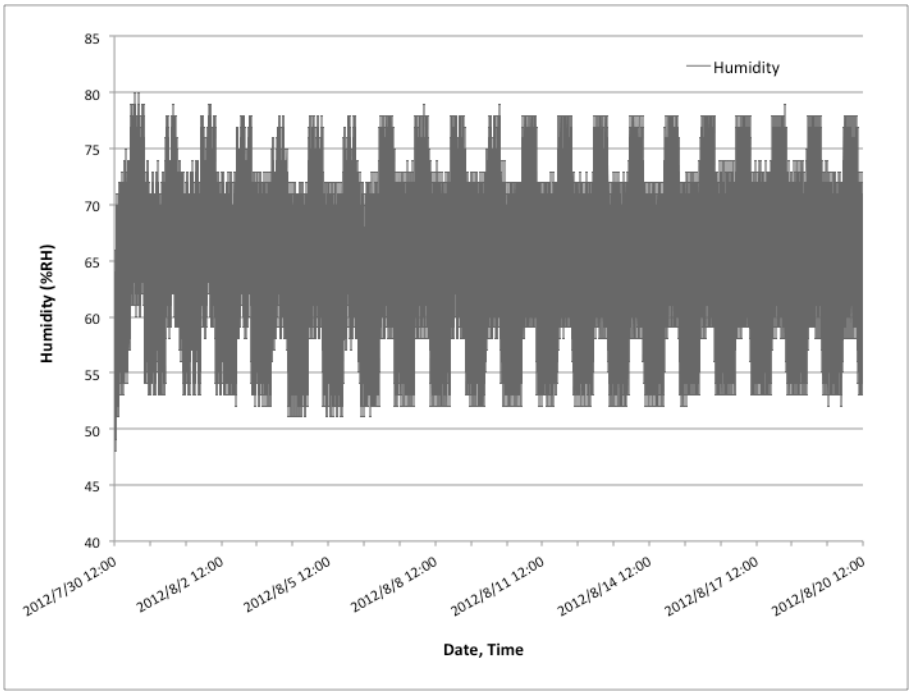


Fig. 6.26 Humidity in Chamber (3 Weeks, with Microwave, No.2)

3) Photosynthetic Photon Flux Density

Considering the synchronized fluctuation of microwave output with the light/dark photoperiod, photosynthetic photon flux density (PPFD) was measured at the point of the center on the surface height of the pot No. 1 by a light meter (LI. COR Model LI-250). PPFD was measured as 15 seconds average value. The measurement was conducted 50 times for each, alternately when the microwave power emission was turned on and off (total 100 times). The mean PPFD values are shown in Table 6.6.

Simple turning on and off of the 20 W amplifier affected the PPDF. The reason is unknown why the amplifier affected the PPFD. Significant difference was found by t-test between when the amplifier was turned on and off. However, the difference of mean PPFD was approximately 0.5 %.

Table 6.6 Mean PPFD

| | Without Microwave | With Microwave | Significance |
|---|---|---|---|
| PPFD ($\mu$mol $m^{-2}$ $s^{-1}$) | 141.43 | 142.18 | * |

4) Growth Measurement

Fig. 6.27 shows an example of scanned image of leaves. Leaves were cut to fit to the flat panel of the image scanner. Table 6.7, 6.8, and 6.9 show the result of mean value and variance of each plot for dry matter, fresh matter and leaf area of 1, 3, and 5 weeks. For fresh matter of 3 and 5 weeks, only above-ground part was measured. In Table 6.7, figures are total value of each plot.


Fig. 6.27 Example of Scanned Image

Table 6.7 Result of 1 Week Experiment

| | | Control | Experimental |
|---|---|---|---|
| Dry Matter (mg) | (Mean) | 6.43 | 4.90 |
| Fresh Matter (mg) | (Mean) | 89.37 | 93.62 |
| Cotyledon ($mm^2$) | (Mean) | 140.335 | 155.106 |

Table 6.8 Result of 3 Weeks Experiment

| | | Control | Experimental |
|---|---|---|---|
| Dry Matter (mg) | (Mean) | 152.17 | 155.00 |
| Fresh Matter of Above-Ground (mg) | (Mean) | 2091.86 | 2031.57 |
| Cotyledon ($mm^2$) | (Mean) | 652.168 | 612.013 |
| Second Leaves ($mm^2$) | (Mean) | 2768.709 | 2846.106 |
| Third Leaves ($mm^2$) | (Mean) | 1943.075 | 1893.755 |

Table 6.9 Result of 5 Weeks Experiment

| | | Control | Experimental |
|---|---|---|---|
| Dry Matter (mg) | (Mean) | 1079.65 | 1731.57 |
| Fresh Matter of Above-Ground (mg) | (Mean) | 15032.53 | 22799.73 |
| Cotyledon ($mm^2$) | (Mean) | 549.283 | 576.477 |
| Second Leaves ($mm^2$) | (Mean) | 3619.424 | 4652.716 |
| Third Leaves ($mm^2$) | (Mean) | 5424.615 | 8516.143 |
| Forth Leaves ($mm^2$) | (Mean) | 7710.967 | 10678.204 |

5) Statistical Analysis of 1 and 3 Weeks Experiment

Differences among the means were analyzed using Wilcoxon signed-rank test, at the 5 % level of significance. Power density of microwave at each position of pot was different, thus, for each experiment of 1, 3, and 5 weeks, mean value of pairs of each pot position were tested. Table 6.10, 6.11, and 6.12 show the results of this analysis.

In 1 and 3 weeks experiment, no significance was found for all measured values. Obvious differences of weight and leaf area were not found between control and experimental plots.

Table 6.10 Result of Wilcoxon Signed-Rank Test
(1 Week Experiment)

| | Significance |
|---|---|
| Dry Matter | n.s. |
| Fresh Matter | n.s. |
| Cotyledon | n.s. |

Table 6.11 Result of Wilcoxon Signed-Rank Test
(3 Week Experiment)

| | Significance |
|---|---|
| Dry Matter | n.s. |
| Fresh Matter of Above-Ground | n.s. |
| Cotyledon | n.s. |
| Second Leaves | n.s. |
| Third Leaves | n.s. |

Table 6.12 Result of Wilcoxon Signed-Rank Test
(5 Week Experiment)

| | Significance |
|---|---|
| Dry Matter | * |
| Fresh Matter of Above-Ground | * |
| Cotyledon | n.s. |
| Second Leaves | n.s. |
| Third Leaves | * |
| Forth Leaves | n.s. |

6) Statistical Analysis of 5 Weeks Experiment

In 5 weeks experiment, significance was observed in dry matter, fresh matter of above-ground part, and third leaves area. As mentioned above, approximately 0.5 % difference of PPFD was found between the control and experimental plots. However, this difference can be considered enough small not to affect the growth in the both pots. In total 14 items in Table 6.10, 6.11, and 6.12, four items showed larger values of the control plots than those of the experimental plots. The rest of them showed the differences large enough from the 0.5 % difference of measured PPFD.

No significances were found in 1 and 3 weeks experiments, while in 5 weeks experiments dry matter, fresh matter of above-ground, and third leaves area showed the significances. This does not mean that there were no effects on inner plant biochemical responses at an early stage. These results may suggest that changes in outer forms require certain long time.

Atmospheric temperature and light intensity were set as the same in both experimental and control plots. However, soil temperature and plant body temperature were not measured. Under higher power density, even if there is no effect of microwave itself on plants, temperature of plants could be increased by thermal effect of

microwave. Considering no significance in 3 weeks experiments, it can be thought that there was no significant differences of soil temperature between experimental and control plots. Temperature of direct measurement of plant body was not obtained. However, as plants grow, height of plant body increases and the top of the plant approaches to the patch antenna. This means that there is a possibility of temperature increase in plant body. To estimate this effect, Wilcoxon signed-rank test at the 5 % level of significance for 5 weeks experiments that does not include the pot No. 7, 8 and 10, which were near the patch antenna, was conducted. Table 6.13 shows the result, which indicates the significances of dry matter and fresh matter of above-ground part. Significance of third leaves area, which is shown in Table 6.12, was not found in this test. This result does not show the direct indication that there was no differences of plant body temperature. However, it suggests little or no difference of temperature. A new method and experimental apparatus that enable to distinguish the difference between thermal and non-thermal effects of microwave should be introduced.

Table 6.13 Result of Wilcoxon Signed-Rank Test
(5 Weeks Experiment, excluding Pot No. 7, 8, and 10)

| | Significance |
|---|---|
| Dry Matter | * |
| Fresh Matter of Above-Ground | * |
| Cotyledon | n.s. |
| Second Leaves | n.s. |
| Third Leaves | n.s. |
| Forth Leaves | n.s. |

## 6.3 Discussion

In the two experiments (6.1 Effects on Germination Stage, 6.2 Long-Term Effects on Growth of Spinach), differences between exposed and not exposed plant growth were found. One of the main points of these experiments was to determine whether these differences were derived from thermal or non-thermal effect of microwave exposure.

The results of the first experiment suggested the existence of non-thermal effect by showing more similar pattern to non-thermal effect in Fig. 6.2. The relation between microwave power density and measure values also suggested the non-thermal effect (Fig. 6.17, 6.18, and 6.19). In the second experiment, Wilcoxon signed-rank test at the 5 % level of significance for 5 weeks experiments that does not include the pot No. 7, 8 and 10, which were near the patch antenna, was conducted to estimate the non-thermal effect (Table 6.13). The result of this Wilcoxon signed-rank test suggested the significances under temperatures with no or little differences. This also indicated the possibility of non-thermal effect of microwave exposure.

The outcomes of the two experiments in this chapter were different from the results of Skiles that reported no significant differences of chlorophyll content by SPAD measurement, fresh weight, and dry weight (Skiles, 2006). However Skiles's experiments were conducted in the undivided same field for both control and reference plots at the same time. This design of experiment contains the dependency of location in each plot. This is the reason why the growth camber with the controlled environment was used and Wilcoxon signed-rank test related to the location of the pots was conducted in the second experiment.

Results of Shmutz *et al*. that reported no visual symptoms of damage contain two main different points from the experiments in this chapter. One is that their experiment was conducted in a wide open-air field. The other is they exposure the microwave and observed the plants for very long-term of 3.5 years (Shmutz *et al*., 1996).

Open-air field is affected by various outer environmental factors and dependency of location is considered stronger than that in controlled environment such as in a growth chamber. These disturbances affect the possibility that the differences may be reduced or eliminated.

Shmuts *et al*. reported decrease of the foliar concentrations of calcium and sulfur in beech trees during the first 2 years and no significance of them in the third year in their paper. Their result suggests that the inner change may not cause the effects on outer

figure immediately and that plans may have stability or restoring ability against the effects. The result of the second experiment in this chapter indicated that the changes were found after 5 weeks. This result shows that outer change of plants may appear after certain period with accumulation of effects of inner substances. However, the first experiment of this chapter showed the changes of root growth in short-term (96 hours).

There is a possibility that these changes will disappear for longer-term than 5 weeks. Roux *et al*. reported the change of relative quantity of *calmodulin-N6*, *cmbp*, and *pin2* related to the time after end of EMF exposure. The results showed that the increase of relative quantity of them after 15 min, decrease after 30 min, and again increase after 60 min. This suggests that the response of plants is not constant and it can be fluctuate after the exposure. This can be considered as adaptability or flexibility of plants against the environment. In the two experiments, plants were exposed to continuous microwave during the experiment period. In these periods, inner responses of plants might not be constant.

In the first experiment of germination stage, differences were found between with and without microwave exposure. There is a possibility that in the germination stage, plants were affected by microwave exposure, and plants showed adaptability against the effect of microwave after germination stage, and after 5 weeks, accumulated effects caused the differences. As mentioned above, these differences can be eliminated after longer-term by adaptability and flexibility of plants (Shmutz *et al*., 1996).

Ursache *et al*. reported the decrease of chlorophyll A and B, and carotenes and slight increase of dry and fresh matter (Ursache *et al*., 2009). This indicates that relationship between change of inner biochemical contents and outer change of mass is not simple and cannot be directly connected. In the experiments in this chapter, differences of dry and fresh matter were shown. To investigate the change in inner plant substances that caused the significances in this study, the measurements of biochemical contents and presumption of the mechanism including homeostasis should be conducted.

[References]

Chen, Y.P., Y.J. Liu, X.L. Wang, Z.Y. Ren, M.Yue. 2005. Effect of Microwave and He-Ne laser on enzyme activity and biophoton emission of *Isatis indigotica* fort. Journal of Integrative Plant Biology 47 (7): 849-855.

Iguchi, H., J. Miyasaka, Y. Ogawa, H. Shimizu, H. Nakashima, K. Ohdoi, N. Shinohara, T. Mitani. 2010. Effects of Microwave on Plant Growth after Germination. IEICE Technical Report (In Japanese with English abstract).

Jonas, H. 1979. Circadian Response to Microwaves by *Mimosa pudica* L. Z. Pflanzenphysiol., 91: 95-101.

Jonas, H., 1983. Responses of Maize Seedlings to Microwave Irradiations. Environmental Pollution (Series B) 6: 207-219.

Roux, D., A. Vian, S. Girard, P. Bonnet, F. Paladian, E. Davies, G. Ledoigt. 2006. Electromagnetic fields (900 MHz) evoke consistent molecular responses in tomato plants. Physiologia Plantarum 128: 283-288.

Schmutz, P., J. Siegenthaler, C. Stäger, D. TaTjan, J. B. Bucher. 1996. Long-term exposure of young spruce and beech trees to 2450-MHz microwave radiation. The Science of the Total Environment, 180: 43-48.

Skiles, J. W. 2006. Plant response to microwaves at 2.45 GHz. Acta Astronautica 58: 258–263.

Ursache, M., G. Mindru, D.E. Creangă, F.M. Tufescu, C. Goiceanu 2009. The Effects of High Frequency Electromagnetic Waves on the Vegetal Organisms. Rom. Journ. Phys., 54(1–2): 133–145.

Vian, A., D. Roux, S. Girard, P. Bonnet, F. Paladian, E. Davies, G. Ledoigt. 2006. Microwave Irradiation Affects Gene Expression in Plants. Plant Signaling & Behavior, 1(2): 67-69.

# 7. Conclusions

## 7.1 Microwave Power Transmission to Agricultural Model Vehicle

As described in previous chapters (Chapter 3 to 5), microwave power transmission to model agricultural vehicles and running of them were realized through the experiments. From the first step of experiments using small model vehicle with fixed receiving antennas (rectenna panels), microwave power transmission and tracking of transmission system were obtained. However, the beam of microwave was spread because of using of a horn antenna as the transmitting antenna. This decreased the transmitting efficiency of microwave power (less than 2%).

As the second step, the larger scaled vehicle with rotating rectenna panels was introduced. This model vehicle was designed as the same size with a small sewing machine. To increase the transmitting efficiency, the parabolic antenna was used as the transmitting antenna. This parabolic antenna enabled to increase the transmitting efficiency from 2 % to 5% compared to the first step experiment. From these experiments, the problems such as slower response of detecting and tracking of the running vehicle were revealed. This slow response was derived from the low processing speed of image detection and slower rotation of cameras and the turntable of the transmitting antenna. To obtain higher response and good tracking of the vehicle, higher performance of tracking and detecting system are desired.

To determine the required response and required power transmission, the smaller vehicle was introduced again. This new small vehicle was equipped with rotating rectenna panel. The new transmitting system was developed as a smaller device with higher response speed. From these experiments, the characteristics of transmitting and receiving antennas were obtained and these characteristics were used to determine the required response of both transmitting and receiving system. Also the received power and the response of the system were measured. However, also in these experiments, lower efficiency of transmission was the problem for smooth running of the vehicle.

## 7.2 Effects of Microwave Power Transmission on Crops

The results of the spinach germination experiment in Chapter 6 suggested the existence of non-thermal effect, showing similar pattern to non-thermal effect (Fig. 6.2). Also the relation between microwave power density and measure values suggested the

non-thermal effect. In the spinach growth experiment for 1 to 5 weeks, Wilcoxon signed-rank test at the 5 % level of significance for 5 weeks experiments that does not include the pot No. 7, 8 and 10 (which were near the patch antenna) suggested the significances under temperatures with no or little differences and the possibility of non-thermal effect of microwave exposure.

Through two types of experiments of microwave effects on plants, negative effects were not observed. These results showed the applicability of microwave transmission in crop fields. However, some effects that enhanced the growth were observed. At this moment, the reason is not clear and more investigation is required.

## 7.3 Future of Microwave Power Transmission for Agricultural Machinery and Other Moving Devices

In this study, the possibility and the problems of microwave power transmission to the running agricultural vehicle were examined. To realize the microwave-driven agricultural vehicle, higher response and efficiency of transmission are the key to this application. However, these problems were not the ones that cannot be overcome by conventional technologies, such as more powerful PC, miniaturization of devices for the weight saving of the vehicle, and introduction of phased array patch antenna for narrow beam of transmitted microwave.

As another way to improve the performance of the system, batteries as a buffer on the vehicle can be considered. This buffer batteries can stable the power supply to the motors under the fluctuation of microwave power transmission. The vehicle runs mainly by the batteries. These batteries can be charged continuously during its farm work.

Other than the application of microwave-driven agricultural vehicle in open-air fields, this technology is considered to have a potential for wireless power supply in greenhouses. Several studies of wireless microwave power transmission in weak power levels have been started to supply electricity to mobile equipment like mobile phones or notebook computers in a room with this facility (ubiquitous power supply). Also transmission of microwave power to the running vehicle is applicable not only to the agricultural fields, but also the wider area of application such as the wireless power transmission to the vehicle on the moon and other planets. Also the vehicle used in disaster situation has a potential of this application.

# Acknowledgements

The author expresses his sincere gratitude to Emeritus Professor Akira Oida, Kyoto University, the proponent of the microwave-driven agricultural vehicle and the pioneer of this research field. He guided the author to study this completely new research field. His thoughtful advice was indispensable to complete this study.

The author also expresses grateful gratitude to Professor Hiroshi Shimizu, Laboratory of Agricultural Systems Engineering, Graduate School of Agriculture, Kyoto University. Without his precise advice and guidance, the author could not complete this doctoral thesis. He always gave timely indication and great help to the author.

Special acknowledgements are due to Professor Naoshi Kondo and Michihisa Iida, the members of the dissertation committee with Professor Shimizu for their greatly helpful suggestions to this reseach.

Also the author would like to express special thanks to Emeritus Professor Minoru Yamazaki, Kyoto University, who was a supervisor of the author during the author's first several years of the career.

Special acknowledgements are due to Associate Professor Hiroshi Nakashima and Assistant Professor Katsuaki Ohdoi, colleagues and co-researchers of this study. We spent a lot of time to conduct the difficult experiments, to improve the system, and to discuss the plan and results of this study. Without their collaboration, this research would not complete.

Also special acknowledgements are due to Emeritus Professor Hiroshi Matsumoto, Emeritus Professor Kozo Hashimoto, Professor Naoki Shinohara, and Associate Professor Tomohiko Mitani, Kyoto University. Emeritus Professor Hiroshi Matsumoto welcomed Professor Oida's first proposal of joint-research of the microwave-driven agricultural vehicle, and without his help, we could not start this project. Professor Hashimoto, Professor Shinohara, and Associate Professor Mitani were co-researchers with us from the first step of this study. Without their facilities, an anechoic chamber of METLAB, Research Institute for Sustainable Humanosphere, Kyoto University, this study could not be conducted and completed. They also gave the author precise advices

to point out the problems of the experiments.

The author would like to express utmost gratitude to Associate Professor Yuichi Ogawa, co-researcher of the study on microwave effects on plants. He always gave the author precise, helpful, and thoughtful comments and suggestions.

This study contains the significant amount of the result of the author's co-research with his graduate and under-graduate students. Mr. Masatoshi Watanabe, Mr. Yuya Yamanaka, and Mr. Shinya Nakagawa were devoted to the development of the transmitting and receiving system and the vehicles. Mr. Hiroyuki Iguchi and Mr. Ryosuke Yamamoto worked with the author to conduct the experiments of microwave effects on plants. The time of collaboration with them was a great memory of happy research time of the author.

Mr. Tomoya Kubota, Mr,Yasunori Matsui, Mr. Shinji Ohnishi, Mr. Shinji, Yamada, Mr. Hideaki Miyanaga, Mr. Masaru Sasaki, Mr. Shinji Kitamura, Mr. Kazuyuki Matsuoka, Mr. Hideya Saito, Ms. Hiromi Matsumoto were also devoted to the research on microwave-driven agricultural vehicles and effects of microwave on plants. The author would like to thank to them for their efforts to contribute to the project.